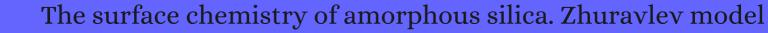
CITATION REPORT List of articles citing



DOI: 10.1016/s0927-7757(00)00556-2 Colloids and Surfaces A: Physicochemical and Engineering Aspects, 2000, 173, 1-38.

Source: https://exaly.com/paper-pdf/31381818/citation-report.pdf

Version: 2024-04-18

This report has been generated based on the citations recorded by exaly.com for the above article. For the latest version of this publication list, visit the link given above.

The third column is the impact factor (IF) of the journal, and the fourth column is the number of citations of the article.

#	Paper IF	Citations
1717	Structurally bound water and surface characterization of amorphous silica. 1989 , 61, 1969-1976	62
1716	Surface coverages of bonded-phase ligands on silica: a computational study. 2001 , 73, 4006-11	25
1715	Fabrication and Characterization of SiO2 Particles Generated by Spray Method for Standards Aerosol 2001 , 34, 1285-1292	37
1714	Hydrogen Production via Catalytic Decomposition of Methane. 2001 , 199, 9-18	201
1713	Pure Na-4-mica: Synthesis and Characterization. 2002 , 14, 2582-2589	50
1712	Evidence of the Existence of Three Types of Species at the QuartzAqueous Solution Interface at pH 0110: XPS Surface Group Quantification and Surface Complexation Modeling. 2002, 106, 2937-2945	205
1711	Investigation on elastomerBilica interactions by inverse gas chromatography and image analysis aided transmission electron microscopy. 2002 , 41, 451-471	15
1710	Templated Site-Selective Deposition of Titanium Dioxide on Self-Assembled Monolayers. 2002 , 14, 1236-1241	98
1709	Optical aspects of Na+ ions adsorption on sol-gel porous films used in optical fiber sensors. 2002 , 250, 168-74	6
1708	Preparation of End-Tethered DNA Monolayers on Siliceous Surfaces Using Heterobifunctional Cross-Linkers. 2003 , 19, 6968-6975	61
1707	Graft polymerization of vinyl acetate onto silica. 2003 , 87, 300-310	42
1706	Surface hydroxylation and silane grafting on fumed and thermal silica. 2003 , 264, 354-61	120
1705	Chemisorption of HSi(OH)3 on silica surfaces: an ab initio periodic study. 2003 , 620, 291-300	10
1704	Supercritical fluid generated stationary phases for liquid chromatography and capillary electrochromatography. 2003 , 75, 5860-9	14
1703	Adsorption and Diffusion of Single Molecules at Chromatographic Interfaces. 2003, 107, 6258-6268	67
1702	Drying of Silica Gels to Obtain Aerogels:Phenomenology and Basic Techniques. 2003 , 21, 593-628	76
1701	Novel Preparation of Hybrid Polypropylene/Silica Nanocomposites in a Slurry-Phase Polymerization Reactor. 2003 , 42, 3750-3757	20

1700	Hysteresis Caused by Water Molecules in Carbon Nanotube Field-Effect Transistors. 2003 , 3, 193-198		808
1699	Sintering Characteristics of Nano-Ceramic Coatings. 2003 , 218-220, 51-66		2
1698	Attachment of solid particles to air bubbles in surfactant-free aqueous solutions. 2004 , 59, 2639-2645		58
1697	Adsorption of zinc on colloidal silica, triple layer modelization and aggregation data. <i>Colloids and Surfaces A: Physicochemical and Engineering Aspects</i> , 2004 , 244, 131-140	5.1	19
1696	Diffusion of Single Streptocyanine Molecules in the Nanoporous Network of Sol © el Glasses © 2004 , 108, 14699-14709		77
1695	Lipid membrane formation by vesicle fusion on silicon dioxide surfaces modified with alkyl self-assembled monolayer islands. 2004 , 20, 7526-31		41
1694	Hydrolysis of a two-membered silica ring on the amorphous silica surface. 2004 , 120, 1044-54		52
1693	Grafted metallocalixarenes as single-site surface organometallic catalysts. 2004 , 126, 16478-86		85
1692	Biospecificity of glass surfaces: streptavidin attachment to silica. 2004 , 349, 260-266		6
1691	Hydrophobisation of mesoporous EAl2O3 with organochlorosilanesEfficiency and structure. 2005 , 83, 1-9		27
1690	Low-temperature reaction of trialkoxysilanes on silica gel: a mild and controlled method for modifying silica surfaces. 2005 , 281, 410-6		25
1689	Structured water in partially dehydrated yeast cells and at partially hydrophobized fumed silica surface. 2005 , 283, 329-43		31
1688	Physisorbed water layer formation on fully hydroxylated mesoporous silicas. 2005 , 291, 353-60		12
1687	Influence of mobile phase composition and thermodynamics on the normal phase chromatography of echinocandins. 2005 , 1098, 55-65		9
1686	Experimental and QM/MM investigation of the hydrated silica surface reactivity. 2005, 405, 459-464		7
1685	Partially hydrophobized silica supported Pd catalyst for hydrogenation reactions in aqueous media. 2005 , 294, 121-130		19
1684	Correlation between the growth-per-cycle and the surface hydroxyl group concentration in the atomic layer deposition of aluminum oxide from trimethylaluminum and water. 2005 , 245, 6-10		80
1683	Water adsorption on plasma sprayed transition metal oxides. 2005 , 249, 115-126		24

1682	Water/silica nanoparticle interfacial kinetics of sulfate, hydrogen phosphate, and dithiocyanate radicals. 2005 , 81, 1526-33	7
1681	Molecular Dynamics Simulation of the Structure and Hydroxylation of Silica Glass Surfaces. 2005 , 88, 2532-2539	139
1680	Investigation of factors affecting the adsorption of functional molecules onto gel silicas. 1. Flow microcalorimetry and infrared spectroscopy. 2005 , 287, 379-87	17
1679	Dispersion and aggregation of nanoparticles derived from colloidal droplets under low-pressure conditions. 2005 , 288, 423-31	32
1678	Mechanism of formation of silicalilicate thin films on zinc. 2005 , 488, 45-55	15
1677	Temperature Dependence of the Concentration of Silanol Groups in Silica Precipitated from a Hydrothermal Solution. 2005 , 31, 661-670	25
1676	Fabrication of silica nano wires on the internal perimeter of narrow bore fused silicia tubing by non-isothermal etching. 2005 , 40, 583-589	7
1675	Solid-Liquid Interactions and Functional Surface Wettability. 2005 , 58, 644	12
1674	Environmental Photochemistry in Heterogeneous Media. 2005 , 49-75	2
1673	Surface hydration and its effect on fluorinated SAM formation on SiO2 surfaces. 2005 , 21, 11795-801	41
1672	Quasi-ice monolayer on atomically smooth amorphous SiO2 at room temperature observed with a high-finesse optical resonator. 2005 , 95, 166104	46
1671	Anatomy of Catalytic Centers in Phillips Ethylene Polymerization Catalyst. 1-35	15
1670	Adsorption of ethylene glycol vapor on (alpha-AI2O3 (0001) and amorphous SiO2 surfaces: observation of molecular orientation and surface hydroxyl groups as sorption sites. 2005 , 39, 206-12	45
1669	Theoretical study of the interaction between selected adhesives and oxide surfaces. 2005 , 109, 5060-6	14
1668	Thermally- and photoinduced changes in the water wettability of low-surface-area silica and titania. 2005 , 21, 2400-7	106
1667	FTIR investigation of the H2, N2, and C2H4 molecular complexes formed on the Cr(II) sites in the Phillips catalyst: a preliminary step in the understanding of a complex system. 2005 , 109, 15024-31	43
1666	Effect of OH and silanol groups in the removal of dyes from aqueous solution using diatomite. 2005 , 39, 922-32	209
1665	The structure of active centers and the ethylene polymerization mechanism on the Cr/SiO2 catalyst: a frontier for the characterization methods. 2005 , 105, 115-84	359

(2006-2005)

1664	Probing strong adsorption of solute onto C18-silica gel by fluorescence correlation imaging and single-molecule spectroscopy under RPLC conditions. 2005 , 77, 2303-10	39
1663	Redox-active silica nanoparticles. Part 1. Electrochemistry and catalytic activity of spherical, nonporous silica particles with nanometric diameters and covalently bound redox-active modifications. 2006 , 22, 10605-11	46
1662	Energetics of small molecule and water complexation in hydrophobic calixarene cavities. 2006 , 22, 4004-14	31
1661	Thermodynamic study of water adsorption in high-silica zeolites. 2006 , 110, 14849-59	85
1660	Highly magnetic silica-coated iron nanoparticles prepared by the arc-discharge method. 2006 , 17, 1188-1192	78
1659	Salt permeation and exclusion in hydroxylated and functionalized silica pores. 2006 , 96, 095504	65
1658	Characterisation of the grafting of (3-aminoethyl)aminopropyltrimethoxy silane on precipitated silica. 2006 , 30, 797	17
1657	A Mo(VI) alkylidyne complex with polyhedral oligomeric silsesquioxane ligands: homogeneous analogue of a silica-supported alkyne metathesis catalyst. 2006 , 128, 14742-3	74
1656	Structural Investigations of Silica Polyamine Composites: Surface Coverage, Metal Ion Coordination, and Ligand Modification. 2006 , 45, 6538-6547	30
1655	11B NMR investigation of boron interaction with mineral surfaces: Results for boehmite, silica gel and illite. 2006 , 70, 3231-3238	25
1654	Interactions of biopolymers with silica surfaces: Force measurements and electronic structure calculation studies. 2006 , 70, 3803-3819	34
1653	Water-silica force field for simulating nanodevices. 2006 , 110, 21497-508	248
1652	Nanophase Materials. 2006,	3
1651	X-ray absorption and x-ray fluorescence for the characterization of titanium oxide-modified HPLC silicas. 2006 , 35, 101-105	3
1650	High surface area microporous tabular SiO2 nanoparticles synthesized from octylamine/water bilayer systems. <i>Colloids and Surfaces A: Physicochemical and Engineering Aspects</i> , 2006 , 286, 27-32	2
1649	Increasing the hydrothermal stability of mesoporous SiO2 with methylchlorosilanes日日tructural日study. 2006 , 88, 63-71	25
1648	States of H2O adsorbed on oxides: An investigation by near and mid infrared spectroscopy. 2006 , 307, 13-20	60
1647	Influence of silica fillers during the electron irradiations of DGEBA/TETA epoxy resins, part I: Study of the chemical modification on model compounds. 2006 , 91, 2110-2118	22

1646	Influence of oxygen, hydrogen, helium, argon and vacuum on the surface behavior of molten InSb, other semiconductors, and metals on silica. 2006 , 290, 319-333	6
1645	Determination of hydroxyls density in the silica-mesostructured cellular foams by thermogravimetry. 2006 , 443, 49-52	19
1644	Density of silanol groups on the surface of silica precipitated from a hydrothermal solution. 2006 , 80, 1119-1128	42
1643	The Role of CaO in the ZieglerNatta Catalyst for Propylene Polymerization. 2006 , 109, 147-152	5
1642	Laser-assisted fabrication of submicron-structured hydrophilic/ hydrophobic templates for the directed self-assembly of alkylsiloxane monolayers into confined domains. 2006 , 82, 15-18	23
1641	Immobilized polymeric stationary phases using metalized silica supports. 2006 , 29, 782-9	14
1640	Modelling of non-contact atomic force microscopy imaging of individual molecules on oxide surfaces. 2006 , 17, 2062-2072	18
1639	The role of molecular modeling in bionanotechnology. 2006 , 3, S40-53	58
1638	In situ spectroscopic ellipsometry study on the growth of ultrathin TiN films by plasma-assisted atomic layer deposition. 2006 , 100, 023534	81
1637	From cluster to bulk: size dependent energetics of silica and silica-water interaction. 2006 , 124, 024722	13
1636	Biosilica-coated Ecarrageenan microspheres for yeast alcohol dehydrogenase encapsulation. 2007 , 18, 1517-1526	5
1635	Development of a classical force field for the oxidized Si surface: application to hydrophilic wafer bonding. 2007 , 127, 204704	59
1634	Preparation and characterization of amorphous silica nanowires from natural chrysotile. 2007 , 353, 1534-1539	76
1633	Adsorption behavior and activity of horseradish peroxidase onto polysaccharide-decorated particles. 2007 , 41, 404-9	17
1632	Origin of Gate Hysteresis in Carbon Nanotube Field-Effect Transistors. 2007 , 111, 12504-12507	110
1631	Charge inversion of divalent ionic solutions in silica channels. 2007 , 75, 061202	50
1630	Molecular Simulation of the Phase Behavior of Water Confined in Silica Nanopores. 2007 , 111, 7938-7946	65
1629	Microporous structure and enhanced hydrophobicity in methylated SiO2 for molecular separation. 2007 , 17, 1509	32

1628	Structural assessment and catalytic consequences of the oxygen coordination environment in grafted Ti-calixarenes. 2007 , 129, 1122-31	60
1627	Determining the Structure of Silica-Supported Monomeric Vanadium Oxide Catalysts Based on Synthesis Method and Spectral Data from Theoretical Calculations. 2007 , 111, 7071-7077	11
1626	Hydration of MCM-41 Studied by Sorption Calorimetry. 2007, 111, 12906-12913	62
1625	Speciation of Silanol Groups in Precipitated Silica Nanoparticles by 1H MAS NMR Spectroscopy. 2007 , 111, 9066-9071	37
1624	Synthesis and Characterization of Butoxylated Silica Nanoparticles. Reaction with Benzophenone Triplet States. 2007 , 111, 7623-7628	17
1623	Strong adhesion of water to CeO2(111). 2007 , 18, 044025	51
1622	Surface-Grafted, Molecularly Imprinted Polymers Grown from Silica Gel for Chromatographic Separations. 2007 , 46, 2117-2124	55
1621	Optical and EPR properties of point defects at a crystalline silica surface: Ab initio embedded-cluster calculations. 2007 , 75,	45
1620	Pyrolysis studies of polyethylene terephthalate/silica nanocomposites. 2007, 104, 9-14	21
1619	Functionalization of Cubic Ia3d Mesoporous Silica for Immobilization of Penicillin G Acylase. 2007 , 17, 2160-2166	52
1618	On the H-exchange of ammonia and silica hydroxyls in the presence of Rh nanoparticles. 2007 , 253, 3600-3607	' 5
1617	Redox-active silica nanoparticles. 2007 , 53, 1244-1251	26
1616	Effects of pore sizes of porous silica gels on desorption activation energy of water vapour. 2007 , 27, 869-876	79
1615	Functionalization of SBA-15 by an acid-catalyzed approach: A surface characterization study. 2007 , 106, 129-139	55
1614	Rate and molecular weight distribution modeling of syndiospecific styrene polymerization over silica-supported metallocene catalyst. 2007 , 48, 6519-6531	18
1613	Water sorption in silicone foam containing diatomaceous earth. 2007 , 306, 228-40	13
1612	How pre-melting on surrounding interfaces broadens solid[Iquid phase transitions. 2007, 3, 890-894	34
1611	Equilibrium sorption of gaseous organic chemicals to fiber filters used for aerosol studies. 2007 , 41, 8241-825	227

1610	Concentration of various forms of water in silica precipitated from a hydrothermal solution. 2007 , 1, 310-318	2
1609	Strain of plates of aluminum, glass, and silicon at sorption of water vapor. 2007 , 77, 393-397	1
1608	Effect of Temperature on the Chromatographic Behavior of Epirubicin and its Analogues on High Purity Silica Using Reversed-Phase Solvents. 2007 , 65, 519-526	42
1607	Molecular dynamics simulation of amorphous SiO2 nanoparticles. 2007 , 111, 12649-56	62
1606	Effect of humidity on the hysteresis of single walled carbon nanotube field-effect transistors. 2008 , 245, 2315-2318	35
1605	Morphology and Viscoelastic Behaviour of a Silica Filled Styrene/Butadiene Random Copolymer. 2008 , 293, 178-187	14
1604	Hysteresis suppression in self-assembled single-wall nanotube field effect transistors. 2008 , 40, 2278-2282	21
1603	Single-ion conductors for lithium batteries via silica surface modification. 2008 , 177, 561-565	19
1602	Functionalized SiO2 with N-, S-containing ligands for Pb(II) and Cd(II) adsorption. <i>Colloids and Surfaces A: Physicochemical and Engineering Aspects</i> , 2008 , 320, 25-35	34
1601	Structural, optical, and electrical properties of self-assembled films of PbSe nanocrystals treated with 1,2-ethanedithiol. 2008 , 2, 271-80	638
1600	Effect of Filler Particle Size on the Properties of Model Nanocomposites. 2008, 41, 1499-1511	118
1599	Molecular Dynamics of Ionic Transport and Electrokinetic Effects in Realistic Silica Channels. 2008 , 112, 10222-10232	92
1598	Silica on Silicon Carbide. 2008 , 33, 1-99	144
1597	Interactions of silica nanoparticles in supercritical carbon dioxide. 2008 , 129, 174704	19
1596	Thermogravimetric and Spectroscopy Analyses of Silicone Nanocomposites. 2008,	3
1595	Nanofilled silicone dielectrics prepared with surfactant for outdoor insulation applications. 2008 , 15, 228-235	44
1594	Stress-Driven Oxidation Chemistry of Wet Silicon Surfaces. 2008 , 112, 12077-12080	27
1593	Surface Properties of Silica-Based Biomaterials: Ca Species at the Surface of Amorphous Silica As Model Sites. 2008 , 112, 16879-16892	29

1592	Multinuclear Solid-State NMR Studies of Ordered Mesoporous Bioactive Glasses. 2008 , 112, 5552-5562	111
1591	Multiscale Modeling of the Atomic Layer Deposition of HfO2 Thin Film Grown on Silicon: How to Deal with a Kinetic Monte Carlo Procedure. 2008 , 4, 1915-27	38
1590	Water diffusion in nanoporous glass: an NMR study at different hydration levels. 2008, 112, 3927-30	25
1589	Atomic Resolution Imaging on CeO2(111) with Hydroxylated Probes. 2008, 112, 2045-2049	19
1588	Water penetration of damaged self-assembled monolayers. 2008, 24, 5734-9	35
1587	Structural, electronic, and vibrational properties of water molecules adsorbed on silica clusters. 2008 , 77,	8
1586	Flame Hydrolysis. 2008, 286	
1585	Solid phase microextraction fibers coated with sol-gel aminopropylsilica/polydimethylsiloxane: development and its application to screening of beer headspace. 2008 , 24, 1141-6	10
1584	Hysteresis in In2O3:Zn nanowire field-effect transistor and its application as a nonvolatile memory device. 2008 , 93, 183111	12
1583	Aging evaluation of silicone rubber nanocomposites. 2009,	5
1583 1582	Aging evaluation of silicone rubber nanocomposites. 2009, Controlled grafting modification of silica gel via RAFT polymerization under ultrasonic irradiation. 2009, 114, 402-406	5
1582	Controlled grafting modification of silica gel via RAFT polymerization under ultrasonic irradiation.	
1582 1581	Controlled grafting modification of silica gel via RAFT polymerization under ultrasonic irradiation. 2009 , 114, 402-406 Size-dependent physicochemical and optical properties of silica nanoparticles. 2009 , 114, 328-332	58
1582 1581	Controlled grafting modification of silica gel via RAFT polymerization under ultrasonic irradiation. 2009 , 114, 402-406 Size-dependent physicochemical and optical properties of silica nanoparticles. 2009 , 114, 328-332	58 179
1582 1581 1580	Controlled grafting modification of silica gel via RAFT polymerization under ultrasonic irradiation. 2009, 114, 402-406 Size-dependent physicochemical and optical properties of silica nanoparticles. 2009, 114, 328-332 Exploiting the Kubas Interaction in the Design of Hydrogen Storage Materials. 2009, 21, 1787-1800 The Role of the Oxygen/Water Redox Couple in Suppressing Electron Conduction in Field-Effect	58 179 121
1582 1581 1580	Controlled grafting modification of silica gel via RAFT polymerization under ultrasonic irradiation. 2009, 114, 402-406 Size-dependent physicochemical and optical properties of silica nanoparticles. 2009, 114, 328-332 Exploiting the Kubas Interaction in the Design of Hydrogen Storage Materials. 2009, 21, 1787-1800 The Role of the Oxygen/Water Redox Couple in Suppressing Electron Conduction in Field-Effect Transistors. 2009, 21, 3087-3091 High-temperature chlorination-reduction sequence for the preparation of silicon hydride modified	58 179 121 258
1582 1581 1580 1579	Controlled grafting modification of silica gel via RAFT polymerization under ultrasonic irradiation. 2009, 114, 402-406 Size-dependent physicochemical and optical properties of silica nanoparticles. 2009, 114, 328-332 Exploiting the Kubas Interaction in the Design of Hydrogen Storage Materials. 2009, 21, 1787-1800 The Role of the Oxygen/Water Redox Couple in Suppressing Electron Conduction in Field-Effect Transistors. 2009, 21, 3087-3091 High-temperature chlorination-reduction sequence for the preparation of silicon hydride modified silica surfaces. 2009, 15, 936-46 Bioinspired control of colloidal silica in vitro by dual polymeric assemblies of zwitterionic	58 179 121 258 15

1574	Estimation of the interaction energy between small molecules and a silica model as an approach for predicting the interaction order between elastomers and silica. 2009 , 58, 811-816		12
1573	Surface functionalization with phosphazene substratespart VII. Silicon-based materials functionalized with hexachlorocyclophosphazene. 2009 , 41, 27-33		13
1572	Gas permeation through porous glass membranes. 2009 , 336, 17-31		56
1571	Composite fuel cell membranes based on an inert polymer matrix and proton-conducting hybrid silica particles. 2009 , 338, 100-110		61
1570	Mixed-emulsifier stabilised emulsions: Investigation of the effect of monoolein and hydrophilic silica particle mixtures on the stability against coalescence. 2009 , 329, 284-91		72
1569	Pyrogenic silica ageing under humid atmosphere. 2009 , 190, 225-229		24
1568	Surface modification of silica particles by dry coating: Characterization and powder ageing. 2009 , 190, 200-209		58
1567	Optimization of hydrogen storage capacity in silica-supported low valent Ti systems exploiting Kubas binding of hydrogen. 2009 , 694, 2793-2800		19
1566	Evidence of 13C non-covalent isotope effects obtained by quantitative 13C nuclear magnetic resonance spectroscopy at natural abundance during normal phase liquid chromatography. 2009 , 1216, 7043-8		21
1565	Investigation of the states of water and OH groups on the surface of silica. <i>Colloids and Surfaces A: Physicochemical and Engineering Aspects</i> , 2009 , 334, 112-115	5.1	87
1564	IR spectroscopic study of the basicity of aminated silica gels. 2009 , 54, 1798-1803		4
1563	Relaxation Dynamics of Hydration Water at Activated Silica Interfaces in High-Performance Elastomer Composites. 2009 , 42, 2127-2134		29
1562	Thermally induced radical hydrosilylation for synthesis of C18 HPLC phases from highly condensed SiH terminated silica surfaces. 2009 , 25, 13481-7		9
1561	A dynamic magic angle spinning NMR study of the local mobility of alanine in an aqueous environment at the inner surface of mesoporous materials. 2009 , 113, 6267-82		33
1560	Study of Charge Diffusion at the Carbon NanotubeBiO2 Interface by Electrostatic Force Microscopy. 2009 , 113, 15476-15479		4
1559	Observation of graphene bubbles and effective mass transport under graphene films. 2009 , 9, 332-7		164
1558	Porosities accessible to HTO and iodide on water-saturated compacted clay materials and relation with the forms of water: A low field proton NMR study. 2009 , 73, 7290-7302		18
1557	Adsorption of Acetone on Nonporous and Mesoporous Silica. 2009 , 113, 16517-16529		16

(2010-2009)

1556	Anti-fogging nanofibrous SiO(2) and nanostructured SiO(2)-TiO(2) films made by rapid flame deposition and in situ annealing. 2009 , 25, 12578-84	137
1555	In situspectroscopic ellipsometry as a versatile tool for studying atomic layer deposition. 2009 , 42, 073001	232
1554	Quantification of water and silanol species on various silicas by coupling IR spectroscopy and in-situ thermogravimetry. 2009 , 25, 5825-34	161
1553	Elucidating the bimodal acid-base behavior of the water-silica interface from first principles. 2009 , 131, 18358-65	187
1552	Nucleation and growth of atomic layer deposition of HfO2 gate dielectric layers on silicon oxide: a multiscale modelling investigation. 2009 , 11, 3701-9	21
1551	Erosion resistance and mechanical properties of silicone nanocomposite insulation. 2009 , 16, 52-59	51
1550	Evaluation of the Adsorption States of H2O on Oxide Surfaces by Vibrational Absorption: Near- and Mid-Infrared Spectroscopy. 2009 , 17, 373-384	40
1549	Improvement in the Durability of Carbon Nanotube-Supported Ruthenium Catalysts by Coverage with Silica Layers. 2010 , 83, 953-959	5
1548	A mechanism of changes in the electron work function upon water chemisorption on a Si(100) surface. 2010 , 84, 1266-1269	5
1547	Porous Silica in Transition Metal Polymerization Catalysts. 2010 , 29-52	3
1546	Functionalized porous glass for the removal and the confinement of ruthenium from radioactive solutions. 2010 , 400, 25-31	8
1545	Redox-active silica nanoparticles. Part 4. Synthesis, size distribution, and electrochemical adsorption behavior of ferrocene- and (diamine)(diphosphine)-ruthenium(II)-modified StBer silica colloidal particles. 2010 , 14, 289-303	10
1544	The impact of microwave energy on the results of silica gel hydrothermal modification. 2010 , 16, 485-493	6
1543	Molecular dynamics simulation of wetting behavior at CO2/water/solid interfaces. 2010, 55, 2252-2257	44
1542	Combined modeling and experimental studies of hydroxylated silica nanoparticles. 2010 , 45, 5084-5088	22
1541	Thermal pretreatment of silica composite filler materials. 2010 , 99, 237-243	28
1540	Hot Surface Activation of Molecular Complexes: Insight from Modeling Studies. 2010, 122, 1988-1992	12
1539	"Hot" surface activation of molecular complexes: insight from modeling studies. 2010 , 49, 1944-8	43

1538	O/W emulsions stabilised by both low molecular weight surfactants and colloidal particles: The effect of surfactant type and concentration. 2010 , 352, 128-35	133
1537	Differentiating and characterizing geminal silanols in silicas by (29)Si NMR spectroscopy. 2010 , 352, 163-70	26
1536	The separation of uranium ions by natural and modified diatomite from aqueous solution. 2010 , 181, 700-7	146
1535	Green solvent extraction of a triblock copolymer from mesoporous silica: Application to the adsorption of carbon dioxide under static and dynamic conditions. 2010 , 128, 26-33	14
1534	In vitro stability of SBA-15 under physiological conditions. 2010 , 132, 442-452	63
1533	Preparation of MEMO silane-coated SiO2 nanoparticles under high pressure of carbon dioxide and ethanol. 2010 , 52, 276-284	25
1532	Metallocene catalyst supported on silicahagnesia xerogels for ethylene polymerization. 2010 , 382, 106-114	9
1531	Inverse gas chromatography for determining the dispersive surface energy of porous silica. <i>Colloids and Surfaces A: Physicochemical and Engineering Aspects</i> , 2010 , 357, 21-26	32
1530	A new route to synthesis of surface hydrophobic silica with long-chain alcohols in water phase. Colloids and Surfaces A: Physicochemical and Engineering Aspects, 2010 , 369, 218-222 5.1	22
1529	Membrane electrode assembly with Pt/SiO2/C anode catalyst for proton exchange membrane fuel cell operation under low humidity conditions. 2010 , 55, 8894-8900	26
1528	A high-performance, safer and semi-automated approach for the delta18O analysis of diatom silica and new methods for removing exchangeable oxygen. 2010 , 24, 2655-64	37
1527	Interface Investigation in Nanostructured BaTiO3/Silica Composite Ceramics. 2010, 93, 865-874	42
1526	SBR/silica composites modified by a polymerizable protic ionic liquid. 2010 , 42, 555-561	19
1525	Generation of chemisorbed benzyl radicals on silica nanoparticles. 2010 , 86, 1208-14	3
1524	An effect of Ecattering by absorption bserved in near-infrared properties of nanoporous silica. 2010 , 107, 083106	22
1523	Impact of negative line tension on the shape of nanometer-size sessile droplets. 2010 , 105, 076103	64
1522	Electrical properties and memory effects of field-effect transistors from networks of single- and double-walled carbon nanotubes. 2010 , 21, 115204	47
1521	A reactive molecular dynamics simulation of the silica-water interface. 2010 , 132, 174704	359

(2010-2010)

1520	Host and adsorbate dynamics in silicates with flexible frameworks: empirical force field simulation of water in silicalite. 2010 , 132, 094501	12
1519	Tailoring the Hydrophobic Character of Mesoporous Silica by Silylation for VOC Removal. 2010 , 45, 768-775	28
1518	Intrinsic doping and gate hysteresis in graphene field effect devices fabricated on SiO2 substrates. 2010 , 22, 334214	91
1517	Hydrophobic Behavior of Dehydroxylated Silica Surfaces: A B3LYP Periodic Study. 2010 , 114, 19984-19992	22
1516	Ion-specific effects under confinement: the role of interfacial water. 2010 , 4, 2035-42	120
1515	Measurement of the Reactive Surface Area of Clay Minerals Using Solid-State NMR Studies of a Probe Molecule 2010 , 114, 5491-5498	35
1514	Confinement effects on monosaccharide transport in nanochannels. 2010 , 114, 11117-26	35
1513	Facile route to morphologically tailored silver patches on colloidal particles. 2010 , 26, 13564-71	26
1512	Effect of particle structure and surface chemistry on PMMA adsorption to silica nanoparticles. 2010 , 26, 5077-87	28
1511	Linking Surface Potential and Deprotonation in Nanoporous Silica: Second Harmonic Generation and Acid/Base Titration. 2010 , 114, 18465-18473	50
1510	The Formation of Gold Clusters Supported on Mesoporous Silica Material Surfaces: A Molecular Picture. 2010 , 114, 9002-9007	27
1509	Phase transition broadening due to interfacial premelting: a new quantitative access to intermolecular interactions within submonolayer films at solid/vapor interfaces. 2010 , 26, 6394-9	12
1508	Grafting of lanthanide complexes on silica surfaces: a theoretical investigation. 2010 , 114, 6322-30	25
1507	H-Bonding of Furan and Its Hydrogenated Derivatives with the Isolated Hydroxyl of Amorphous Silica: An IR Spectroscopic and Thermodynamic Study. 2010 , 114, 18233-18239	18
1506	The characterization of phospholipid functional group probe species on respirable silicon-containing dusts by solid-state 13C and 31P nuclear magnetic resonance spectroscopy. 2010 , 64, 328-36	1
1505	Synthesis of monodisperse Fe3O4@silica coreBhell microspheres and their application for removal of heavy metal ions from water. 2010 , 492, 656-661	118
1504	Remediation of cadmium contaminated irrigation and drinking water: a large scale approach. 2010 , 198, 89-92	11
1503	Thermally Induced Structural Modification of Silica Nanoparticles Investigated by Raman and Infrared Absorption Spectroscopies. 2010 , 114, 13991-13997	30

1502	Silicon nanoparticle photophysics and singlet oxygen generation. 2010 , 26, 10953-60	35
1501	Chemisorbed Thiols on Silica Particles: Characterization of Reactive Sulfur Species. 2010 , 114, 5080-5087	10
1500	Hydration of cellulose/silica hybrids assessed by sorption isotherms. 2010 , 114, 4047-55	25
1499	Molecular level characterization of the inorganic-bioorganic interface by solid state NMR: alanine on a silica surface, a case study. 2010 , 114, 5989-96	46
1498	Reconstruction and stability of tristobalite 001, 101, and 111 surfaces during dehydroxylation. 2010 , 12, 14930-40	50
1497	Performance of silicone rubber nanocomposites in salt-fog, inclined plane, and laser ablation tests. 2010 , 17, 206-213	34
1496	Elaboration of copper hydroxide phase modified diatomite and their application in lead ions immobilization. 2011 , 35, 461-468	9
1495	Thermal annealing activates amplified photoluminescence of germanium metabolically doped in diatom biosilica. 2011 , 21, 10658	13
1494	Photoinduced hole trapping in single semiconductor quantum dots at specific sites at silicon oxide interfaces. 2011 , 13, 17084-92	30
1493	The Surface Modification of Silica with Vinyltriethoxysilane. 2011 , 399-401, 1123-1130	4
1492	Influence of Polyamines and Related Macromolecules on Silicic Acid Polycondensation: Relevance to Boluble Silicon Pools 2011 , 23, 4676-4687	52
1491	Safranine-T Triplet-State Quenching by Modified Silica Nanoparticles. 2011 , 115, 18122-18130	10
1490	Silanol-Related and Unspecific Adsorption of Molecular Ammonia on Highly Dehydrated Silica. 2011 , 115, 23344-23353	17
1489	Flexible, low-voltage, and low-hysteresis PbSe nanowire field-effect transistors. 2011 , 5, 10074-83	50
1488	Effect of CO Pressure Gradients on the Photochemistry and Thermal Chemistry of Fe(CO)5 Physisorbed into Porous Vycor Glass. 2011 , 115, 20824-20831	7
1487	Carbon dioxide sorbents with propylamine groups-silica functionalized with a fractional factorial design approach. 2011 , 27, 3822-34	40
1486	Evaluations of the BET, I-point, and \(\phi\)lot procedures for the routine determination of external specific surface areas of highly dispersed and porous silicas. 2011 , 27, 187-95	7
1485	Ga-Modified (Si��a�) Sol��el Glasses: Possible Relationships between Surface Chemical Properties and Bioactivity. 2011 , 115, 22461-22474	16

(2011-2011)

1484	Investigating the quartz (1010)/water interface using classical and ab initio molecular dynamics. 2011 , 27, 8700-9	55
1483	Molecular nature of support effects in single-site heterogeneous catalysts: silicavs.alumina. 2011 , 2, 1449	95
1482	Radical Grafting of Tetrafluoroethylene and Vinylidene Fluoride Telomers onto Silica Bearing Vinyl Groups. 2011 , 44, 6249-6257	21
1481	Polyoxometalate grafting onto silica: stability diagrams of H3PMo12O40 on {001}, {101}, and {111} tristobalite surfaces analyzed by DFT. 2011 , 13, 15955-9	21
1480	Controlled silanization of silica nanoparticles to stabilize foams, climbing films, and liquid marbles. 2011 , 27, 12869-76	19
1479	Influence of the Chemical Composition on Nature and Activity of the Surface Layer of Zn-Substituted Sol © el (Bioactive) Glasses. 2011 , 115, 2196-2210	22
1478	An SCC-DFTB/MD Study of the Adsorption of Zwitterionic Glycine on a Geminal Hydroxylated Silica Surface in an Explicit Water Environment. 2011 , 115, 9615-9621	36
1477	Silica-supported aminoxyls as reactive materials for NOx removal. 2011 , 21, 982-990	10
1476	Formation of Pyrogenic Silica: Spectroscopic and Quantum Chemical Insight. 2011 , 36, 47-65	7
1475	Silicon, silica and its surface patterning/activation with alkoxy- and amino-silanes for nanomedical applications. 2011 , 6, 281-300	28
1474	Probing charge transfer at surfaces using graphene transistors. 2011 , 11, 132-7	248
1473	Structural studies of water in hydrophilic and hydrophobic mesoporous silicas: an x-ray and neutron diffraction study at 297 K. 2011 , 134, 064509	33
1472	Simulations of the Quartz(101 1)/Water Interface: A Comparison of Classical Force Fields, Ab Initio Molecular Dynamics, and X-ray Reflectivity Experiments. 2011 , 115, 2076-2088	145
1471	Multilayer Metal Film Plating on Glass. 2011 , 25, 1277-1287	2
1470	Tailored covalent grafting of hexafluoropropylene oxide oligomers onto silica nanoparticles: toward thermally stable, hydrophobic, and oleophobic nanocomposites. 2011 , 27, 4057-67	30
1469	Multi-scale modelling of silicon nanocrystal synthesis by Low Pressure Chemical Vapor Deposition. 2011 , 519, 7650-7658	8
1468	Adsorption of Zinc(II) on diatomite and manganese-oxide-modified diatomite: a kinetic and equilibrium study. 2011 , 193, 27-36	145
1467	Composite membranes based on a sulfonated poly(arylene ether sulfone) and proton-conducting hybrid silica particles for high temperature PEMFCs. 2011 , 36, 10891-10900	37

1466	New adsorbents based on microemulsion modified diatomite and activated carbon for removing organic and inorganic pollutants from waste lubricants. 2011 , 173, 115-128	42
1465	Energetics of protein adsorption on amine-functionalized mesostructured cellular foam silica. 2011 , 1218, 7796-803	28
1464	Application of Hierarchical Porous Silica with a Stable Large Porosity for EGalactosidase Immobilization. 2011 , 3, 1948-1954	26
1463	Increasing Selective CO2 Adsorption on Amine-Grafted SBA-15 by Increasing Silanol Density. 2011 , 115, 21264-21272	172
1462	Effect of a formulation named Lirallon mechanical properties of a composite based on silica and unsaturated polyester resin. 2011 , 66, 77-94	5
1461	Mechanism of Cd (II) sorption on silica synthesized by solgel method. 2011 , 169, 78-83	21
1460	Spontaneous crystalline-to-amorphous phase transformation of organic or medicinal compounds in the presence of porous media, part 1: thermodynamics of spontaneous amorphization. 2011 , 100, 2801-15	33
1459	A New Modifier for Silica in Reinforcing SBR Elastomers for the Tyre Industry. 2011 , 296, 455-464	37
1458	Novel Triclosan-Bound Hybrid-Silica Nanoparticles and their Enhanced Antimicrobial Properties. 2011 , 21, 4295-4304	31
1457	One-pot colloidal synthesis of plasmonic patchy particles. 2011 , 23, 2644-9	53
1456	A dry milling approach for the synthesis of highly active nanoparticles supported on porous materials. 2011 , 4, 1561-5	64
1455	Effect of silica modification on the chemical interactions in NBR-based composites. 2011 , 122, 2130-2138	11
1454	Nanoporous silica polyamine composites for metal ion capture from rice hull ash. 2011 , 25, 530-536	7
1453	Annealing of silica to reduce the concentration of isolated silanols and peak tailing in reverse phase liquid chromatography. 2011 , 1218, 5131-5	14
1452	Direct determination of half-life of (214)Pb by gamma spectrometry and comparison with previous indirect measurements. 2011 , 69, 705-10	3
1451	Comparison of mesoporous silicon and non-ordered mesoporous silica materials as drug carriers for itraconazole. 2011 , 414, 148-56	108
1450	Strengthening of basalt fibers with nano-SiO2@poxy composite coating. 2011 , 32, 4180-4186	97
1449	Inversion of particle-stabilized emulsions of partially miscible liquids by mild drying of modified silica particles. 2011 , 359, 126-35	51

1448	Synthesis powder precursor of LAS ceramics via pH controlled wet chemical process. 2011 , 211, 256-263	3
1447	Light-ion-irradiation-induced thermal spikes in nanoporous silica. 2011 , 44, 085406	16
1446	Characterization and Properties of Sol-Gel-Derived Polyurethane Acrylate/Silica Hybrid Materials. 2011 , 306-307, 1229-1232	
1445	Study on adsorption of dyes from wastewater by diatomite. 2011 ,	
1444	Effect of hydration on the dielectric properties of C-S-H gel. 2011 , 134, 034509	37
1443	Controlling surface hydroxylation of nanoporous silica by ion bombardment. 2012 , 45, 445307	1
1442	In situ study of the atomic layer deposition of HfO2 on Si. 2012 , 30, 01A143	12
1441	Electrical transport properties of individual WS2 nanotubes and their dependence on water and oxygen absorption. 2012 , 101, 113112	35
1440	Interpreting atomic force microscopy measurements of hydrodynamic and surface forces with nonlinear parametric estimation. 2012 , 83, 103702	6
1439	Formation of Silica Glaze Rock Coatings through Water Vapor Interactions. 2012 , 33, 21-31	9
1438	EFFECTS AND ROLE OF WATER ENVIRONMENT ON A GEMINAL HYDROXYLATED SILICA SURFACE \(\begin{align*} SELF-CONSISTENT CHARGE DENSITY FUNCTIONAL TIGHT BINDING THEORY BASED MOLECULAR DYNAMICS SIMULATION. 2012 , 11, 155-162	12
1437	Particle-wall interactions in micro/nanofluidics. 2012,	1
1436	Mechanical modification of silica powders. 2012 , 120, 429-435	9
1435	A New Method of Silane Coupling Treatment: Chemical Surface Modifications of Metal Oxides with Hydrosilane. 2012 , 41, 853-854	2
1434	Electronic Transport in Graphene. 2012 , 17-49	
1433	Chemistry of aqueous silica nanoparticle surfaces and the mechanism of selective peptide adsorption. 2012 , 134, 6244-56	299
1432	Spontaneous crystalline-to-amorphous phase transformation of organic or medicinal compounds in the presence of porous media, part 3: effect of moisture. 2012 , 29, 2698-709	14
1431	Characterization of medicinal compounds confined in porous media by neutron vibrational spectroscopy and first-principles calculations: a case study with ibuprofen. 2012 . 29, 2432-44	12

1430	Effect of operating conditions on the hydrophobisation of silica-based porous particles in a fluidised-bed reactor: Temperature effect. 2012 , 23, 596-600	2
1429	The pozzolanic reactivity of monodispersed nanosilica hydrosols and their influence on the hydration characteristics of Portland cement. 2012 , 42, 1563-1570	167
1428	Effects of Surface Chemistry of Substrates on Raman Spectra in Graphene. 2012 , 116, 4732-4737	31
1427	Triplet state of 4-methoxybenzyl alcohol chemisorbed on silica nanoparticles. 2012 , 11, 1032-40	8
1426	Grafted poly(1- g- 暇lucan) strands on silica: a comparative study of surface reactivity as a function of grafting density. 2012 , 28, 431-7	30
1425	Dependence of surface properties of silylated silica on the length of silane arms. 2012 , 18, 307-320	12
1424	Aqueous NaCl and CsCl solutions confined in crystalline slit-shaped silica nanopores of varying degree of protonation. 2012 , 28, 1256-66	71
1423	Dielectric Study of Hydration Water in Silica Nanoparticles. 2012 , 116, 24340-24349	70
1422	Interactions and binding energies of dimethyl methylphosphonate and dimethyl chlorophosphate with amorphous silica. 2012 , 28, 10962-7	34
1421	Integrating functional oxides with graphene. 2012 , 152, 1365-1374	37
1420	Asymmetric orientation of toluene molecules at oil-silica interfaces. 2012 , 137, 064703	12
1419	A low field NMR study of water adsorbed on silica and alumina surfaces. 2012 , 19, 313-320	1
1418	Synthesis of silver nanoparticle necklaces without explicit addition of reducing or templating agents. 2012 , 48, 4287-9	16
1417	Molecular Dynamics Simulations of Water Structure and Diffusion in Silica Nanopores. 2012 , 116, 11556-1156	4184
1416	Spectroscopic Investigation of the Canopy Configurations in Nanoparticle Organic Hybrid Materials of Various Grafting Densities during CO2 Capture. 2012 , 116, 516-525	36
1415	Enhancing Hysteresis in Graphene Devices Using Dielectric Screening. 2012 , 33, 1195-1197	2
1414	Preparation and characterization of composites built of poly(N-benzophenoyl methacrylamide-co-N-hydroxyethyl acrylamide) cores and silica raspberry-like shells with dual orthogonal functionality. 2012 , 386, 167-73	7
1413	Application of clickable nanoporous silica surface for immobilization of ionic liquids. 2012 , 27, 932-938	9

1	Chemical origins of frictional aging. 2012 , 109, 186102	62
1411	Efficient simultaneous fluorescence orientation, spectrum, and lifetime detection for single molecule dynamics. 2012 , 137, 164202	19
1410	Ion exclusion and electrokinetic effects resulting from electro-osmotic flow of salt solutions in charged silica nanopores. 2012 , 14, 5935-44	24
1409	The electronic property of graphene adsorbed on the siloxane and silanol surface structures of SiO2: A theoretical prediction. 2012 , 101, 253107	6
1408	Molecular orientation transformation in initial growth stage of disk-like phthalocyanine during organic vapor deposition process. 2012 , 3, 528-536	21
1407	Changes in the Silanol Protonation State Measured In Situ at the Silica Aqueous Interface. 2012 , 3, 231-235	34
1406	Initial Stages of Atomic Layer Deposition of Tantalum Nitride on SiO2 and Porous Low- Substrates Modified by a Branched Interfacial Organic Layer: Chemisorption and the Transition to Steady-State Growth. 2012 , 116, 21948-21960	3
1405	Simulation of Forces between Humid Amorphous Silica Surfaces: A Comparison of Empirical Atomistic Force Fields. 2012 , 116, 26247-26261	60
1404	New hybrid membranes based on phosphonic acid functionalized silica particles for PEMFC. 2012 , 50, 1308-1316	13
1403	Ab initio derived force-field parameters for molecular dynamics simulations of deprotonated	- 8
-4 °)	amorphous-SiO2/water interfaces. 2012 , 249, 292-305	58
1402		813
	Hysteresis in single-layer MoS2 field effect transistors. 2012 , 6, 5635-41 Sources of Hysteresis in Carbon Nanotube Field-Effect Transistors and Their Elimination Via	
1402	Hysteresis in single-layer MoS2 field effect transistors. 2012 , 6, 5635-41 Sources of Hysteresis in Carbon Nanotube Field-Effect Transistors and Their Elimination Via	813
1402 1401	Hysteresis in single-layer MoS2 field effect transistors. 2012 , 6, 5635-41 Sources of Hysteresis in Carbon Nanotube Field-Effect Transistors and Their Elimination Via Methylsiloxane Encapsulants and Optimized Growth Procedures. 2012 , 22, 2276-2284 Nature and structure of aluminum surface sites grafted on silica from a combination of high-field	813
1402 1401 1400	Hysteresis in single-layer MoS2 field effect transistors. 2012 , 6, 5635-41 Sources of Hysteresis in Carbon Nanotube Field-Effect Transistors and Their Elimination Via Methylsiloxane Encapsulants and Optimized Growth Procedures. 2012 , 22, 2276-2284 Nature and structure of aluminum surface sites grafted on silica from a combination of high-field aluminum-27 solid-state NMR spectroscopy and first-principles calculations. 2012 , 134, 6767-75	813 93 58
1402 1401 1400 1399	Hysteresis in single-layer MoS2 field effect transistors. 2012 , 6, 5635-41 Sources of Hysteresis in Carbon Nanotube Field-Effect Transistors and Their Elimination Via Methylsiloxane Encapsulants and Optimized Growth Procedures. 2012 , 22, 2276-2284 Nature and structure of aluminum surface sites grafted on silica from a combination of high-field aluminum-27 solid-state NMR spectroscopy and first-principles calculations. 2012 , 134, 6767-75 Effect of nano-SiO2 on the compatibility of PVA/RSF blend. 2012 , 21, 523-530	813 93 58
1402 1401 1400 1399 1398	Hysteresis in single-layer MoS2 field effect transistors. 2012, 6, 5635-41 Sources of Hysteresis in Carbon Nanotube Field-Effect Transistors and Their Elimination Via Methylsiloxane Encapsulants and Optimized Growth Procedures. 2012, 22, 2276-2284 Nature and structure of aluminum surface sites grafted on silica from a combination of high-field aluminum-27 solid-state NMR spectroscopy and first-principles calculations. 2012, 134, 6767-75 Effect of nano-SiO2 on the compatibility of PVA/RSF blend. 2012, 21, 523-530 Chemisorption and Dehydration of Ethanol on Silica: Effect of Temperature on Selectivity. 2012, 55, 84-92 Synthesis, characterization and examination of Gd[DO3A-hexylamine]-functionalized silica	813 93 58 5

1394	Adsorption of biomolecules on mesostructured cellular foam silica: Effect of acid concentration and aging time in synthesis. 2012 , 149, 60-68	32
1393	Quantification of chemisorption and physisorption of carbon dioxide on porous silica modified by propylamines: Effect of amine density. 2012 , 159, 42-49	63
1392	Modified heat-treatment process of precursor powders for Bi-2212 tapes preparation. 2012 , 27, 268-271	4
1391	Tuning the hydrophobicity of mesoporous silica materials for the adsorption of organic pollutant in aqueous solution. 2012 , 201-202, 107-14	40
1390	Adsorptive removal of nitrate and phosphate anions from aqueous solutions using functionalised SBA-15: Effects of the organic functional group. 2012 , 90, 34-40	18
1389	Application of mesoporous silicon dioxide and silicate in oral amorphous drug delivery systems. 2012 , 101, 444-63	154
1388	Thiol-containing ionic liquid for the modification of styreneButadiene rubber/silica composites. 2012 , 123, 1252-1260	29
1387	Nano-sized silica supported Me2Si(Ind)2ZrCl2/MAO catalyst for ethylene polymerization. 2012 , 123, 1169-117	756
1386	Synthesis and characterization of novel ultraviolet-curing polyurethane acrylate/epoxy acrylate/SiO2 hybrid materials via solgel reaction. 2013 , 127, 2905-2909	11
1385	The first-principles molecular dynamics study of quartz water interface. 2013 , 113, 401-412	5
1384	Surface modification of ultrafine precipitated silica with 3-methacryloxypropyltrimethoxysilane in carbonization process. <i>Colloids and Surfaces A: Physicochemical and Engineering Aspects</i> , 2013 , 418, 174-179	52
1383	Diffusion transport of nanoparticles at nanochannel boundaries. 2013 , 15, 1	13
1382	Enhanced Photon Management of Thin-Film Silicon Solar Cells Using Inverse Opal Photonic Crystals with 3D Photonic Bandgaps. 2013 , 1, 692-698	26
1381	Reverse osmosis performance of organosilica membranes and comparison with the pervaporation and gas permeation properties. 2013 , 59, 1298-1307	46
1380	High fluorescence of thioflavin T confined in mesoporous silica xerogels. 2013 , 29, 10238-46	18
1379	Sulfur Promotion in Conjugated Isomerization of Safflower Oil over Bifunctional Structured Rh/SBA-15 Catalysts. 2013 , 5, 1917-1934	6
1378	Structural investigation of cobalt-doped silica derived from solgel synthesis. 2013, 378, 1-6	4
1377	Observation of the Ambient Effect in BTI Characteristics of Back-Gated Single Layer Graphene Field Effect Transistors. 2013 , 60, 2682-2686	11

1376	Chemoaffinity material for plasmid DNA analysis by high-performance liquid chromatography with condition-dependent switching between isoform and topoisomer selectivity. 2013 , 85, 2913-20	17
1375	Role of hydrogen bonding on the adsorption of several amino acids on SiO2 and Si3N4 and selective polishing of these materials using ceria dispersions. <i>Colloids and Surfaces A:</i> 5.1 <i>Physicochemical and Engineering Aspects</i> , 2013 , 429, 67-73	27
1374	Utilizing Taguchi design of experiment to study the surface treatment of a nanosilica with an acrylic silane coupling agent and revealing the dispersibility of particles in a urethane acrylate resin. 2013 , 10, 537-547	7
1373	In situ repair of high-performance, flexible nanocrystal electronics for large-area fabrication and operation in air. 2013 , 7, 8275-83	48
1372	The influence of different preparation methods on the aggregation status of pyrogenic nanosilicas used in concrete. 2013 , 46, 135-143	32
1371	Influence of surface conductivity on the apparent zeta potential of amorphous silica nanoparticles. 2013 , 410, 81-93	97
1370	Silica nanoparticles as carriers of antifouling ligands for PVDF ultrafiltration membranes. 2013 , 433, 135-151	117
1369	Reactions of d(0) tungsten alkylidyne complexes with O2 or H2O. Formation of an oxo siloxy complex through unusual silyl migrations. 2013 , 49, 9555-7	21
1368	Energetics of liposomes encapsulating silica nanoparticles. 2013 , 19, 2459-72	19
1367	Reversible wettability control of silicon nanowire surfaces: From superhydrophilicity to superhydrophobicity. 2013 , 527, 179-185	21
1366	Anti-fogging and anti-reflective silica nanofibrous film fabricated by seedless flame method. 2013 , 108, 200-203	18
1365	Organic/inorganic nanocomposite coating of bisphenol A diglycidyl ether diacrylate containing silica nanoparticles via electron beam curing process. 2013 , 76, 1119-1126	25
1364	Microemulsion-assisted synthesis of hierarchical porous Ni(OH)2/SiO2 composites toward efficient removal of formaldehyde in air. 2013 , 42, 10190-7	94
1363	Interstitial O2 distribution in amorphous SiO2 nanoparticles determined by Raman and photoluminescence spectroscopy. 2013 , 114, 104305	21
1362	Vibrational spectra of a ferrocenyl phosphine derivative chemisorbed on 3-aminopropylsilyl modified silica gel. 2013 , 69, 57-64	2
1361	Antireflective coatings based on amorphous submicron silica particles for silicate glass: Preparation, morphology of surface, optical properties. 2013 , 8, 756-764	O
1360	Anhydrous proton conducting materials based on sulfonated dimethylphenethylchlorosilane grafted mesoporous silica/ionic liquid composite. 2013 , 5, 11535-43	19
1359	Silica nanoparticles and polyethyleneimine (PEI)-mediated functionalization: a new method of PEI covalent attachment for siRNA delivery applications. 2013 , 24, 2076-87	59

1358	An Original 🗓 lick and Bind 🖺 approach for Immobilizing Copper Hexacyanoferrate Nanoparticles on Mesoporous Silica. 2013 , 25, 4447-4453	60
1357	Optical Tracking of Single Ag Clusters in Nanostructured Water Films. 2013 , 117, 24822-24829	4
1356	Cr-doped porous silica glass as a model material to describe Phillips catalyst properties. 2013 , 308, 319-327	12
1355	Synthesis of Sulfonic Acid Functionalized Silica Honeycombs. 2013 , 52, 15293-15297	6
1354	Lithographically defined macroscale modulation of lateral fluidity and phase separation realized via patterned nanoporous silica-supported phospholipid bilayers. 2013 , 135, 15718-21	8
1353	Charge transport in diatomaceous earth studied by broadband dielectric spectroscopy. 2013 , 80-81, 226-235	9
1352	Titration of free hydroxyl and strained siloxane sites on silicon dioxide with fluorescent probes. 2013 , 29, 11868-75	11
1351	Preparation of chitin-silica composites by in vitro silicification of two-dimensional lanthella basta demosponge chitinous scaffolds under modified StBer conditions. 2013 , 33, 3935-41	61
1350	CO2 adhesion on hydrated mineral surfaces. 2013 , 47, 11858-65	42
1349	Atomic structure and dehydration mechanism of amorphous silica: Insights from 29Si and 1H solid-state MAS NMR study of SiO2 nanoparticles. 2013 , 120, 39-64	44
1348	Novel silica membrane material for molecular sieve applications. 2013 , 179, 22-29	14
1347	Influence of capillary bridge formation onto the silica nanoparticle interaction studied by grand canonical Monte Carlo simulations. 2013 , 29, 12410-20	39
1346	A comparative study on bulk and nanoconfined water by time-resolved optical Kerr effect spectroscopy. 2013 , 167, 293-308	30
1345	Dehydroxilation and crystallization of glasses: A DTA study. 2013 , 381, 12-16	5
1344	Effects of catalyst thickness on the fabrication and performance of carbon nanotube-templated thin layer chromatography plates. 2013 , 31, 031203	21
1343	Height distribution of atomic force microscopy images as a tool for atomic layer deposition characterization. 2013 , 31, 01A104	3
1342	Effect of thermal treatment and moisture content on the charge of silica particles in non-polar media. 2013 , 9, 7242	16
1341	Redox-active silica nanoparticles. Part 6. Synthesis and spectroscopic and electrochemical characterization of viologen-modified StBer silica particles with diameters of approximately 125 nm. 2013 , 17, 79-97	11

1340	Activity improvement of xylylenediamine as a base catalyst by incorporation in SBA-15 mesoporous material. 2013 , 380, 144-151	1
1339	Effect of calcium carbonate on PET physical properties and thermal stability. 2013 , 244, 45-51	23
1338	Energy-enhanced atomic layer deposition for more process and precursor versatility. 2013 , 257, 3254-3270	72
1337	Silica/potassium ferrite nanocomposite: Structural, morphological, magnetic, thermal and in vitro cytotoxicity analysis. 2013 , 178, 1230-1239	15
1336	Enrichment of tritiated water using mesoporous silica. 2013 , 179, 217-223	2
1335	Optical and morphological properties of infrared emitting functionalized silica nanoparticles. 2013 , 142, 763-769	6
1334	Molecular Dynamics Simulation of Water/CO2-quartz Interfacial Properties: Application to Subsurface Gas Injection. 2013 , 37, 5387-5402	58
1333	Effect of silica particles on stability of highly concentrated water-in-oil emulsions with non-ionic surfactant. 2013 , 75, 95-102	12
1332	Influence of Water and Filler Content on the Dielectric Response of Silica-Filled Rubber Compounds. 2013 , 46, 2407-2416	40
1331	Cu nanoparticles on 2D and 3D silica substrates: controlled size and density, and critical size in catalytic silicon nanowire growth. 2013 , 1, 1583	17
1330	Silica surface features and their role in the adsorption of biomolecules: computational modeling and experiments. 2013 , 113, 4216-313	414
1329	From well-defined Pt(II) surface species to the controlled growth of silica supported Pt nanoparticles. 2013 , 42, 238-48	34
1328	Mesoporous silica nanoparticles in medicinerecent advances. 2013 , 65, 689-702	509
1327	Direct observation of ozone formation on SiO2surfaces in O2discharges. 2013 , 46, 032001	16
1326	Structure of Monomeric Chromium(VI) Oxide Species Supported on Silica: Periodic and Cluster DFT Studies. 2013 , 117, 8138-8149	60
1325	Hydroxylation of Metal-Supported Sheet-Like Silica Films. 2013 , 117, 8336-8344	29
1324	Bandgap Opening of Bilayer Graphene by Dual Doping from Organic Molecule and Substrate. 2013 , 117, 12873-12881	66
1323	The Structure of Silica Surfaces Exposed to Atomic Oxygen. 2013 , 117, 9311-9321	22

1322	Reversible Activity Modulation of Surface-Attached Grubbs Second Generation Type Catalysts Using Redox-Responsive Polymers. 2013 , 46, 4255-4267	49
1321	Quantification of silanol sites for the most common mesoporous ordered silicas and organosilicas: total versus accessible silanols. 2013 , 15, 642-50	79
1320	Optical probing of the electronic interaction between graphene and hexagonal boron nitride. 2013 , 7, 1533-41	48
1319	Theoretical Study of the Adsorption of Organophosphorous Compounds to Models of a Silica Surface. 2013 , 117, 14625-14634	17
1318	Tailoring the affinity of organosilica membranes by introducing polarizable ethenylene bridges and aqueous ozone modification. 2013 , 5, 6147-54	40
1317	Thermal restructuring of silica-grafted -CrO2Cl and -VOCl2 species. 2013 , 42, 12725-32	19
1316	Silica-supported Ti chloride tetrahydrofuranates, precursors of Ziegler-Natta catalysts. 2013 , 42, 12706-13	29
1315	Infrared Spectra and Binding Energies of Chemical Warfare Nerve Agent Simulants on the Surface of Amorphous Silica. 2013 , 117, 15685-15697	56
1314	Effect of surface charge density on the affinity of oxide nanoparticles for the vapor-water interface. 2013 , 29, 5023-9	50
1313	Local Charge Storage in Thin Silicon Oxide Films: Mechanisms and Possible Applications. 2013 , 117, 5358-536	3 9
1313 1312	Local Charge Storage in Thin Silicon Oxide Films: Mechanisms and Possible Applications. 2013, 117, 5358-536 Adsorption of Water Acetonitrile Mixtures to Model Silica Surfaces. 2013, 117, 6620-6631	3 9
1312	Adsorption of WaterAcetonitrile Mixtures to Model Silica Surfaces. 2013, 117, 6620-6631 Dating chert (diagenetic silica) using in-situ produced 10Be: Possible complications revealed	45
1312 1311	Adsorption of WaterAcetonitrile Mixtures to Model Silica Surfaces. 2013, 117, 6620-6631 Dating chert (diagenetic silica) using in-situ produced 10Be: Possible complications revealed through a comparison with 36Cl applied to coexisting limestone. 2013, 17, 81-93	45 26
1312 1311 1310	Adsorption of Water Acetonitrile Mixtures to Model Silica Surfaces. 2013, 117, 6620-6631 Dating chert (diagenetic silica) using in-situ produced 10Be: Possible complications revealed through a comparison with 36Cl applied to coexisting limestone. 2013, 17, 81-93 A comparative study of the catalysis of peptide bond formation by oxide surfaces. 2013, 15, 13371-80 Biocompatibility of calcined mesoporous silica particles with ventricular myocyte structure and	45 26 45
1312 1311 1310 1309	Adsorption of Water Acetonitrile Mixtures to Model Silica Surfaces. 2013, 117, 6620-6631 Dating chert (diagenetic silica) using in-situ produced 10Be: Possible complications revealed through a comparison with 36Cl applied to coexisting limestone. 2013, 17, 81-93 A comparative study of the catalysis of peptide bond formation by oxide surfaces. 2013, 15, 13371-80 Biocompatibility of calcined mesoporous silica particles with ventricular myocyte structure and function. 2013, 26, 26-36	45 26 45 6
1312 1311 1310 1309 1308	Adsorption of Water Acetonitrile Mixtures to Model Silica Surfaces. 2013, 117, 6620-6631 Dating chert (diagenetic silica) using in-situ produced 10Be: Possible complications revealed through a comparison with 36Cl applied to coexisting limestone. 2013, 17, 81-93 A comparative study of the catalysis of peptide bond formation by oxide surfaces. 2013, 15, 13371-80 Biocompatibility of calcined mesoporous silica particles with ventricular myocyte structure and function. 2013, 26, 26-36 Understanding the role of defect sites in glucan hydrolysis on surfaces. 2013, 135, 4398-402 Thermal restructuring of silica-grafted TiCl(x) species and consequences for epoxidation catalysis.	45 26 45 6 49

Effects of a silane coupling agent on the tensile adhesive strengt 2013 , 129, 2922-2930	th between resin and titanium.
1303 Room-Temperature ALD of Metal Oxide Thin Films by Energy-Enl	hanced ALD. 2013 , 19, 125-133 58
Roles of Oxygen and Interfacial Stabilization in Enhancing the Cy Anodes for Rechargeable Lithium Batteries. 2013 , 160, A906-A91	
Enhanced adsorption of anionic dyes from aqueous solution by g diatomite. 2013 , 51, 6526-6535	emini cationic surfactant-modified 6
1300 A Model of Silica Dissolution Based on Acid Dissociation of Interr	nal Silanol. 2013 , 86, 520-525 2
Fluorescent Silica Nanoparticles in the Detection and Control of 2013, 1-7	the Growth of Pathogen. 2013 ,
1298 Silica: An efficient catalyst for one-pot regioselective synthesis o	f dithioethers. 2014 , 10, 26-33
Electric-field-induced forces between two surfaces filled with an adsorbed water. 2014 , 66, 31301	insulating liquid: the role of
1296 A new and effective method for thermostatting confined fluids.	2014 , 140, 054502 17
Atomic layer deposition of aluminum-free silica onto patterned c preparation of microfabricated thin-layer chromatography plates	
1294 Effects of Interfacial Bonding on Friction and Wear at Silica/Silica	Interfaces. 2014 , 56, 481-490 43
The structure and activity of potassium supported on SBA-15 mo theory study. 2014 , 13, 1350076	lecular sieve: Density functional
1292 Mesoporous Silica Drug Delivery Systems. 2014 , 665-693	6
1291 A Study of Oxalic Acid Adsorption on the Surface of Natural Mica	ı. 2014 , 884-885, 12-15
1290 Epoxy Resin Composite Based on Functional Hybrid Fillers. 2014 ,	7, 6064-6091 31
VIP service life assessment: Interactions between barrier laminat significance of silica core ageing. 2014 , 85, 617-630	es and core material, and 30
The Free Volume of Condensed Phases Confined in a Nanopore a and Compared to PALS. 2014 , 125, 785-788	as Seen by Computer Simulations
THERMOGRAVIMETRIC ANALYSIS OF THE KINETICS OF THE READ SILICA. 2014 , 87, 443-450	CTION OF ALKOXYSILANE WITH 4

1286	Deposition of a SiOx Film Showing Enhanced Surface Passivation. 2014 , 55, 769-776	3
1285	Covalent functionalization of silica surface using "inert" poly(dimethylsiloxanes). 2014 , 30, 14797-807	29
1284	Silica-surface reorganization during organotin grafting evidenced by IIISn DNP SENS: a tandem reaction of gem-silanols and strained siloxane bridges. 2014 , 16, 17822-7	33
1283	Optical investigation of diffusion of single Ag markers in confined water films. 2014 , 16, 1	4
1282	Hydrophobation of silica surface by silylation with new organo-silanes bearing a polybutadiene oligomer tail. 2014 , 35, 1603-1613	11
1281	The thermal conductivity of clustered nanocolloids. 2014 , 2, 066102	7
1280	Identification and Characterization of Surface Hydroxyl Groups by Infrared Spectroscopy. 2014 , 99-318	53
1279	Stepwise Solid-Phase Synthesis and Solid-State Electrochemistry of Redox-Active Viologen Core/Shell-Structured Modified Silica Materials. 2014 , 1, 263-280	3
1278	On the redox origin of surface trapping in AlGaN/GaN high electron mobility transistors. 2014 , 115, 124506	20
1277	Compartmentalization of bacteria in microcapsules. 2014 , 50, 15427-30	17
1276	Recovery of high specific area silica and sodium fluoride from sodium hexafluorosilicate. 2014 , 21, 4084-4090	4
1275	Silanol-Assisted Aldol Condensation on Aminated Silica: Understanding the Arrangement of Functional Groups. 2014 , 6, 255-264	38
1274	Enzymes immobilized in mesoporous silica: a physical-chemical perspective. 2014 , 205, 339-60	156
1273	Effects of heat treatment on various properties of organic[horganic hybrid silica derived from phenyltriethoxysilane. 2014 , 144, 132-138	5
1272	Electrostatic lofting of dust aggregates near the terminator of airless bodies and its implication for the formation of exozodiacal disks. 2014 , 100, 64-72	16
1271	Exploring the potential of siloxane surface modified nano-SiO2 to improve the Portland cement pastes hydration properties. 2014 , 54, 99-105	51
1270	Asphaltene Adsorption, a Literature Review. 2014 , 28, 2831-2856	338
1269	Thermal conductivity of heat treated mesoporous silica particles. 2014 , 190, 109-116	23

1268	Reactivity of Bis[3-(triethoxysilyl)propyl] Tetrasulfide (TESPT) Silane Coupling Agent over Hydrated Silica: Operando IR Spectroscopy and Chemometrics Study. 2014 , 118, 4056-4071	34
1267	New nanostructured sorbents for desulfurization of natural gas. 2014 , 8, 8-19	20
1266	Characterization of Plasma Polymerized Hexamethyldisiloxane Films Prepared by Arc Discharge. 2014 , 34, 271-285	12
1265	The properties of glass fibres after conditioning at composite recycling temperatures. 2014 , 61, 201-208	49
1264	Simulation-Experimental Approach to Investigate the Role of Interfaces in Self-Replenishing Composite Coatings. 2014 , 1, 1400053	11
1263	Removal of silicon in acid leaching and flocculation processes during zirconium oxychloride octahydrate production. 2014 , 40, 8801-8808	6
1262	Robust and selective nano cavities for protein separation: an interpenetrating polymer network modified hierarchically protein imprinted hydrogel. 2014 , 1345, 154-63	41
1261	Highly efficient and flexible electrospun carbon-silica nanofibrous membrane for ultrafast gravity-driven oil-water separation. 2014 , 6, 9393-401	195
1260	The isolated flat silicon nanocrystals (2D structures) stabilized with perfluorophenyl ligands. 2014 , 16, 1	12
1259	Silica-reinforced tire tread compounds compatibilized by using epoxidized natural rubber. 2014 , 51, 69-79	117
1258	Surface properties of CNTs and their interaction with silica. 2014 , 413, 43-53	34
1257	Strengthening coating based on silica nanoparticles for soda-lime-silica glass. 2014 , 50, 63-67	1
1256	Studies on an Ionic Liquid Confined in Silica Nanopores: Change in Tg and Evidence of OrganicIhorganic Linkage at the Pore Wall Surface. 2014 , 118, 1530-1539	58
1255	Interactions at the silica-peptide interface: the influence of particle size and surface functionality. 2014 , 30, 227-33	43
1254	Surface functionalization of SBA-15 nanorods for anticancer drug delivery. 2014 , 92, 1296-1303	52
1253	Effectiveness of grafting modes of methoxycinnamate sunscreen onto silica particles. <i>Colloids and Surfaces A: Physicochemical and Engineering Aspects</i> , 2014 , 441, 653-663	9
1252	An improved surface passivation method for single-molecule studies. 2014 , 11, 1233-6	85
1251	Few-layer black phosphorus field-effect transistors with reduced current fluctuation. 2014 , 8, 11753-62	245

1250	Role of microstructure on corrosion initiation of an experimental tool alloy: A Quantitative Nanomechanical Property Mapping study. 2014 , 89, 236-241	6
1249	Correlation of Enhanced Strength and Internal Structure for Heat-Treated Submicron StBer Silica Particles. 2014 , 31, 664-674	27
1248	SAXS studies on silica nanoparticle aggregation in a humid atmosphere. 2014 , 16, 1	5
1247	Preparation and Characterization of Magnetite-Silica Nano-Composite as Adsorbents for Removal of Methylene Blue Dyes from Environmental Water Samples. 2014 , 896, 525-531	7
1246	PEI@SiO2: synthesis from diatomite and application for capturing phenolic compounds from aqueous solution. 2014 , 4, 26309-26315	4
1245	Formation of hybrid poly(styrene-co-maleic anhydride)-silica microcapsules. 2014 , 2, 4826-4835	10
1244	Detection of Low-Density Surface Sites on Silica: Experimental Evidence of Intrinsic Oxygen-Vacancy Defects. 2014 , 26, 2166-2171	11
1243	Immobilization of papain on nanoporous silica. 2014 , 4, 13304-13312	10
1242	Improving catalase-based propelled motor endurance by enzyme encapsulation. 2014, 6, 8907-13	33
1241	ZnO superstructures via oriented aggregation initiated in a block copolymer melt. 2014 , 16, 1502-1513	21
1240	Shear dynamics of nanoconfined ionic liquids. 2014 , 16, 8247-56	52
1239	Back gated multilayer InSe transistors with enhanced carrier mobilities via the suppression of carrier scattering from a dielectric interface. 2014 , 26, 6587-93	331
1238	Accurate amorphous silica surface models from first-principles thermodynamics of surface dehydroxylation. 2014 , 30, 5133-41	69
1237	pH Dependent Electronic and Geometric Structures at the WaterBilica Nanoparticle Interface. 2014 , 118, 29007-29016	28
1236	Surface Modification of Silica-Based Marine Sponge Bioceramics Induce Hydroxyapatite Formation. 2014 , 14, 4545-4552	10
1235	Thermally induced structural modifications and O2 trapping in highly porous silica nanoparticles. 2014 , 148, 956-963	2
1234	Study on superhydrophobic surfaces of octanol grafted electrospun silica nanofibers. 2014 , 148, 798-802	10
1233	XPS Investigation of the Atomic Layer Deposition Half Reactions of Bis(N-tert-butyl-N?-ethylpropionamidinato) Cobalt(II). 2014 , 26, 2642-2646	20

1232	Si/SiO2 quantum dots cause cytotoxicity in lung cells through redox homeostasis imbalance. 2014 , 220, 102-15	31
1231	Poly(ethylene oxide) brushes prepared by the grafting tolmethod as a platform for the assessment of cell receptor gand binding. 2014 , 58, 11-22	8
1230	Density functional calculations of amines on the (101) face of quartz. 2014 , 69, 57-64	43
1229	Study of Gas Adsorption on Biphasic Nanostructured Surfaces. 2014 , 55, 373-382	
1228	Coverage-Dependent Luminescence from Two-Dimensional Systems of Covalently Attached Perylene Fluorophores on Silica. 2014 , 118, 2104-2114	9
1227	Silica-based materials as drug adsorbents: first principle investigation on the role of water microsolvation on Ibuprofen adsorption. 2014 , 118, 5801-7	40
1226	Kinetic analysis of the thermal processing of silica and organosilica. 2014 , 118, 5270-7	13
1225	Tuning Spatial Distribution of Surface Hydroxyls on a Metal-Supported Single-Layer Silica. 2014 , 5, 1701-4	10
1224	Water Behavior in MCM-41 As a Function of Pore Filling and Temperature Studied by NMR and Molecular Dynamics Simulations. 2014 , 118, 23701-23710	23
1223	Force Field and a Surface Model Database for Silica to Simulate Interfacial Properties in Atomic Resolution. 2014 , 26, 2647-2658	244
1223		244
	Resolution. 2014, 26, 2647-2658 Fluid adsorption in linear pores: a molecular simulation study of the influence of heterogeneities	
1222	Resolution. 2014, 26, 2647-2658 Fluid adsorption in linear pores: a molecular simulation study of the influence of heterogeneities on the hysteresis loop and the distribution of metastable states. 2014, 40, 690-697 Probing the Adsorption/Desorption of CO2 on Amine Sorbents by Transient Infrared Studies of	6
1222	Resolution. 2014, 26, 2647-2658 Fluid adsorption in linear pores: a molecular simulation study of the influence of heterogeneities on the hysteresis loop and the distribution of metastable states. 2014, 40, 690-697 Probing the Adsorption/Desorption of CO2 on Amine Sorbents by Transient Infrared Studies of Adsorbed CO2 and C6H6. 2014, 53, 4224-4231 Conformational transitions and stop-and-go nanopore transport of single-stranded DNA on	6 25
1222 1221 1220	Resolution. 2014, 26, 2647-2658 Fluid adsorption in linear pores: a molecular simulation study of the influence of heterogeneities on the hysteresis loop and the distribution of metastable states. 2014, 40, 690-697 Probing the Adsorption/Desorption of CO2 on Amine Sorbents by Transient Infrared Studies of Adsorbed CO2 and C6H6. 2014, 53, 4224-4231 Conformational transitions and stop-and-go nanopore transport of single-stranded DNA on charged graphene. 2014, 5, 5171 Molecular Details of Amorphous Silica Surfaces Determine Binding Specificity to Small Amino Acids.	6 25 78
1222 1221 1220 1219	Resolution. 2014, 26, 2647-2658 Fluid adsorption in linear pores: a molecular simulation study of the influence of heterogeneities on the hysteresis loop and the distribution of metastable states. 2014, 40, 690-697 Probing the Adsorption/Desorption of CO2 on Amine Sorbents by Transient Infrared Studies of Adsorbed CO2 and C6H6. 2014, 53, 4224-4231 Conformational transitions and stop-and-go nanopore transport of single-stranded DNA on charged graphene. 2014, 5, 5171 Molecular Details of Amorphous Silica Surfaces Determine Binding Specificity to Small Amino Acids. 2014, 118, 7901-7909	6 25 78 20
1222 1221 1220 1219 1218	Resolution. 2014, 26, 2647-2658 Fluid adsorption in linear pores: a molecular simulation study of the influence of heterogeneities on the hysteresis loop and the distribution of metastable states. 2014, 40, 690-697 Probing the Adsorption/Desorption of CO2 on Amine Sorbents by Transient Infrared Studies of Adsorbed CO2 and C6H6. 2014, 53, 4224-4231 Conformational transitions and stop-and-go nanopore transport of single-stranded DNA on charged graphene. 2014, 5, 5171 Molecular Details of Amorphous Silica Surfaces Determine Binding Specificity to Small Amino Acids. 2014, 118, 7901-7909 Metal Oxides as Acid-Base Catalytic Materials. 2014, 103-195 Dense and narrowly distributed silica-supported rhodium and iridium nanoparticles: Preparation via	6 25 78 20 5

1214	Proton transfers are key elementary steps in ethylene polymerization on isolated chromium(III) silicates. 2014 , 111, 11624-9	102
1213	Molecular dynamics study of nanoconfined water flow driven by rotating electric fields under realistic experimental conditions. 2014 , 30, 3095-109	24
1212	An advanced fabrication route for alkali silicate glass by non-firing process. 2014 , 25, 360-364	2
1211	Synthesis and fuel cell performance of phosphonated hybrid membranes for PEMFC applications. 2014 , 466, 200-210	12
121 0	Preparation of amorphous silica gel from Algerian siliceous by-product of kaolin and its physico chemical properties. 2014 , 40, 10499-10503	11
1209	Silicon wafer wettability and aging behaviors: Impact on gold thin-film morphology. 2014 , 26, 25-32	16
1208	Molecular dynamics simulations of water on a hydrophilic silica surface at high air pressures. 2014 , 198, 107-113	34
1207	Self-assembly of lipopolysaccharide layers on allantoin crystals. 2014 , 120, 8-14	11
1206	Towards single-gate field effect transistor utilizing dual-doped bilayer graphene. 2014 , 77, 431-441	13
1205	Fabrication of electrospun poly (3-hydroxybutyrate)/poly (Faprolactone)/silica hybrid fibermats with and without calcium addition. 2014 , 55, 222-234	45
1204	Inorganic materials as supports for covalent enzyme immobilization: methods and mechanisms. 2014 , 19, 14139-94	272
1203	Ultra-thin silicate films on metals. 2015 , 27, 443001	11
1202	Influence and mechanism of mechanical grinding on disaggregation of silica white particles in aqueous medium. 2015 , 19, S1-210-S1-214	
1201	Effect of the processing method on the electrical behavior of silicon nitride / epoxy nanocomposites. 2015 ,	2
12 00	The effectiveness of a watersoluble synthetic acrylic polymer in enhancing reinforcing action of silica in carboxylated acrylonitrile butadiene rubber latex. 2015 ,	
1199	Particle-size effects in the formation of bicontinuous Pickering emulsions. 2015 , 92, 032308	29
1198	Experimental constraints on the role of dynamic recrystallization on resetting the Ti-in-quartz thermobarometer. 2015 , 120, 8120-8137	25
1197	Biomimetic Intrafibrillar Mineralization of Type I Collagen with Intermediate Precursors-loaded Mesoporous Carriers. 2015 , 5, 11199	25

1196	Constructing 3D microtubule networks using holographic optical trapping. 2015 , 5, 18085	16
1195	Promoting the Adsorption of Metal Ions on Kaolinite by Defect Sites: A Molecular Dynamics Study. 2015 , 5, 14377	33
1194	Highly-symmetric silicon dioxide shallow shell resonators with angstrom-level roughness. 2015,	5
1193	Aging of glass powder surface. 2015 , 427, 175-183	12
1192	VOx/SiO2 Catalyst Prepared by Grafting VOCl3 on Silica for Oxidative Dehydrogenation of Propane. 2015 , 7, 3332-3339	27
1191	High-Throughput Universal DNA Curtain Arrays for Single-Molecule Fluorescence Imaging. 2015 , 31, 10310-7	41
1190	Mesoporous Silica Nanoparticles Decorated with Carbosilane Dendrons as New Non-viral Oligonucleotide Delivery Carriers. 2015 , 21, 15651-66	38
1189	Synthesis of Silica@Ni-Co Mixed Metal Oxide CoreBhell Nanorattles and Their Potential Use as Effective Adsorbents for Waste Water Treatment. 2015 , 2015, 4260-4274	16
1188	Mechanical Treatment of Silica Powder. 2015 , 62, 519-523	1
1187	Hydroxylation of the silica in microfabricated thin layer chromatography plates as probed by time-of-flight secondary ion mass spectrometry and diffuse reflectance infrared Fourier transform spectroscopy. 2015 , 47, 340-344	2
1186	Silicon-based quantum dots induce inflammation in human lung cells and disrupt extracellular matrix homeostasis. 2015 , 282, 2914-29	26
1185	Solid-State NMR and DFT Combined for the Surface Study of Functionalized Silicon Nanoparticles. 2015 , 21, 16047-58	14
1184	Influence of the grafting topology of hydrophobic silica surfaces on the mechanical properties of silicone high consistency rubbers. 2015 , 64, 1128-1134	7
1183	CO2 wettability of seal and reservoir rocks and the implications for carbon geo-sequestration. 2015 , 51, 729-774	269
1182	Stable Poly(methacrylic acid) Brush Decorated Silica Nano-Particles by ARGET ATRP for Bioconjugation. 2015 , 7, 1427-1443	12
1181	High Temperature Stable Separator for Lithium Batteries Based on SiOland Hydroxypropyl Guar Gum. 2015 , 5, 632-45	23
1180	Effect of the functionalization of silica nanoparticles as a reinforcing agent on dental composite materials. 2015 ,	3
1179	Structural stability and polarisation of ionic liquid films on silica surfaces. 2015 , 17, 17661-9	15

1178	Atomistic Description of Pressure-Driven Flow of Aqueous Salt Solutions through Charged Silica Nanopores. 2015 , 119, 12298-12311	21
1177	Photoluminescent SBA-16 Rhombic Dodecahedral Particles: Assembly, Characterization, and ab Initio Modeling. 2015 , 7, 12740-50	3
1176	Exploration and exploitation of water in colloidal crystals. 2015 , 27, 2686-714	25
1175	Highly effective continuous-flow monolithic silica microreactors for acid catalyzed processes. 2015 , 489, 203-208	25
1174	Charge trapping at the MoS2-SiO2 interface and its effects on the characteristics of MoS2 metal-oxide-semiconductor field effect transistors. 2015 , 106, 103109	138
1173	Insights into the role of surface hydroxyl of the silica fillers in the bulk properties of resulting underfills. 2015 ,	1
1172	Vapors in the ambient∆ complication in tribological studies or an engineering solution of tribological problems?. 2015 , 3, 85-114	24
1171	COHESION OF AMORPHOUS SILICA SPHERES: TOWARD A BETTER UNDERSTANDING OF THE COAGULATION GROWTH OF SILICATE DUST AGGREGATES. 2015 , 812, 67	62
1170	Characterization of Nanoparticles by Solvent Infrared Spectroscopy. 2015 , 87, 12313-7	16
1169	Proton Migration on Hydrated Surface of Cubic ZrO2: Ab initio Molecular Dynamics Simulation. 2015 , 119, 28925-28933	39
1168	Capillary Dynamics of Water/Ethanol Mixtures. 2015 , 54, 12196-12203	19
1167	Further Investigation of Slurry Additives for Selective Polishing of SiO2Films over Si3N4Using Ceria Dispersions. 2015 , 4, P5025-P5028	7
1166	Low-cost mesoporous adsorbents amines-impregnated for CO2 capture. 2015 , 21, 597-609	14
1165	Effects of Pressure, Thermal Treatment, and O2 Loading in MCM41, MSU-H, and MSU-F Mesoporous Silica Systems Probed by Raman Spectroscopy. 2015 , 119, 27434-27441	4
1164	Thermal and hydrolytic stability of grafted ester groups of carboxylic acids on the silica surface. 2015 , 122, 517-523	5
1163	Dynamics of ultrathin gold layers on vitreous silica probed by density functional theory. 2015 , 17, 27488-95	5
1162	Piperazine and its carboxylic acid derivatives-functionalized mesoporous silica as nanocarriers for gemcitabine: adsorption and release study. 2015 , 49, 66-74	32
1161	Flower-, wire-, and sheet-like MnO2-deposited diatomites: Highly efficient absorbents for the removal of Cr(VI). 2015 , 29, 71-81	56

1160	Analysis of ionic strength effects on the adsorption of simple amino acids. 2015, 443, 153-61	16
1159	Manipulating surface wettability and oil absorbency of diatomite depending on processing and ambient conditions. 2015 , 332, 22-31	18
1158	Effects of amine structure and base strength on acidBase cooperative aldol condensation. 2015 , 246, 35-45	36
1157	Pore-scale analysis of formation damage in Bentheimer sandstone with in-situ NMR and micro-computed tomography experiments. 2015 , 129, 48-57	54
1156	Potential applications of cyclodextrins in enhanced oil recovery. <i>Colloids and Surfaces A: Physicochemical and Engineering Aspects</i> , 2015 , 469, 42-50 5.1	13
1155	Insights into the origin of the separation selectivity with silica hydride adsorbents. 2015 , 119, 3063-9	21
1154	Structural and Electronic Properties of Pt13 Nanoclusters on Amorphous Silica Supports. 2015 , 119, 2503-25	51228
1153	The use of mesoporous silica in the removal of Cu(I) from the cyanidation process. 2015 , 50, 439-446	3
1152	Optical breathing of nano-porous antireflective coatings through adsorption and desorption of water. 2014 , 4, 6595	18
1151	Mesoporous Hybrid Thin Film Membranes with [email[protected] Architectures: Controlling Ionic Gating through the Tuning of Polyelectrolyte Density. 2015 , 27, 808-821	49
1150	Physics and chemistry of antimicrobial behavior of ion-exchanged silver in glass. 2015 , 7, 2195-201	12
1149	Gas-phase dehydration of vicinal diols to epoxides: Dehydrative epoxidation over a Cs/SiO2 catalyst. 2015 , 323, 85-99	21
1148	Adsorption of charged and neutral polymer chains on silica surfaces: the role of electrostatics, volume exclusion, and hydrogen bonding. 2015 , 91, 012601	25
1147	Modification of graphene/SiO2 interface by UV-irradiation: effect on electrical characteristics. 2015 , 7, 2439-43	33
1146	Support Effects of Ni2P Catalysts on the Hydrodeoxygenation of Guaiacol: In Situ XAFS Studies. 2015 , 58, 211-218	26
1145	A molecular dynamics study on mass transport characteristics in the vicinity of SiO2Water/IPA interfaces. 2015 , 84, 584-591	10
1144	Carbonate and sandstone reservoirs wettability improvement without using surfactants for Chemical Enhanced Oil Recovery (C-EOR). 2015 , 153, 408-415	68
1143	Effect of Interfaces on the Glass Transition of Supported and Freestanding Polymer Thin Films. 2015 , 48, 4132-4141	70

1142	Specific Interactions of Neutral Side Chains of an Adsorbed Protein with the Surface of ⊞Quartz and Silica Gel. 2015 , 119, 8679-84	
1141	In Vivo Integrity and Biological Fate of Chelator-Free Zirconium-89-Labeled Mesoporous Silica Nanoparticles. 2015 , 9, 7950-9	116
1140	Speciation of adsorbates on surface of solids by infrared spectroscopy and chemometrics. 2015 , 891, 79-89	4
1139	Molecular dynamics studies of aqueous silica nanoparticle dispersions: salt effects on the double layer formation. 2015 , 27, 325101	15
1138	Molecular Modeling of Glassy Surfaces. 2015 , 345-365	1
1137	Grafting of lanthanide complexes on silica surfaces dehydroxylated at 200 °C: a theoretical investigation. 2015 , 39, 7703-7715	13
1136	The dependence of phase change enthalpy on the pore structure and interfacial groups in hydrated salts/silica composites via sol-gel. 2015 , 448, 100-5	28
1135	Fibre-reinforced glass/silicate composites: effect of fibrous reinforcement on intumescence behaviour of silicate matrices as a fire barrier application. 2015 , 86, 80-88	5
1134	Mechanisms of criticality in environmental adhesion loss. 2015 , 11, 3994-4001	21
1133	Effect of Aluminum Alkyls on a Homogeneous and Silica-Supported Phenoxy-Imine Titanium Catalyst for Ethylene Trimerization. 2015 , 5, 5068-5076	26
1132	QENS and NMR Study of Water Dynamics in SBA-15 with a Low Water Content. 2015 , 119, 16578-16586	13
1131	First-Principles Calculations of Lithiation of a Hydroxylated Surface of Amorphous Silicon Dioxide. 2015 , 119, 16424-16431	30
1130	Computational Study of Acidic and Basic Functionalized Crystalline Silica Surfaces as a Model for Biomaterial Interfaces. 2015 , 31, 6321-31	11
1129	Nanocomposited silicone hydrogels with a laser-assisted surface modification for inhibiting the growth of bacterial biofilm. 2015 , 3, 3234-3241	8
1128	Improved catalytic methane combustion of Pd/CeO2 catalysts via porous glass integration. 2015 , 179, 313-320	55
1127	Robust polymeric coating enables the stable operation of silicon micro-plate anodes recovered from photovoltaic industry waste for high-performance Li-ion batteries. 2015 , 3, 15432-15443	31
1126	Organic Modification of Hydroxylated Nanoparticles: Silica, Sepiolite, and Polysaccharides. 2015 , 1-35	
1125	Role of PdAg interface in Pd-Ag/SiO2 bimetallic catalysts in low-temperature oxidation of carbon monoxide. 2015 , 56, 379-385	15

1124	Use of diatomite for the removal of lead ions from water: thermodynamics and kinetics. 2015 , 29, 696-704	6
1123	Energy Landscape of Water and Ethanol on Silica Surfaces. 2015 , 119, 15428-15433	27
1122	Support Functionalization To Retard Ostwald Ripening in Copper Methanol Synthesis Catalysts. 2015 , 5, 4439-4448	69
1121	Functionalization of Silica Nanoparticles and Native Silicon Oxide with Tailored Boron-Molecular Precursors for Efficient and Predictive p-Doping of Silicon. 2015 , 119, 13750-13757	22
1120	Cell Penetrating Peptide Adsorption on Magnetite and Silica Surfaces: A Computational Investigation. 2015 , 119, 8239-46	28
1119	Surface vibrational structure of colloidal silica and its direct correlation with surface charge density. 2015 , 31, 3621-6	27
1118	Ceria-Based Slurries for Non-Prestonian Removal of Silicon Dioxide Films. 2015 , 4, P36-P41	13
1117	Coating of silica particles by fluorinated diblock copolymers and use of the resultant silica for superamphiphobic surfaces. 2015 , 64, 153-162	24
1116	Synthesis and small angle X-ray scattering (SAXS) characterization of silica spheres covered with gel-like particles formed by means of solvent evaporation. 2015 , 278, 257-265	13
1115	Simple thiol-ene click chemistry modification of SBA-15 silica pores with carboxylic acids. 2015 , 450, 316-324	20
1115	Simple thiol-ene click chemistry modification of SBA-15 silica pores with carboxylic acids. 2015 , 450, 316-324 A direct method of quantification of maximal chemisorption of 3-aminopropylsilyl groups on silica gel using DRIFT spectroscopy. 2015 , 149, 69-74	5
	A direct method of quantification of maximal chemisorption of 3-aminopropylsilyl groups on silica	
1114	A direct method of quantification of maximal chemisorption of 3-aminopropylsilyl groups on silica gel using DRIFT spectroscopy. 2015 , 149, 69-74 A facile preparation method for synthesis of silica sulfuric acid/poly(o-methoxyaniline) coreBhell	5
1114	A direct method of quantification of maximal chemisorption of 3-aminopropylsilyl groups on silica gel using DRIFT spectroscopy. 2015 , 149, 69-74 A facile preparation method for synthesis of silica sulfuric acid/poly(o-methoxyaniline) coreBhell nanocomposite. 2015 , 26, 645-657 Acid-base dissociation mechanisms and energetics at the silica-water interface: An activationless	5
1114 1113 1112	A direct method of quantification of maximal chemisorption of 3-aminopropylsilyl groups on silica gel using DRIFT spectroscopy. 2015, 149, 69-74 A facile preparation method for synthesis of silica sulfuric acid/poly(o-methoxyaniline) coreshell nanocomposite. 2015, 26, 645-657 Acid-base dissociation mechanisms and energetics at the silica-water interface: An activationless process. 2015, 451, 231-44 Thermodynamic frameworks of adsorption kinetics modeling: Dynamic water uptakes on silica gel	5 12 70
1114 1113 1112 1111	A direct method of quantification of maximal chemisorption of 3-aminopropylsilyl groups on silica gel using DRIFT spectroscopy. 2015, 149, 69-74 A facile preparation method for synthesis of silica sulfuric acid/poly(o-methoxyaniline) coreEhell nanocomposite. 2015, 26, 645-657 Acid-base dissociation mechanisms and energetics at the silica-water interface: An activationless process. 2015, 451, 231-44 Thermodynamic frameworks of adsorption kinetics modeling: Dynamic water uptakes on silica gel for adsorption cooling applications. 2015, 84, 296-302 Synthesis and application of silica hybrids grafted with new guanidine-containing polymers as	5 12 70 53
1114 1113 1112 1111 1110	A direct method of quantification of maximal chemisorption of 3-aminopropylsilyl groups on silica gel using DRIFT spectroscopy. 2015, 149, 69-74 A facile preparation method for synthesis of silica sulfuric acid/poly(o-methoxyaniline) coreBhell nanocomposite. 2015, 26, 645-657 Acid-base dissociation mechanisms and energetics at the silica-water interface: An activationless process. 2015, 451, 231-44 Thermodynamic frameworks of adsorption kinetics modeling: Dynamic water uptakes on silica gel for adsorption cooling applications. 2015, 84, 296-302 Synthesis and application of silica hybrids grafted with new guanidine-containing polymers as highly effective adsorbents for bilirubin removal. 2015, 293, 1667-1674	5 12 70 53 23

1106	Computer Simulations of Quartz (101) Water Interface over a Range of pH Values. 2015, 119, 9274-9286	74
1105	Heterolytic Activation of C-H Bonds on Cr(III)-O Surface Sites Is a Key Step in Catalytic Polymerization of Ethylene and Dehydrogenation of Propane. 2015 , 54, 5065-78	88
1104	Amine-functionalized magnetic nanocomposite particles for efficient immobilization of lipase: effects of functional molecule size on properties of the immobilized lipase. 2015 , 5, 33313-33327	36
1103	Water Contact Angle Dependence with Hydroxyl Functional Groups on Silica Surfaces under CO2 Sequestration Conditions. 2015 , 49, 14680-7	74
1102	Thermal pretreatments of superficially porous silica particles for high-performance liquid chromatography: Surface control, structural characterization and chromatographic evaluation. 2015 , 1419, 45-57	6
1101	Effect of Siloxane Ring Strain and Cation Charge Density on the Formation of Coordinately Unsaturated Metal Sites on Silica: Insights from Density Functional Theory (DFT) Studies. 2015 , 5, 7177-7185	32
1100	Effect of Support Preparation and Nanoparticle Size on CatalystBupport Interactions between Pt and Amorphous Silica. 2015 , 119, 19934-19940	45
1099	Enhanced Nucleation of Lysozyme Using Inorganic Silica Seed Particles of Different Sizes. 2015 , 15, 3582-3593	3 9
1098	Chemisorption and thermally induced transformations of polydimethylsiloxane on the surface of nanoscale silica and ceria/silica. 2015 , 120, 203-211	16
1097	Multifunctional Engineering Aluminum Surfaces for Self-Propelled Anti-Condensation. 2015 , 17, 961-968	19
1096	Silica-Grafted SnIV Catalysts in Hydrogen-Transfer Reactions. 2015 , 7, 3270-3278	22
1095	Comparative safety evaluation of silica-based particles. 2015 , 30, 355-63	29
1094	Physisorption data for methyl-hybrid silica gels. 2015 , 75, 508-518	5
1093	Silylation from supercritical carbon dioxide: a powerful technique for modification of surfaces. 2015 , 50, 7159-7181	19
1092	Use of activated silica sol as a coagulant aid to remove aluminium from water defluoridated by electrocoagulation. 2015 , 1-10	
1091	High performance shear thickening fluid based on calcinated colloidal silica microspheres. 2015 , 24, 085033	10
1090	Quantification of silane molecules on oxidized silicon: are there options for a traceable and absolute determination?. 2015 , 87, 10117-24	41
1089	Ion-specific adsorption and electroosmosis in charged amorphous porous silica. 2015 , 17, 24683-95	46

(2015-2015)

1088	SBA-15 materials: calcination temperature influence on textural properties and total silanol ratio. 2015 , 21, 659-669	24
1087	A highly stable Pd/SiO2/cordierite monolith catalyst for 2-ethyl-anthraquinone hydrogenation. 2015 , 5, 100968-100977	19
1086	Surface area enhancement by mesoporous silica deposition on microcantilever sensors for small molecule detection. 2015 , 3, 12507-12513	13
1085	Intrinsic surface areas and bond site concentrations of silica aerogels of different densities. 2015 , 106, 100-104	5
1084	Mesoporous Silica Nanoparticles under Sintering Conditions: A Quantitative Study. 2015 , 31, 13011-21	16
1083	Dynamic nuclear polarization in solid samples by electrical-discharge-induced radicals. 2015 , 261, 95-100	8
1082	Adsorption of 2-Chloroethyl Ethyl Sulfide on Silica: Binding Mechanism and Energy of a Bifunctional Hydrogen-Bond Acceptor at the GasBurface Interface. 2015 , 119, 365-372	26
1081	Tribology of Si/SiO2 in humid air: transition from severe chemical wear to wearless behavior at nanoscale. 2015 , 31, 149-56	59
1080	Understanding StBer silica's pore characteristics measured by gas adsorption. 2015 , 31, 824-32	45
1079	Study on the response of InAs nanowire transistors to H2O and NO2. 2015 , 209, 456-461	13
1078	Effect of nano-silica on the corrosion behavior of silicate conversion coatings on hot-dip galvanized steel. 2015 , 66, 459-464	16
1077	Effect of Silica Ratio on the Corrosion Behavior of Nano-silica Potassium Silicate Coatings on Aluminum Alloy 2024. 2015 , 24, 839-847	10
1076	Mechanistic aspects of formation of sintering-resistant palladium nanoparticles over SiO2 prepared using Pd(acac)2 as precursor. 2015 , 504, 179-186	12
1075	Co-catalytic enhancement of H2 production by SiO2 nanoparticles. 2015 , 242, 146-152	13
1074	Influence of temperature and pressure on quartz-water-COIL ontact angle and COEwater interfacial tension. 2015 , 441, 59-64	125
1073	Reaction-dependent heteroatom modification of acidBase catalytic cooperativity in aminosilica materials. 2015 , 504, 429-439	20
1072	Liquid marbles for high-throughput biological screening of anchorage-dependent cells. 2015, 4, 264-70	32
1071	In situ cracking of silica beads in the SEM and TEM Æffect of particle size on structureproperty correlations. 2015 , 270, 337-347	26

1070	Implications of silica on biorefineries Interactions with organic material and mineral elements in grasses. 2015 , 9, 109-121	26
1069	Synthesis and study of new functionalized silica aerogel poly(methyl methacrylate) composites for biomedical use. 2015 , 36, 348-358	18
1068	Release of potassium accompanying the dissolution of rice straw phytolith. 2015 , 119, 371-376	33
1067	Tailoring the properties of sub-3 th silica core-shell particles prepared by a multilayer-by-multilayer process. 2015 , 437, 50-57	9
1066	Kinetic behavior of the reaction between silica and epoxidized liquid rubber. 2016 , 26, 291-296	4
1065	Optimal Surface Amino-Functionalization Following Thermo-Alkaline Treatment of Nanostructured Silica Adsorbents for Enhanced COIAdsorption. 2016 , 9,	11
1064	Conventional glass-ionomer cements. 2016 , 107-136	1
1063	Silica nanoparticles loaded on activated carbon for simultaneous removal of dichloromethane, trichloromethane, and carbon tetrachloride. 2016 , 27, 1719-1729	17
1062	Ga[OSi(O(t)Bu)3]3ITHF, a thermolytic molecular precursor for high surface area gallium-containing silica materials of controlled dispersion and stoichiometry. 2016 , 45, 11025-34	17
1061	Evaluation of thermally pretreated silica stationary phases under hydrophilic interaction chromatography conditions. 2016 , 39, 1611-8	
1060	Solid-state synthesis of a new coreBhell nanocomposite of polyaniline and silica via oxidation of aniline hydrochloride by FeCl3.6H2O. 2016 , 27, 1038-1049	10
1059	Effect of Electrolyte Concentration on the Stern Layer Thickness at a Charged Interface. 2016 , 128, 3854-3858	17
1058	Ethylene polymerization using vanadium catalyst supported on silica modified by pyridinium ionic liquid. 2016 , 65, 1089-1097	7
1057	Adsorption of anionic surfactant (sodium dodecyl sulfate) on silica. 2016 , 62, 223-229	33
1056	Soft electrostatic repulsion in particle monolayers at liquid interfaces: surface pressure and effect of aggregation. 2016 , 374,	22
1055	Quantum-chemical approach to optimization of the synthesis conditions of two-component phosphorus-titanium oxide structures on silica surface. 2016 , 86, 2263-2272	4
1054	Impact of Support Interactions for Single-Atom Molybdenum Catalysts on Amorphous Silica. 2016 , 55, 12350-12357	20
1053	Improved oil recovery in nanopores: NanoIOR. 2016 , 6, 28128	21

1052	XPS study of thermal and electron-induced decomposition of Ni and Co acetylacetonate thin films for metal deposition. 2016 , 34, 041515		10	
1051	Electronic transport properties of graphene channel with metal electrodes or insulating substrates in 10 nm-scale devices. 2016 , 120, 154301		3	
1050	Inherent substrate-dependent growth initiation and selective-area atomic layer deposition of TiO2 using Water-freeImetal-halide/metal alkoxide reactants. 2016 , 34, 01A148		51	
1049	Precursor dependent nucleation and growth of ruthenium films during chemical vapor deposition. 2016 , 34, 041514		9	
1048	Scratch and wear resistance of nano-silica-modified silicate conversion coating on aluminium. 2016 , 32, 1346-1353		2	
1047	Extraction behaviors of uranyl peroxo cage clusters by mesoporous silica SBA-15. 2016 , 310, 453-462		4	
1046	Comparison of surface properties of silica xero- and hydrogels hydrothermally modified using mechanochemical, microwave and classical methods. <i>Colloids and Surfaces A: Physicochemical and Engineering Aspects</i> , 2016 , 504, 139-153	5.1	19	
1045	Adsorption of Substituted Benzene Derivatives on Silica: Effects of Electron Withdrawing and Donating Groups. 2016 , 120, 13024-13031		21	
1044	CoreBhell Nanoplasmonic Sensing for Characterization of Biocorona Formation and Nanoparticle Surface Interactions. 2016 , 1, 798-806		20	
1043	Assessment of biochemical and immunomodulatory activity of sulphated polysaccharides from Ulva intestinalis. 2016 , 91, 269-77		33	
1042	Probing Surface Hydrogen Bonding and Dynamics by Natural Abundance, Multidimensional, 170 DNP-NMR Spectroscopy. 2016 , 120, 11535-11544		59	
1041	Surface Reactions of Mesoporous Bioactive Glasses Monitored by Solid-State NMR: Concentration Effects in Simulated Body Fluid. 2016 , 120, 4961-4974		23	
1040	Laminated altered layers in historical glass: Density variations of silica nanoparticle random packings as explanation for the observed lamellae. 2016 , 442, 1-16		16	
1039	Spectroscopy and Ultrafast Vibrational Dynamics of Strongly Hydrogen Bonded OH Species at the #Al2O3(112 0)/H2O Interface. 2016 , 120, 16153-16161		33	
1038	Nanoporous chalcogenides for adsorption and gas separation. 2016 , 18, 13449-58		10	
1037	Quantitative morphological characterization of bicontinuous Pickering emulsions via interfacial curvatures. 2016 , 12, 4082-92		22	
1036	Remarks on the Interpretation of IR-Absorption Studies Applied to the Surfaces of Silica Nanoparticles. 2016 , 120, 9229-9235			
1035	Pressure and Temperature Dependence of Contact Angles for CO2/Water/Silica Systems Predicted by Molecular Dynamics Simulations. 2016 , 30, 5027-5034		29	

1034	Fully atomistic molecular dynamics simulation of nanosilica-filled crosslinked polybutadiene. 2016 , 653, 90-95	28
1033	Number density distribution of solvent molecules on a substrate: a transform theory for atomic force microscopy. 2016 , 18, 15534-44	12
1032	Electrokinetics of the silica and aqueous electrolyte solution interface: Viscoelectric effects. 2016 , 234, 108-131	26
1031	Thermosensitive silica-pluronic-starch model coating dispersion-part I: The effect of Pluronic block copolymer adsorption on the colloidal stability and rheology. <i>Colloids and Surfaces A:</i> 5.1 <i>Physicochemical and Engineering Aspects</i> , 2016 , 506, 245-253	5
1030	Pervaporative desulfurization of model gasoline using PDMS/BTESE-derived organosilica hybrid membranes. 2016 , 154, 188-196	13
1029	Magnetic polymer-silica composites as bioluminescent sensors for bilirubin detection. 2016 , 183, 422-429	12
1028	Flammability and oxidation kinetics of hydrophobic silica aerogels. 2016 , 320, 350-358	33
1027	. 2016,	O
1026	Elemental areal density calculation and oxygen speciation for flat glass surfaces using x-ray photoelectron spectroscopy. 2016 , 450, 185-193	23
1025	Engineering Intrinsically Zirconium-89 Radiolabeled Self-Destructing Mesoporous Silica Nanostructures for In Vivo Biodistribution and Tumor Targeting Studies. 2016 , 3, 1600122	61
1024	Hydrogen Recombination Rates on Silica from Atomic-Scale Calculations. 2016 , 120, 24137-24147	8
1023	Monolayer Tantalum Oxide on Mesoporous Silica Substrate. 2016 , 1, 3124-3131	4
1022	Syngas production through methane oxy-steam reforming over a Ni/SiO2 nanocatalyst prepared by a modified impregnation method. 2016 , 11, 890-895	2
1021	In-situ infrared spectroscopy as a non-invasive technique to study carbon sequestration at high pressure and high temperature. 2016 , 51, 126-135	3
1020	Mn porphyrins immobilized on non-modified and chloropropyl-functionalized mesoporous silica SBA-15 as catalysts for cyclohexane oxidation. 2016 , 526, 9-20	37
1019	Chromium-based catalysts for ethane dehydrogenation: Effect of SBA-15 support. 2016 , 234, 370-376	39
1018		20
1017	Thermosensitive Silica-Pluronic-Starch model coating dispersion-Part II: The relationship between rheology and microstructure. <i>Colloids and Surfaces A: Physicochemical and Engineering Aspects</i> , 2016 5.1 , 509, 415-426	2

1016	SilicaEpoxy Vitrimer Nanocomposites. 2016 , 49, 5893-5902	117
1015	Understanding Acoustic Cavitation Initiation by Porous Nanoparticles: Toward Nanoscale Agents for Ultrasound Imaging and Therapy. 2016 , 28, 5962-5972	45
1014	Thermoreversible Gels Composed of Colloidal Silica Rods with Short-Range Attractions. 2016 , 32, 8424-35	20
1013	Anchoring and promotion effects of metal oxides on silica supported catalytic gold nanoparticles. 2016 , 482, 135-141	12
1012	Surface Structure and Acidity Properties of Mesoporous Silica SBA-15 Modified with Aluminum and Titanium: First-Principles Calculations. 2016 , 120, 18105-18114	17
1011	Depositing SiO2 on Al2O3: a Route to Tunable Brfisted Acid Catalysts. 2016 , 6, 6156-6164	36
1010	SynthesisBtructureHunction Relationships of Silica-Supported Niobium(V) Catalysts for Alkene Epoxidation with H2O2. 2016 , 6, 6124-6134	60
1009	Unraveling the Mystery of StBer Silica's Microporosity. 2016 , 32, 9180-7	16
1008	Controlled chemical modification of the internal surface of photonic crystal fibers for application as biosensitive elements. 2016 , 60, 283-289	7
1007	Molecular Dynamics Study on Mechanism of Preformed Particle Gel Transporting Through Nanopores: Deformation and Dehydration. 2016 , 120, 19389-19395	8
1006	Enhanced energy harvesting by concentration gradient-driven ion transport in SBA-15 mesoporous silica thin films. 2016 , 16, 3824-3832	54
1005	Opportunities of Immobilized Homogeneous Metathesis Complexes as Prominent Heterogeneous Catalysts. 2016 , 8, 3010-3030	36
1004	Effects of Aspect Ratio on Water Immersion into Deep Silica Nanoholes. 2016 , 32, 8759-66	
1003	Vapor-enhanced covalently bound ultra-thin films on oxidized surfaces for enhanced resolution imaging. 2016 , 4, 8634-8647	9
1002	Hydration in silica based mesoporous materials: a DFT model. 2016 , 18, 32962-32972	37
1001	W(h)ither dielectrics?. 2016 ,	3
1000	Can Point Defects in Surfaces in Solution be Atomically Resolved by Atomic Force Microscopy?. 2016 , 117, 226101	15
999	H Formation on Cosmic Grain Siliceous Surfaces Grafted with Fe : A Silsesquioxanes-Based Computational Model. 2016 , 17, 3390-3394	4

998	Thermal Behavior of d-Ribose Adsorbed on Silica: Effect of Inorganic Salt Coadsorption and Significance for Prebiotic Chemistry. 2016 , 22, 15834-15846	11
997	Size-dependent interactions of silica nanoparticles with a flat silica surface. 2016 , 483, 177-184	18
996	Hollow Nanospheres with Fluorous Interiors for Transport of Molecular Oxygen in Water. 2016 , 1, 3306-3309	
995	Adsorption of III/V ions (In(III), Ga(III) and As(V)) onto SiO2, CeO2 and Al2O3 nanoparticles used in the semiconductor industry. 2016 , 3, 1014-1026	11
994	Hydrogen cleavage by solid-phase frustrated Lewis pairs. 2016 , 52, 10478-81	33
993	Cation Dependent Carbonate Speciation and the Effect of Water. 2016 , 120, 17570-17578	6
992	The secret life of Pickering emulsions: particle exchange revealed using two colours of particle. 2016 , 6, 31401	45
991	Approachable Way to Synthesize 3D Silica Hollow Nanospheres with Mesoporous Shells via Simple Template-Assisted Technique. 2016 , 1, 5961-5966	1
990	New Insights into Formation of Molecular Sieve SAPO-34 for MTO Reactions. 2016 , 120, 25945-25957	11
989	Response to Extreme Temperatures of Mesoporous Silica MCM-41: Porous Structure Transformation Simulation and Modification of Gas Adsorption Properties. 2016 , 32, 11422-11431	11
988	Modified macromolecules in the prevention of silica scale. 2016 , 88, 1037-1047	10
987	Quantum-chemical analysis and experimental synthesis of titanium-vanadium-containing coatings on the silica surface from a mixture of TiCl4 and VOCl3 vapors. 2016 , 86, 2113-2123	5
986	Effect of Synthesis on Quality, Electronic Properties and Environmental Stability of Individual Monolayer Ti3C2 MXene Flakes. 2016 , 2, 1600255	649
985	Silica and Titania Nanodispersions. 2016 , 159-210	
984	Transmission and fluorescence X-ray absorption spectroscopy cell/flow reactor for powder samples under vacuum or in reactive atmospheres. 2016 , 87, 073108	20
983	Effect of Electrolyte Concentration on the Stern Layer Thickness at a Charged Interface. 2016 , 55, 3790-4	192
982	Early entombment within silica minimizes the molecular degradation of microorganisms during advanced diagenesis. 2016 , 437, 98-108	61
981	The effect of support pretreatment on activity of Ag/SiO 2 catalysts in low-temperature CO oxidation. 2016 , 278, 150-156	32

(2016-2016)

980	Atomic-level organization of vicinal acid-base pairs through the chemisorption of aniline and derivatives onto mesoporous SBA15. 2016 , 7, 6099-6105		12
979	Effect of pretreatment temperature on the surface modification of diatomite with trimethylchlorosilane. 2016 , 23, 1439-1449		12
978	High efficiency reductive degradation of a wide range of azo dyes by SiO 2 -Co core-shell nanoparticles. 2016 , 199, 504-513		67
977	Preliminary kinetic data of silicic acid species prior to the formation of exoskeletal structures. 2016 , 181, 18-24		2
976	Effects of Salinity-Induced Chemical Reactions on Biotite Wettability Changes under Geologic CO2 Sequestration Conditions. 2016 , 3, 92-97		18
975	Sum Frequency Generation Spectroscopy and Molecular Dynamics Simulations Reveal a Rotationally Fluid Adsorption State of Pinene on Silica. 2016 , 120, 12578-12589		18
974	A temperature-controlled method to produce Janus nanoparticles using high internal interface systems: Experimental and theoretical approaches. <i>Colloids and Surfaces A: Physicochemical and Engineering Aspects</i> , 2016 , 506, 56-62	5.1	53
973	Development of superhydrophobicity in fluorosilane-treated diatomaceous earth polymer coatings. 2016 , 386, 178-186		29
972	Detecting Opal-CT Formation Resulting From Thermal Recovery Methods in Diatomites. 2016,		О
971	Plasma-Enhanced Chemical Vapor Deposition (PE-CVD) yields better Hydrolytical Stability of Biocompatible SiOx Thin Films on Implant Alumina Ceramics compared to Rapid Thermal Evaporation Physical Vapor Deposition (PVD). 2016 , 8, 17805-16		28
970	Elucidation of Anchoring and Restructuring Steps during Synthesis of Silica-Supported Vanadium Oxide Catalysts. 2016 , 28, 5495-5504		31
969	Interactions between silica nanoparticles and phospholipid membranes. 2016 , 1858, 2163-2170		36
968	Compatibilization of silica-filled natural rubber compounds by combined effects of functionalized low molecular weight rubber and silane. 2016 , 48, 145-163		9
96 7	Removal of anionic dye using amine-functionalized mesoporous hollow shells prepared from corn cob silica. 2016 , 42, 5937-5950		7
966	Gamma irradiation effect on bioactive glasses synthesized with polyethylene-glycol template. 2016 , 42, 1990-1997		5
965	Multi-responsive hybrid Janus nanoparticles: Surface functionalization through solvent physisorption. 2016 , 75, 363-370		8
964	CO2 hydrogenation on Pt, Pt/SiO2 and Pt/TiO2: Importance of synergy between Pt and oxide support. 2016 , 343, 115-126		174
963	Siloxane D4 adsorption by mesoporous aluminosilicates. 2016 , 289, 356-364		31

962	Evolution of Crystal Structure During the Initial Stages of ZnO Atomic Layer Deposition. 2016 , 28, 592-600	23
961	Molecular dynamics study on mechanism of preformed particle gel transporting through nanopores: surface hydration. 2016 , 6, 7172-7180	9
960	Materials Fundamentals of Drug Controlled Release. 2016 , 17-55	
959	Molecular dynamics simulations of oil transport through inorganic nanopores in shale. 2016 , 171, 74-86	186
958	Synthesis and characterization of bifunctional surfaces with tunable functional group pairs. 2016 , 648, 284-290	5
957	Poly(methyl methacrylate) nanotubes in AAO templates: Designing nanotube thickness and characterizing the T-confinement effect by DSC. 2016 , 82, 327-336	25
956	Immobilized Grubbs catalysts on mesoporous silica materials: insight into support characteristics and their impact on catalytic activity and product selectivity. 2016 , 6, 2580-2597	19
955	Exploring Pd adsorption, diffusion, permeation, and nucleation on bilayer SiO2/Ru as a function of hydroxylation and precursor environment: From UHV to catalyst preparation. 2016 , 652, 286-293	7
954	Magnetic silica hybrids modified with guanidine containing co-polymers for drug delivery applications. 2016 , 64, 20-28	15
953	Charge-tunable insertion process of carbon nanotubes into DNA nanotubes. 2016 , 66, 20-5	11
952	Thermal transformation of bioactive caffeic acid on fumed silica seen by UV-Vis spectroscopy, thermogravimetric analysis, temperature programmed desorption mass spectrometry and quantum chemical methods. 2016 , 470, 132-141	18
951	High azobenzene functionalization enhances stability of the cis isomer: Periodic mesoporous organosilica network on the way to new light triggered applicable materials. 2016 , 228, 30-36	7
950	Influence of the Silica Support on the Structure and the Morphology of Silver Nanoparticles: A Molecular Simulation Study. 2016 , 120, 8323-8332	12
949	Surfactant adsorption to soil components and soils. 2016 , 231, 59-102	60
948	Stable Aqueous Dispersions of Hydrophobically Modified Titanium Dioxide Pigments through Polyanion Adsorption: Synthesis, Characterization, and Application in Coatings. 2016 , 32, 1929-38	8
947	Amorphous SiO2 surface models: energetics of the dehydroxylation process, strain, ab initio atomistic thermodynamics and IR spectroscopic signatures. 2016 , 18, 7475-82	93
946	Surficial Siloxane-to-Silanol Interconversion during Room-Temperature Hydration/Dehydration of Amorphous Silica Films Observed by ATR-IR and TIR-Raman Spectroscopy. 2016 , 32, 1568-76	69
945	Isolation of a wide range of minerals from a thermally treated plant: Equisetum arvense, a Mare's tale. 2016 , 21, 101-12	10

944	Unraveling the Dynamics of Aminopolymer/Silica Composites. 2016 , 32, 2617-25		9
943	Deuterium MAS NMR and Local Molecular Dynamic Model to Study Adsorption Desorption Kinetics of a Dipeptide at the Inner Surfaces of SBA-15. 2016 , 120, 2797-2806		11
942	Assessing the Potential for Drug-Nanoparticle Surface Interactions To Improve Drug Penetration into the Skin. 2016 , 13, 1375-84		5
941	Bioactive glass-gelatin hybrids: building scaffolds with enhanced calcium incorporation and controlled porosity for bone regeneration. 2016 , 4, 2486-2497		25
940	Catalysis of HMX Decomposition and Combustion. 2016 , 193-230		9
939	NbOx/SiO2 in the gas-phase Beckmann rearrangement of cyclohexanone oxime to Eaprolactam: Influence of calcination temperature, niobia loading and silylation post-treatment. 2016 , 185, 272-280		9
938	Selective Plasma Oxidation of Ultrasmall Si Nanowires. 2016 , 120, 472-477		4
937	Simulations of inorganic-bioorganic interfaces to discover new materials: insights, comparisons to experiment, challenges, and opportunities. 2016 , 45, 412-48		143
936	Using Hydrogen To Expand the Inherent Substrate Selectivity Window During Tungsten Atomic Layer Deposition. 2016 , 28, 117-126		54
935	Influence of Protein Surface Coverage on Anomalously Strong Adsorption Sites. 2016 , 8, 511-20		14
934	Electron stimulated hydroxylation of a metal supported silicate film. 2016 , 18, 3755-64		32
933	Combined influence of pore size distribution and surface hydrophilicity on the water adsorption characteristics of micro- and mesoporous silica. 2016 , 226, 221-228		39
932	Surface Organometallic and Coordination Chemistry toward Single-Site Heterogeneous Catalysts: Strategies, Methods, Structures, and Activities. 2016 , 116, 323-421		485
932			485
	Strategies, Methods, Structures, and Activities. 2016 , 116, 323-421 Water Incorporation in Graphene Transferred onto SiO2/Si Investigated by Isotopic Labeling. 2016 ,		
931	Strategies, Methods, Structures, and Activities. 2016 , 116, 323-421 Water Incorporation in Graphene Transferred onto SiO2/Si Investigated by Isotopic Labeling. 2016 , 120, 201-206 Assessing the use of nanoimmobilized laccases to remove micropollutants from wastewater. 2016 ,		9
931	Strategies, Methods, Structures, and Activities. 2016, 116, 323-421 Water Incorporation in Graphene Transferred onto SiO2/Si Investigated by Isotopic Labeling. 2016, 120, 201-206 Assessing the use of nanoimmobilized laccases to remove micropollutants from wastewater. 2016, 23, 3217-28 Receding and advancing (CO 2 + brine + quartz) contact angles as a function of pressure,	5.1	9

926	Calcium silicate hydrate (C-S-H) gel solubility data and a discrete solid phase model at 25 LC based on two binary non-ideal solid solutions. 2016 , 79, 1-30	52
925	Monolayers of charged particles in a Langmuir trough: Could particle aggregation increase the surface pressure?. 2016 , 462, 223-34	29
924	Adhesion between highly stretchable materials. 2016 , 12, 1093-9	73
923	Processing and characterization of diatom nanoparticles and microparticles as potential source of silicon for bone tissue engineering. 2016 , 59, 471-479	32
922	Silica nanoparticles (SiO 2): Influence of relative humidity in stone consolidation. 2016 , 18, 258-270	33
921	Systematic investigation of the pore structure and surface properties of SBA-15 by water vapor physisorption. 2016 , 220, 183-187	17
920	Wettability alteration of oil-wet carbonate by silica nanofluid. 2016 , 461, 435-442	247
919	Oil absorbency of diatomite-embedded polypropylene meltblown composite structures. 2017 , 46, 1552-1578	1
918	Experimental and analytical investigation of water diffusion process in nano-carbon/alumina/silica filled epoxy nanocomposites. 2017 , 13, 607-615	21
917	Temperature Stability and Photocatalytic Activity of Nanocrystalline Cristobalite Powders with Cu Dopant. 2017 , 9, 943-948	14
916	Effect of Cu and Zr Co-doped SiO2 Nanoparticles on the Stability of Phases (Quartz-Tridymite-Cristobalite) and Degradation of Methyl Orange at High Temperature. 2017 , 9, 293-299	7
915	Global optimisation of hydroxylated silica clusters: A cascade Monte Carlo Basin Hopping approach. 2017 , 1102, 38-43	10
914	Waste-free synthesis of silica nanospheres and silica nanocoatings from recycled ethanol∃mmonium solution. 2017 , 71, 841-848	6
913	General Aspects Regarding the HPLC Analytical Column. 2017 , 231-277	
912	Enhancement of water barrier properties and tribological performance of hybrid glass fiber/epoxy composites with inclusions of carbon and silica nanoparticles. 2017 , 28, 1115-1124	19
911	Aggregation state and magnetic properties of magnetite nanoparticles controlled by an optimized silica coating. 2017 , 121, 044304	18
910	A novel hydrothermal releasing synthesis of modified SiO2 material and its application in phenol removal process. 2017 , 34, 723-733	2
909	Ion beam-induced hydroxylation controls molybdenum disulfide growth. 2017 , 4, 021017	6

(2017-2017)

908	Nanoparticle decoration with surfactants: Molecular interactions, assembly, and applications. 2017 , 72, 1-58	313
907	Transition Metal Induced Crystallization of Ultrathin Silica Films. 2017 , 29, 931-934	7
906	Progress in Nanotheranostics Based on Mesoporous Silica Nanomaterial Platforms. 2017 , 9, 10309-10337	84
905	Insights on Interfacial Structure, Dynamics, and Proton Transfer from Ultrafast Vibrational Sum Frequency Generation Spectroscopy of the Alumina(0001)/Water Interface. 2017 , 121, 5168-5177	45
904	Synthesis and dissolution behaviour of CaO/SrO-containing solgel-derived 58S glasses. 2017 , 52, 8858-8870	10
903	Bifunctional Succinylated Polylysine-Coated Mesoporous Silica Nanoparticles for pH-Responsive and Intracellular Drug Delivery Targeting the Colon. 2017 , 9, 9470-9483	57
902	Freezing and Melting of Silver Nanoparticles on Silica Substrate Using a Simple Interatomic Potential for AgBiO2 Interaction on the Basis of ab Initio Calculations and Experimental Data. 2017 , 121, 3615-3622	10
901	Structure and Function of Adsorbed Hemoglobin on Silica Nanoparticles: Relationship between the Adsorption Process and the Oxygen Binding Properties. 2017 , 33, 3241-3252	22
900	Surface chemistry of group 11 atomic layer deposition precursors on silica using solid-state nuclear magnetic resonance spectroscopy. 2017 , 146, 052812	11
899	Synthesis of advanced phosphatic geopolymers utilizing fly ash by way of greener route. 2017 , 6, 168-177	9
898	Growth-Induced Strain in Chemical Vapor Deposited Monolayer MoS2: Experimental and Theoretical Investigation. 2017 , 4, 1700031	35
897	Octadecyl-modified silicas obtained by non-hydrolytic condensation of a C18-hybrid silica sol on a silica surface. 2017 , 466-467, 8-14	4
896	Adsorption energy as a metric for wettability at the nanoscale. 2017 , 7, 46317	10
895	Thermal desorption-Gas chromatographic methodology for the determination of residual solvents in mesoporous silica. 2017 , 1500, 160-166	6
894	Characteristics of nanoporous silica aerogel under high temperature from 950 LC to 1200 LC. 2017 , 129, 82-90	49
893	Designing polyethylene characteristics by modification of the support for FI catalyst. 2017 , 434, 1-6	7
892	Study of the physicochemical interactions between Thermomyces lanuginosus lipase and silica-based supports and their correlation with the biochemical activity of the biocatalysts. 2017 , 79, 525-532	5
891	Polarization-Dependent Electronic Transport in Graphene/Pb(Zr,Ti)O3 Ferroelectric Field-Effect Transistors. 2017 , 3, 1700020	45

890	Effect of seawater ionic composition modified by nanofiltration on enhanced oil recovery in Berea sandstone. 2017 , 203, 222-232	19
889	Characterization and dissolution properties of phytolith occluded phosphorus in rice straw. 2017 , 171, 19-24	32
888	Pleiotropic Role of Recombinant Silaffin-Like Cationic Polypeptide P5S3: Peptide-Induced Silicic Acid Stabilization, Silica Formation and Inhibition of Silica Dissolution. 2017 , 2, 6-17	6
887	Spectral green cathodoluminescence emission from surfaces of insulators with metal-hydroxyl bonds. 2017 , 190, 128-135	16
886	High-resolution 29Si CP/MAS solid state NMR spectroscopy and DFT investigation on the role of geminal and single silanols in grafting chromium species over Phillips Cr/silica catalyst. 2017 , 543, 26-33	9
885	On the Thermodynamics and Experimental Control of Twinning in Metal Nanocrystals. 2017 , 129, 8773-8777	6
884	Electroosmotic flow and ionic conductance in a pH-regulated rectangular nanochannel. 2017, 29, 062002	14
883	Modeling hydroxylated nanosilica: Testing the performance of ReaxFF and FFSiOH force fields. 2017 , 146, 224704	9
882	Naturally organic functionalized 3D biosilica from diatom microalgae. 2017 , 132, 22-29	34
881	Circularly Polarized Luminescence of Silica-Grafted Europium Chiral Derivatives Prepared through a Sequential Functionalization. 2017 , 56, 7010-7018	22
880	Enhancing internalization of silica particles in myocardial cells through surface modification. 2017 , 79, 831-840	8
879	Unexpected gas sensing properties of SiO2/SnO2 coreBhell nanofibers under dry and humid conditions. 2017 , 5, 6369-6376	23
878	The bouncing threshold in silica nanograin collisions. 2017 , 19, 16555-16562	15
877	On the Thermodynamics and Experimental Control of Twinning in Metal Nanocrystals. 2017 , 56, 8647-8651	14
876	Continuous thermal control of hydrophilicity/hydrophobicity changes of hybrid films and of their directionality: Kinetics and substrate effects. 2017 , 505, 692-702	2
875	Thermal Transport in Supported Graphene: Substrate Effects on Collective Excitations. 2017, 7,	8
874	Surface structures of sodium borosilicate glasses from molecular dynamics simulations. 2017 , 100, 2516-2524	18
873	The elusive silica/water interface: isolated silanols under water as revealed by vibrational sum frequency spectroscopy. 2017 , 19, 10343-10349	72

872	Epoxy-matrix composites filled with surface-modified SiO2 nanoparticles. 2017 , 127, 399-408	15
871	Sculptured anti-reflection coatings for high power lasers. 2017 , 7, 1249	30
870	Kinetics of Valeric Acid Ketonization and Ketenization in Catalytic Pyrolysis on Nanosized SiO , EAl O , CeO /SiO , Al O /SiO and TiO /SiO. 2017 , 18, 1943-1955	19
869	Surface Structure and Stability of Partially Hydroxylated Silica Surfaces. 2017 , 33, 3882-3891	29
868	Hybrid nanocomposites made of diol-modified silanes and nanostructured calcium hydroxide. Applications to Alum-treated wood. 2017 , 89, 29-39	10
867	A Generalized Method for the Synthesis of Ligand-Free M@SiO (M = Ag, Au, Pd, Pt) Yolk-Shell Nanoparticles. 2017 , 33, 3281-3286	20
866	Copolymerization of ethylene with norbornene or 1-octene using supported ionic liquid systems. 2017 , 74, 2799-2817	5
865	A molecular dynamics study of the interaction of water with the external surface of silicalite-1. 2017 , 19, 2950-2960	21
864	Investigating the Interaction of Water Vapour with Aminopropyl Groups on the Surface of Mesoporous Silica Nanoparticles. 2017 , 18, 839-849	18
863	Understanding inherent substrate selectivity during atomic layer deposition: Effect of surface preparation, hydroxyl density, and metal oxide composition on nucleation mechanisms during tungsten ALD. 2017 , 146, 052811	39
862	Strain effect and dual initiation pathway in CrIII/SiO2 polymerization catalysts from amorphous periodic models. 2017 , 346, 50-56	38
861	Molecular layer deposition using cyclic azasilanes, maleic anhydride, trimethylaluminum, and water. 2017 , 35, 01B136	7
860	Single-site zinc on silica catalysts for propylene hydrogenation and propane dehydrogenation: Synthesis and reactivity evaluation using an integrated atomic layer deposition-catalysis instrument. 2017 , 345, 170-182	55
859	THz dynamics of nanoconfined water by ultrafast optical spectroscopy. 2017 , 28, 014009	4
858	Dehydroxylation and diagenetic variations in diatom oxygen isotope values. 2017 , 199, 185-195	12
857	Reaction Engineering of Polyolefins: The Role of Catalyst Supports in Ethylene Polymerization on Metallocene Catalysts. 2017 , 19-63	2
856	Photocatalytic Water Splitting: Quantitative Approaches toward Photocatalyst by Design. 2017 , 7, 8006-8022	424
855	Alcohols react with MCM-41 at room temperature and chemically modify mesoporous silica. 2017 , 7, 9960	20

854	Poisoning of Hydrogen Recombination on Silica Due to Water Adsorption. 2017, 121, 16366-16372	2
853	A water window on surface chemistry. 2017 , 357, 755-756	1
852	Shear Thickening Electrolytes for High Impact Resistant Batteries. 2017 , 2, 2084-2088	23
851	Direct Relationship Between Interfacial Microstructure and Confined Crystallization in Poly(Ethylene Oxide)/Silica Composites: The Study of Polymer Molecular Weight Effects. 2017 , 55, 1608-1616	11
850	SiO Fibers by Centrifugal Spinning with Excellent Textural Properties and Water Adsorption Performance. 2017 , 2, 5052-5059	15
849	Measuring Competing Equilibria at a Silica Surface through the Contact Angle of a Nonpolar Liquid. 2017 , 33, 9632-9636	1
848	Investigating Alkylsilane Monolayer Tribology at a Single-Asperity Contact with Molecular Dynamics Simulation. 2017 , 33, 11270-11280	16
847	Target-or-Clear Zirconium-89 Labeled Silica Nanoparticles for Enhanced Cancer-Directed Uptake in Melanoma: A Comparison of Radiolabeling Strategies. 2017 , 29, 8269-8281	44
846	Influence of operating conditions and immobilization on activity of alcohol dehydrogenase for the conversion of formaldehyde to methanol. 2017 , 41, 11391-11397	13
845	Beyond Ordered Materials: Understanding Catalytic Sites on Amorphous Solids. 2017 , 7, 7543-7557	84
844	Oil shale powders and their interactions with ciprofloxacin, ofloxacin, and oxytetracycline antibiotics. 2017 , 24, 25977-25985	7
843	Characteristics of polymorphic foam for inhibiting spontaneous coal combustion. 2017 , 206, 334-341	32
842	Role of Surface Chemistry in Grain Adhesion and Dissipation during Collisions of Silica Nanograins. 2017 , 844, 105	6
841	Correlation of silane grafting density with rheological properties of silica filled rubber: Coupling of flow and temperature. 2017 , 94, 299-310	6
840	The silanol content and in vitro cytolytic activity of flame-made silica. 2017, 507, 95-106	19
839	Determination of the Solid Electrolyte Interphase Structure Grown on a Silicon Electrode Using a Fluoroethylene Carbonate Additive. 2017 , 7, 6326	117
838	Quasi-metallic behavior of ZnO grown by atomic layer deposition: The role of hydrogen. 2017 , 122, 025306	14
837	The imprint of thermally induced devolatilization phenomena on radon signal: implications for the geochemical survey in volcanic areas. 2017 , 211, 558-571	6

(2017-2017)

836	catalysts. 2017 , 353, 315-324	29
835	Drying and moisture resorption behaviour of various electrode materials and separators for lithium-ion batteries. 2017 , 364, 84-91	33
834	The effect of amorphous silica on pulp rheology and copper flotation. 2017, 113, 41-46	16
833	Effect of supplementation different hydrophobic silicas on the stability of foams. 2017 , 8, 727-733	
832	Friction and Tribochemical Wear Behaviors of Native Oxide Layer on Silicon at Nanoscale. 2017, 65, 1	23
831	Effects of dope sonication and hydrophilic polymer addition on the properties of low pressure PVDF mixed matrix membranes. 2017 , 540, 200-211	17
830	Bare and Effective Charge of Mesoporous Silica Particles. 2017 , 33, 7343-7351	7
829	Synthesis, thermal behavior and physicochemical characterization of ZrO2/PEG inorganic/organic hybrid materials via solgel technique. 2017 , 130, 535-540	21
828	Effect of Defect Site Preorganization on Fe(III) Grafting and Stability: A Comparative Study of Delaminated Zeolite vs Amorphous Silica Supports. 2017 , 29, 6480-6492	14
827	Zwitterionic surfactant assisted synthesis of Fe doped SnO2-SiO2 nanocomposite with enhanced photocatalytic activity under sun light. 2017 , 223, 167-177	22
826	Surface Organometallic Chemistry: Paving the Way Beyond Well-Defined Supported Organometallics and Single-Site Catalysis. 2017 , 147, 2247-2259	26
825	Insights into Silica Bilayer Hydroxylation and Dissolution. 2017 , 60, 471-480	15
824	Characterization of Supported Platinum Nanocrystallites with Different Sizes and These Effects on a Model Reaction. 2017 , 60, 773-781	
823	Controlling the Surface Hydroxyl Concentration by Thermal Treatment of Layered Double Hydroxides. 2017 , 56, 7842-7850	15
822	Local Structures and Heterogeneity of Silica-Supported M(III) Sites Evidenced by EPR, IR, NMR, and Luminescence Spectroscopies. 2017 , 139, 8855-8867	46
821	Preparation of transparent monolithic methylsilsesquioxane (MSQ) aerogels via ambient pressure drying. 2017 , 7, 32861-32865	2
820	Synthesis of silica Janus nanoparticles by buoyancy effect-induced desymmetrization process and their placement at the PS/PMMA interface. 2017 , 295, 25-36	30
819	Adsorption study of a macro-RAFT agent onto SiO 2 -coated Gd 2 O 3 :Eu 3+ nanorods: Requirements and limitations. 2017 , 394, 519-527	9

818	Cobalt and cobalt-iron spinel oxides as bulk and silica supported catalysts in the ethanol combustion reaction. 2017 , 426, 97-106	10
817	Thermodynamic models of the adsorption and desorption of molecular oxygen at the UV and blue emitting centers in mesoporous silica under variable oxygen pressure. 2017 , 239, 371-380	1
816	Defining the characteristics of spherical Janus particles by investigating the behavior of their corresponding particles at the oil/water interface in a Pickering emulsion. 2017 , 38, 985-991	16
815	A method for defect repair of MFI-type zeolite membranes by multivalent ion infiltration. 2017 , 237, 140-150	15
814	Absorption capacity, kinetics and mechanical behaviour in dry and wet states of hydrophobic DEDMS/TEOS-based silica aerogels. 2017 , 81, 600-610	4
813	A novel 2-step ALD route to ultra-thin MoS films on SiO through a surface organometallic intermediate. 2017 , 9, 538-546	43
812	Adsorption and Dimerization of Late Transition Metal Atoms on the Regular and Defective Quartz (001) Surface. 2017 , 60, 459-470	10
811	Burstable nanostructured micro-raspberries: Towards redispersible nanoparticles from dry powders. 2017 , 490, 401-409	13
810	A review of Fischer Tropsch synthesis process, mechanism, surface chemistry and catalyst formulation. 2017 , 2, 11-31	77
809	Geometry effect on electrokinetic flow and ionic conductance in pH-regulated nanochannels. 2017 , 29, 122006	9
808	. 2017 , 24, 3073-3082	15
807	Adsorption properties of Silochrom chemically modified with nickel acetylacetonate. 2017,	
806	Preparation of Silica Membranes by Atomic Layer Deposition. 2017 , 45-62	3
805	Nanoparticle Incorporation into Desalination and Water Treatment Membranes P otential Advantages and Challenges. 2017 , 261-303	
804	Introduction to Chemically Modified Nanochannels and Nanopores. 2017, 1-25	7
803	Pore-scale modelling of complex conductivity of saturated granular materials. 2017 , 15, 593-602	5
802	The hydrophilic-to-hydrophobic transition in glassy silica is driven by the atomic topology of its surface. 2018 , 148, 074503	26
801	Biogenic porous silica and silicon sourced from Mexican Giant Horsetail (Equisetum myriochaetum) and their application as supports for enzyme immobilization. 2018 , 166, 195-202	20

800	Surface chemical heterogeneity modulates silica surface hydration. 2018, 115, 2890-2895	57
799	What makes lithium substituted polyacrylic acid a better binder than polyacrylic acid for silicon-graphite composite anodes?. 2018 , 384, 136-144	46
798	Simulation of Gas- and Liquid-Phase Layer-By-Layer Deposition of Metal Oxides by Coarse-Grained Modeling. 2018 , 122, 6713-6720	5
797	Evaluating Water Reactivity at Silica Surfaces Using Reactive Potentials. 2018 , 122, 9875-9885	23
796	Si Oxidation and H2 Gassing During Aqueous Slurry Preparation for Li-Ion Battery Anodes. 2018 , 122, 9746-9754	19
795	Identification of Vicinal Silanols and Promotion of Their Formation on MCM-41 via Ultrasonic Assisted One-Step Room-Temperature Synthesis for Beckmann Rearrangement. 2018 , 57, 5550-5557	12
794	High-Magnification SEM Micrograph of Siloxanes. 2018 , 10, 2627-2633	1
793	Structure and Dynamics of Solvated Polymers near a Silica Surface: On the Different Roles Played by Solvent. 2018 , 122, 4573-4582	6
792	Flocculation efficiency of the Sinorhizobium meliloti 1021 exopolysaccharide relative to mineral oxide suspensions [A preliminary study for wastewater treatment. 2018 , 201, 51-59	5
791	Phytolith-associated potassium in fern: characterization, dissolution properties and implications for slash-and-burn agriculture. 2018 , 34, 28-36	13
790	Phosphate ester cleavage by a positively charged porous silica adorned with lanthanum (III). 2018 , 268, 144-152	8
789	Slow crack growth in a cordierite-based glassDeramic missile radome due to stress corrosion. 2018 , 93, 76-86	2
788	Amine-Functionalized Mesoporous Silica Nanoparticles: A New Nanoantibiotic for Bone Infection Treatment. 2018 , 4, 1-12	29
787	One-step preparation of GO/SiO2 membrane for highly efficient separation of oil-in-water emulsion. 2018 , 553, 131-138	52
786	Capillary Condensation of Binary and Ternary Mixtures of n-Pentane-Isopentane-CO in Nanopores: An Experimental Study on the Effects of Composition and Equilibrium. 2018 , 34, 1967-1980	22
7 ⁸ 5	Phase Formation and Evolution in Mg(OH)2deolite Cements. 2018 , 57, 2105-2113	8
7 ⁸ 4	Direct measurement of aerosol glass fiber alignment in a DC electric field. 2018 , 52, 123-135	1
783	Quantification of Zeta-Potential and Electrokinetic Surface Charge Density for Colloidal Silica Nanoparticles Dependent on Type and Concentration of the Counterion: Probing the Outer Helmholtz Plane. 2018 , 122, 4437-4453	34

782	Study of adsorptive materials obtained by wet fine milling and acid activation of vermiculite. 2018 , 155, 37-49	18
781	Whispering gallery mode coulometry of the nanoparticle-microcavity interaction in aqueous solution. 2018 , 112, 051109	5
780	Joint inversion of NMR and SIP data to estimate pore size distribution of geomaterials. 2018, 212, 1791-1805	8
779	The Role of Catalyst Support, Diluent and Co-Catalyst in Chromium-Mediated Heterogeneous Ethylene Trimerisation. 2018 , 61, 213-224	6
778	Interaction of NaOH solutions with silica surfaces. 2018 , 516, 128-137	22
777	Evaluation of VIPs after mild artificial aging during 10 years: Focus on the core behavior. 2018 , 162, 198-207	16
776	Modeling of a Hybrid Langmuir Adsorption Isotherm for Describing Interactions Between Drug Molecules and Silica Surfaces. 2018 , 107, 1392-1397	8
775	Multi-modal stabilisation of emulsions using a combination of hydrophilic particles and an amino acid. <i>Colloids and Surfaces A: Physicochemical and Engineering Aspects</i> , 2018 , 538, 765-773	3
774	On the Relation between the Interfacial Charge of a Discharging Nozzle and Electrification of a Liquid Microjet. 2018 , 47, 16-19	4
773	Modelling the surface of amorphous dehydroxylated silica: the influence of the potential on the nature and density of defects. 2018 , 42, 1356-1367	9
772	Controlled deposition of titanium oxide overcoats by non-hydrolytic sol gel for improved catalyst selectivity and stability. 2018 , 358, 50-61	21
771	Photo-Initiated Reduction of CO by H on Silica Surface. 2018 , 11, 1163-1168	2
770	Mesoporous silica nanoparticles decorated with polycationic dendrimers for infection treatment. 2018 , 68, 261-271	65
7 69	3D Printed Optical Quality Silica and Silicallitania Glasses from Solliel Feedstocks. 2018 , 3, 1700323	45
768	Die Vielfalt des Siliciumdioxids. 2018 , 52, 84-93	2
767	The Multifaceted Role of Methylaluminoxane in Metallocene-Based Olefin Polymerization Catalysis. 2018 , 51, 343-355	53
766	Low temperature bonding of heterogeneous materials using Al2O3 as an intermediate layer. 2018 , 36, 011202	11
765	Thinking outside the box: placing hydrophilic particles in an oil phase for the formation and stabilization of Pickering emulsions. 2018 , 9, 4821-4829	15

(2018-2018)

764	Investigation of thermoplastic powder synergizing polymorphic foam to inhibit coal oxidation at low temperature. 2018 , 226, 490-497	9
763	Predicting the DNP-SENS efficiency in reactive heterogeneous catalysts from hydrophilicity. 2018 , 9, 4866-4872	17
762	The delivery of water by impacts from planetary accretion to present. 2018 , 4, eaar2632	23
761	Pore structure development of silica particles below the isoelectric point. 2018 , 267, 257-264	7
760	Fluorescence imaging of antibiotic clofazimine encapsulated within mesoporous silica particle carriers: relevance to drug delivery and the effect on its release kinetics. 2018 , 20, 11899-11911	10
759	Highly Oriented Liquid Crystalline Epoxy Film: Robust High Thermal-Conductive Ability. 2018 , 3, 3562-3570	23
758	Silicone-urea copolymer as a basis for self-organized multiphase nanomaterials. 2018, 143, 200-211	7
757	Rapid detection of HSO in water: Novel immobilized azo-azomethine colorimetric anion receptors on solid supports. 2018 , 199, 21-31	3
756	Recognition mechanism of aromatic derivatives resolved by argentation chromatography: The driving role played by substituent groups. 2018 , 1019, 135-141	3
755	Calculation of surface potentials at the silical water interface using molecular dynamics: Challenges and opportunities. 2018 , 57, 04FM02	11
754	Photoexcitation effect on the adsorption of hazardous gases on silica surface. 2018 , 341, 93-101	23
753	Wettability of nanofluid-modified oil-wet calcite at reservoir conditions. 2018 , 211, 405-414	77
75 ²	Hydrothermal Sintering for Densification of Silica. Evidence for the Role of Water. 2018 , 38, 1860-1870	33
751	Effect of heat treatment on the surface chemical structure of glass: Oxygen speciation from in situ XPS analysis. 2018 , 101, 644-656	19
75°	Low-temperature CO oxidation over Ag/SiO2 catalysts: Effect of OH/Ag ratio. 2018, 221, 598-609	60
749	Surface modification and characterization of basalt fibers as potential reinforcement of concretes. 2018 , 427, 1248-1256	39
748	Interfacial Water Drives Improved Proton Transport in Siliceous Nanocomposite Nafion Thin Films. 2018 , 19, 538-546	2
747	Thin (single E riple) niobium oxide layers on mesoporous silica substrate. 2018 , 262, 191-198	7

746	Investigation of factors affecting condensation on soiled PV modules. 2018 , 159, 488-500	61
745	Dynamic catalytic adsorptive desulfurization of real diesel over ultra-stable and low-cost silica gel-supported TiO2. 2018 , 64, 2146-2159	33
744	Acidity enhanced [Al]MCM-41 via ultrasonic irradiation for the Beckmann rearrangement of cyclohexanone oxime to e-caprolactam. 2018 , 358, 71-79	23
743	Effect of Ag nanoparticles seeding on the properties of silica spheres. 2018 , 44, 5901-5908	17
742	Role of silanol groups on silica gel on adsorption of benzothiophene and naphthalene. 2018, 215, 463-467	9
741	Selective Separation and Preconcentration of Scandium with Mesoporous Silica. 2018 , 10, 448-457	40
740	A Ceramic-Based Separator for High-Temperature Supercapacitors. 2018 , 6, 306-311	11
739	A comparative study of different nanoclay-reinforced cellulose nanofibril biocomposites with enhanced thermal and mechanical properties. 2018 , 25, 301-315	5
738	A study on optimization of acid sites concentration versus pore dimensions in modified solid acid catalysts for biodiesel production. 2018 , 40, 22-32	1
737	Synthesis of nanometric silica particles via a modified StBer synthesis route. <i>Colloids and Surfaces</i> A: Physicochemical and Engineering Aspects, 2018 , 538, 559-564 5.1	25
736	Direct measurement of the contact angle of water droplet on quartz in a reservoir rock with atomic force microscopy. 2018 , 177, 445-454	30
735	Insignificant influence of the matrix on the melting of ice confined in decorated mesoporous silica. 2018 , 98, 237-249	
734	Influences of polarity and hydration cycles on imbibition hysteresis in silica nanochannels. 2017 , 20, 456-466	5
733	Impact of processing methods on the dissolution of artemether from two non-ordered mesoporous silicas. 2018 , 112, 139-145	11
732	Silica, Amorphous. 2018 , 1-43	2
73 ¹	Electrokinetic flow of an aqueous electrolyte in amorphous silica nanotubes. 2018 , 20, 27838-27848	15
730	The excess electron in polymer nanocomposites. 2018 , 20, 27528-27538	14
729	Nuclearity effects in supported, single-site Fe(ii) hydrogenation pre-catalysts. 2018 , 47, 10842-10846	4

728	Structuration under pressure: Spatial separation of inserted water during pressure-induced hydration in mesolite. 2018 , 103, 175-178	6
727	Optical Fiber Sensor as an Alternative for Colorimetric Image Processing for the Assessment of Dye Concentration. 2018 ,	2
726	The Effect of Support Pretreatment with Ammonia on Pd/SiO2 Catalyst. 2018, 922, 125-129	1
725	Manipulating Thermal Conductance of Supported Graphene via Surface Hydroxylation of Substrates. 2018 , 122, 27689-27695	4
724	Time-Dependent Dynamic Behaviors of a Confined Liquid To Achieve Tailored Adhesion Force with Repeated Contacts Revealed by Atomic Force Microscopy. 2018 , 34, 15211-15227	11
723	Effects of particle size of silica aerogel on its nano-porous structure and thermal behaviors under both ambient and high temperatures. 2018 , 20, 1	5
722	Thin-layer chromatography capability of natural Nev⊟hir volcanic tuff. 2018 , 31, 36-47	
721	A Sustained Release Anchored Biocide System Utilizing the Honeycomb Cellular Structure of Expanded Perlite 2018 , 1, 1959-1971	5
720	Tribo-chemical smoothening process with silica nanoparticles. 2018 , 49, 1423-1438	1
719	Performance Comparison of Three Chemical Vapor Deposited Aminosilanes in Peptide Synthesis: Effects of Silane on Peptide Stability and Purity. 2018 , 34, 11925-11932	1
718	Kinetic and Thermodynamic Study in Pozzolanic Chemical Systems as an Alternative for Chapelle Test. 2018 , 21,	6
717	Synthesis and characterization of amorphous precipitated silica from alkaline dissolution of olivine 2018 , 8, 32651-32658	9
716	Diversification of Device Platforms by Molecular Layers: Hybrid Sensing Platforms, Monolayer Doping, and Modeling. 2018 , 34, 14103-14123	9
715	Influence of the initial chemical conditions on the rational design of silica particles. 2018 , 88, 430-441	16
714	Biological Activation of Bioinert Medical High-Performance Oxide Ceramics by Hydrolytically Stable Immobilization of c(RGDyK) and BMP-2. 2018 , 10, 38669-38680	5
713	Bio-Inspired Hydro-Pressure Consolidation of Silica. 2018 , 28, 1805794	10
712	Interactions between Metal Oxides and Biomolecules: from Fundamental Understanding to Applications. 2018 , 118, 11118-11193	96
711	Improving Polymer Flooding by Addition of Surface Modified Nanoparticles. 2018,	3

710	Analysis on the Influence of Component Ratio on Properties of Silica/Montmorillonite Nanocomposites. 2018 , 11,	6
709	Propylene Oxide Formation on a Silica Surface with Peroxo Defects: Implications in Astrochemistry. 2018 , 122, 9100-9106	3
708	The Effect of Al-Alkyls on the Phillips Catalyst for Ethylene Polymerization: The Case of Diethylaluminum Ethoxide (DEALE). 2018 , 61, 1465-1473	6
707	Zirconium Modification Promotes Catalytic Activity of a Single-Site Cobalt Heterogeneous Catalyst for Propane Dehydrogenation. 2018 , 3, 11117-11127	26
706	Silica Nanofibrous Membranes for the Separation of Heterogeneous Azeotropes. 2018 , 28, 1804138	20
705	Evidence for Copper Dimers in Low-Loaded CuOx/SiO2 Catalysts for Cyclohexane Oxidative Dehydrogenation. 2018 , 8, 9775-9789	8
704	A modified low-temperature wafer bonding method using spot pressing bonding technique and water glass adhesive layer. 2018 , 57, 02BD01	1
703	Effects of nano-confinement on Zn(II) adsorption to nanoporous silica. 2018 , 240, 80-97	15
702	Initiation of heterogeneous Schrock-type Mo and W oxide metathesis catalysts: A quantum thermochemical study. 2018 , 155, 197-208	30
701	Heterobinuclear Light Absorber Coupled to Molecular Wire for Charge Transport across Ultrathin Silica Membrane for Artificial Photosynthesis. 2018 , 10, 31422-31432	8
700	Ionic PMMA/nanosilica interfaces from grafting ionic liquids under supercritical CO2 conditions. 2018 , 109, 82-92	4
699	Formation of porous silica nanoparticles at higher reaction kinetics. 2018 , 339, 801-808	6
698	Comparison of trapped charges and hysteresis behavior in hBN encapsulated single MoS flake based field effect transistors on SiO and hBN substrates. 2018 , 29, 335202	44
697	Effects of surface hydroxylation on adhesion at zinc/silica interfaces. 2018, 20, 15581-15588	4
696	Sorption of cationic organic substances onto synthetic oxides: Evaluation of sorbent parameters as possible predictors. 2018 , 643, 632-639	5
695	Long-term weathering rate of stained-glass windows using H and O isotopes. 2018 , 2,	15
694	Silica-based nanoparticles as drug delivery systems: Chances and challenges. 2018 , 1-40	4
693	Removal of iron from aqueous solution using phytolith-aided aggregation. 2018 , 25, 39-44	1

692	Hydrothermal Transformation of Inorganic and Biogenic Silica as Studied Using in Situ Hydrothermal Infrared Microspectroscopy. 2018 , 72, 1487-1497	1
691	Chemical aging of large-scale randomly rough frictional contacts. 2018 , 98, 023001	9
690	Effect of water vapor on the thermal resistance between amorphous silica nanoparticles. 2018 , 124, 054303	3
689	Impact of polyacrylamide adsorption on flow through porous siliceous materials: State of the art, discussion and industrial concern. 2018 , 531, 693-704	16
688	Cleavage of Organosiloxanes with Dimethyl Carbonate: A Mild Approach To Graft-to-Surface Modification. 2018 , 34, 9719-9730	10
687	What is the role of water in the geopolymerization of metakaolin?. 2018, 182, 360-370	28
686	Probing Hydrogen-Bonding Interactions of Water Molecules Adsorbed on Silica, Sodium Calcium Silicate, and Calcium Aluminosilicate Glasses. 2018 , 122, 17792-17801	20
685	Interaction between porous silica gel microcarriers and peptides for oral administration of functional peptides. 2018 , 8, 10971	4
684	Integrated Mechanochemical/Microwave-Assisted Approach for the Synthesis of Biogenic Silica-Based Catalysts from Rice Husk Waste. 2018 , 6, 11555-11562	13
683	Molecular dynamics simulation of potentiometric sensor response: the effect of biomolecules, surface morphology and surface charge. 2018 , 10, 8650-8666	9
682	Contrasting Roles of Water at Sliding Interfaces between Silicon-Based Materials: First-Principles Molecular Dynamics Sliding Simulations. 2018 , 122, 10459-10467	20
681	Porous Silica in Transition Metal Polymerization Catalysts. 2018 , 31-55	3
680	Iron(III) Ion Adsorption on Macroporous Glass. 2018, 44, 41-46	8
679	General synthesis of silica-based yolk/shell hybrid nanomaterials and tumor vasculature targeting. 2018 , 11, 4890-4904	21
678	Characterization of mesoporous silica used for drug delivery by sorptive interaction - multiple headspace extraction-gas chromatography. 2018 , 187, 35-39	1
677	Quantification of outermost OH group on silica glass surface by high-resolution elastic recoil detection analysis. 2018 , 499, 408-411	2
676	Water Structure Controls Carbonic Acid Formation in Adsorbed Water Films. 2018, 9, 4988-4994	11
675	Influence of moisture absorption on electrical properties and charge dynamics of polyethylene silica-based nanocomposites. 2018 , 51, 425302	3

674	Adsorption of copper (II) on mesoporous silica: the effect of nano-scale confinement. 2018 , 19, 13	26
673	Diffusion of Proteins across Silica Colloidal Crystals. 2018 , 34, 10333-10339	5
672	Lysozyme as a flocculant-inducing agent improving the silica removal from aqueous solutions - A turbidimetric study. 2018 , 226, 187-193	5
671	Silica-Nanochannel-Based Interferometric Sensor for Selective Detection of Polar and Aromatic Volatile Organic Compounds. 2018 , 90, 10780-10785	14
670	Facile bulk preparation and structural characterization of agglomerated Fe2O3/SiO2 nanocomposite particles for nucleic acids isolation and analysis. 2018 , 219, 109-119	2
669	A DFT Study on the Selective Oxidation of Ethane Over Pure SBA-15 and SBA-15-supported Vanadium Oxide. 2018 , 59, 393-404	2
668	New Insights into Adsorption Behaviour of NH3 Molecules on Small (SiO2)n (n=217) Clusters Through Systematic Analysis of Structural and Topological Properties. 2018 , 71, 482	1
667	Dissociation Constants of Silanol Groups of Silic Acids: Quantum Chemical Estimations. 2018 , 59, 261-271	7
666	Durability of silica aerogels dedicated to superinsulation measured under hygrothermal conditions. 2018 , 272, 61-69	11
665	Impacts of environments on nanoscale wear behavior of graphene: Edge passivation vs. substrate pinning. 2018 , 139, 59-66	45
664	Characterisation of silicon, zirconium and aluminium coated titanium dioxide pigments recovered from paint waste. 2019 , 162, 145-152	8
663	Synthesis of lamellar mesostructured phenylene-bridged periodic mesoporous organosilicas (PMO) templated by polyion complex (PIC) micelles. 2019 , 89, 189-195	6
662	Reactive grafting of 3-octanoylthio-1-propyltriethoxysilane in styrene butadiene rubber: Characterization and its effect on silica reinforced tire composites. 2019 , 179, 121693	7
661	Aggregating ability of ferric chloride in the presence of phosphate ligand. 2019 , 164, 114960	3
660	Functionalized Nanoparticles for the Dispersion of Gas Hydrates in Slurry Flow. 2019 , 4, 13496-13508	5
659	Enhancing silica surface deprotonation by using magnetic nanoparticles as heating agents. 2019 , 52, 465001	4
658	Polydimethylsiloxane Sponges Incorporated with Mesoporous Silica Nanoparticles (PDMS/H-MSNs) and Their Selective Solvent Absorptions. 2019 , 58, 21142-21154	7
657	Tunable functionalization of silica coated iron oxide nanoparticles achieved through a silanol-alcohol condensation reaction. 2019 , 55, 10452-10455	7

656	Sensitization of Sm/SnO2(-)SiO2 Nanocomposite with Zwitterionic Surfactant for Enhanced Photocatalytic Performance under Sunlight. 2019 , 93, 1610-1619	3
655	Understanding the catalytic mechanisms of CO2 hydrogenation to methanol on unsupported and supported Ga-Ni clusters. 2019 , 253, 113623	22
654	Contribution of Binary Organic Layers to Soil Water Repellency: A Molecular Level Perspective. 2019 , 123, 7518-7527	3
653	Preparation of nanochitosan-STP from shrimp shell and its application in removing of malachite green from aqueous solutions. 2019 , 7, 103328	31
652	Diffusion Mechanisms for Ions over Hydroxylated Surfaces: Cu on EAl2O3. 2019 , 123, 18502-18507	0
651	Performance of the Halogen Technology for Determining the Moisture Content of Nanoparticulate Powders. 2019 , 43, 757-764	
650	Density Functional Theory Study of the Spontaneous Formation of Covalent Bonds at the Silver/Silica Interface in Silver Nanoparticles Embedded in SiO2: Implications for Ag+ Release. 2019 , 2, 5179-5189	10
649	Measurements of Ion Binding to Lipid-Hosted Ionophores by Affinity Chromatography. 2019 , 35, 9410-9421	6
648	Mechanisms of Silica Fracture in Aqueous Electrolyte Solutions. 2019 , 6,	3
647	Effect of Microcellulose on Wettability of Reservoir Rock Surface Model. 2019 , 811, 55-61	
646	Effect of Microcellulose on Wettability of Reservoir Rock Surface Model. 2019 , 811, 55-61 Polymer modified nanosilica as a sorbent for medical applications. 2019 , 105-124	2
		2 17
646	Polymer modified nanosilica as a sorbent for medical applications. 2019 , 105-124 Nanoscale Mapping of Nonuniform Heterogeneous Nucleation Kinetics Mediated by Surface	
646	Polymer modified nanosilica as a sorbent for medical applications. 2019 , 105-124 Nanoscale Mapping of Nonuniform Heterogeneous Nucleation Kinetics Mediated by Surface Chemistry. 2019 , 141, 13516-13524	17
646 645 644	Polymer modified nanosilica as a sorbent for medical applications. 2019 , 105-124 Nanoscale Mapping of Nonuniform Heterogeneous Nucleation Kinetics Mediated by Surface Chemistry. 2019 , 141, 13516-13524 Understanding the Acidic Properties of the Amorphous Hydroxylated Silica Surface. 2019 , 123, 17343-17352	17
646 645 644	Polymer modified nanosilica as a sorbent for medical applications. 2019, 105-124 Nanoscale Mapping of Nonuniform Heterogeneous Nucleation Kinetics Mediated by Surface Chemistry. 2019, 141, 13516-13524 Understanding the Acidic Properties of the Amorphous Hydroxylated Silica Surface. 2019, 123, 17343-17352 Salt-fog corrosion behavior of C/SiC and its effect on ablation resistance. 2019, 35, 2772-2777 Synthesis and Characterization of Silica-Supported Boron Oxide Catalysts for the Oxidative	17 22 0
646645644643642	Polymer modified nanosilica as a sorbent for medical applications. 2019, 105-124 Nanoscale Mapping of Nonuniform Heterogeneous Nucleation Kinetics Mediated by Surface Chemistry. 2019, 141, 13516-13524 Understanding the Acidic Properties of the Amorphous Hydroxylated Silica Surface. 2019, 123, 17343-17352 Salt-fog corrosion behavior of C/SiC and its effect on ablation resistance. 2019, 35, 2772-2777 Synthesis and Characterization of Silica-Supported Boron Oxide Catalysts for the Oxidative Dehydrogenation of Propane. 2019, 123, 27000-27011 A Comparative Analysis of Different Grades of Silica Particles and Temperature Variants of Food-Grade Silica Nanoparticles for Their Physicochemical Properties and Effect on Trypsin. 2019,	17 22 0
646645644643642641	Polymer modified nanosilica as a sorbent for medical applications. 2019, 105-124 Nanoscale Mapping of Nonuniform Heterogeneous Nucleation Kinetics Mediated by Surface Chemistry. 2019, 141, 13516-13524 Understanding the Acidic Properties of the Amorphous Hydroxylated Silica Surface. 2019, 123, 17343-17352 Salt-fog corrosion behavior of C/SiC and its effect on ablation resistance. 2019, 35, 2772-2777 Synthesis and Characterization of Silica-Supported Boron Oxide Catalysts for the Oxidative Dehydrogenation of Propane. 2019, 123, 27000-27011 A Comparative Analysis of Different Grades of Silica Particles and Temperature Variants of Food-Grade Silica Nanoparticles for Their Physicochemical Properties and Effect on Trypsin. 2019, 67, 12264-12272 Amino Acid-functionalized hollow mesoporous silica nanospheres as efficient biocompatible drug	17 22 0 37

638	Hydrothermally robust Ti/SiO2 epoxidation catalysts via surface modification with oligomeric PMHS. 2019 , 477, 110509	1
637	Structure and dielectric properties of polyethylene nanocomposites containing calcined zirconia. 2019 , 26, 1541-1548	7
636	Atomistic Insights into Cu Chemical Mechanical Polishing Mechanism in Aqueous Hydrogen Peroxide and Glycine: ReaxFF Reactive Molecular Dynamics Simulations. 2019 , 123, 26467-26474	14
635	Dysregulation of cystathionine Elyase promotes prostate cancer progression and metastasis. 2019 , 20, e45986	27
634	Atomic Layer Deposition on Dispersed Materials in Liquid Phase by Stoichiometrically Limited Injections. 2019 , 31, e1904276	10
633	Redox-governed charge doping dictated by interfacial diffusion in two-dimensional materials. 2019 , 10, 4931	14
632	Safer-by-design flame-sprayed silicon dioxide nanoparticles: the role of silanol content on ROS generation, surface activity and cytotoxicity. 2019 , 16, 40	32
631	Origin of weak Lewis acids on silanol nests in dealuminated zeolite Beta. 2019 , 380, 204-214	25
630	Fully Dehydroxylated Silica Generated from Hydrosilane: Surface Defects and Reactivity. 2019 , 123, 23480-23	487
629	Load and Velocity Dependence of Friction Mediated by Dynamics of Interfacial Contacts. 2019 , 123, 116102	15
628	Adsorption of Cu2+ and Mg2+ ions on silica gel derived from rice hulls ash: Experimental and theoretical studies. 2019 , 18, 1950026	1
627	Impact of SiO2 surface composition on trimethylsilane passivation for area-selective deposition. 2019 , 7, 11911-11918	16
626	Modeling of Diffusion and Incorporation of Interstitial Oxygen Ions at the TiN/SiO Interface. 2019 , 11, 36232-36243	4
625	Steam-Stable Basic Immobilized Amine Sorbent Pellets for CO Capture Under Practical Conditions. 2019 , 11, 38336-38346	4
624	Kinetics and thermodynamics of mercury adsorption onto thiolated graphene oxide nanoparticles.	16
	2019 , 173, 114139	
623	Why fumed and precipitated silica have different mechanical behavior: Contribution of discrete element simulations. 2019 , 524, 119646	3
623	Why fumed and precipitated silica have different mechanical behavior: Contribution of discrete	

620	Molecular hydrophobicity at a macroscopically hydrophilic surface. 2019 , 116, 1520-1525	69
619	Synthesis and evaluation of the potential of nonionic surfactants/mesoporous silica systems as nanocarriers for surfactant controlled release in enhanced oil recovery. 2019 , 241, 1184-1194	20
618	Self-Catalyzed, Low-Temperature Atomic Layer Deposition of Ruthenium Metal Using Zero-Valent Ru(DMBD)(CO)3 and Water. 2019 , 31, 1304-1317	11
617	Interaction of water with oxide thin film model systems. 2019 , 34, 360-378	7
616	Effect of Hydrophobic and Hydrophilic Metal Oxide Nanoparticles on the Performance of Xanthan Gum Solutions for Heavy Oil Recovery. 2019 , 9,	20
615	Filtration tests of gaseous ruthenium tetroxide by sand bed and metallic filters. 2019 , 321, 591-598	1
614	Laboratory study of aerosol settling velocities using Laser Doppler velocimetry. 2019, 135, 58-71	5
613	Preferential Adsorption in Mixed Electrolytes Confined by Charged Amorphous Silica. 2019 , 123, 16711-16	720 20
612	Synthesis of methyl palladium complexes on silica as single site catalysts activating CCl bonds in heck reactions. 2019 , 375, 257-266	9
611	Ice nucleation activity of silicates and aluminosilicates in pure water and aqueous solutions Part 2: Quartz and amorphous silica. 2019 , 19, 6035-6058	22
610	Water properties under nano-scale confinement. 2019 , 9, 8246	62
609	Probing Charged Aqueous Interfaces Near Critical Angles: Effect of Varying Coherence Length. 2019 , 123, 16911-16920	31
608	Memory Distance for Interfacial Chemical Bond-Induced Friction at the Nanoscale. 2019 , 13, 7425-7434	4
607	Impact of PAM-Grafted Nanoparticles on the Performance of Hydrolyzed Polyacrylamide Solutions for Heavy Oil Recovery at Different Salinities. 2019 , 58, 9888-9899	16
606	Conduction and Excess Charge in Silicate Glass/Air Interfaces. 2019 , 35, 7703-7712	5
605	Moisture outgassing from siloxane elastomers containing surface-treated-silica fillers. 2019 , 3,	2
604	Surface Reactivity and Leaching of a Sodium Silicate Glass under an Aqueous Environment: A ReaxFF Molecular Dynamics Study. 2019 , 123, 15606-15617	32
603	Cr(VI) reduction by Fe(II) sorbed to silica surfaces. 2019 , 234, 98-107	11

602	Anticorrosive Performance of L. Leaf Extract-Based Hybrid Coating on Steel. 2019 , 4, 10176-10184		12
601	Biocatalytic transamination in a monolithic flow reactor: improving enzyme grafting for enhanced performance 2019 , 9, 18538-18546		20
600	Selective gas conversion of isopropyl alcohol over silver nanoparticles (Ag-NPs) supported on new mesoporous silica precipitated from natural resources. 2019 , 45, 5091-5109		2
599	Disordering of 13C18O bonds in CO2 gas over a heated quartz surface at 50🛭 100 🖰: Insights into the abundance of mass 47 (🗗7) in CO2 gas at thermodynamic equilibrium. 2019 , 524, 213-227		2
598	Investigating the role of SBA-15 silica on the activity of quaternary ammonium halides in the coupling of epoxides and CO2. 2019 , 34, 34-39		14
597	Heavy oil recovery by surface modified silica nanoparticle/HPAM nanofluids. 2019 , 252, 622-634		28
596	Effect of Mineral Surface Properties on Water Behaviors in Pores Constructed by Calcite and Silica Particles. 2019 , 123, 13288-13294		3
595	Effects of slag substitution on physical and mechanical properties of fly ash-based alkali activated binders (AABs). 2019 , 122, 118-135		50
594	CMK-3 nanostructured carbon: Effect of temperature and time carbonization on textural properties and H2 storage. 2019 , 206, 1581-1595		5
593	Influence of oxide substrates on monolayer graphene doping process by thermal treatments in oxygen. 2019 , 149, 546-555		8
592	Amorphous agomelatine stabilization in the presence of pyrogenic silica: Molecular mobility and intermolecular interaction studies. 2019 , 139, 291-300		5
591	Effect of glass aggregates and coupling agent on the mechanical behaviour of polymeric glass composite. 2019 , 227, 119-129		9
590	Role of the Short-Range Order in Amorphous Oxide on MoS2/a-SiO2 and MoS2/a-HfO2 Interfaces. 2019 , 256, 1900002		2
589	Controlling dispersion, stability and polymer content on PDEGMA-functionalized core-brush silica colloids. <i>Colloids and Surfaces A: Physicochemical and Engineering Aspects</i> , 2019 , 574, 12-20	5.1	9
588	Coupling of synthesis and modification to produce hydrophobic or functionalized nano-silica particles. <i>Colloids and Surfaces A: Physicochemical and Engineering Aspects</i> , 2019 , 574, 122-130	5.1	14
587	Development and characterization of membranes derived from SF/GLY/58S hybrid xerogels for the release of inorganic ions as an osteogenic stimulus for bone regeneration. 2019 , 116, 425-437		2
586	Influence of pre-treatment temperature of palm oil fuel ash on the properties and performance of green ceramic hollow fiber membranes towards oil/water separation application. 2019 , 222, 264-277		26
585	Investigation of the Impact of Cross-Polymerization on the Structural and Frictional Properties of Alkylsilane Monolayers Using Molecular Simulation. 2019 , 9,		6

584	Fabrication of highly selective organosilica membrane for gas separation by mixing bis(triethoxysilyl)ethane with methyltriethoxysilane. 2019 , 222, 162-167		10
583	Quartz crystal microbalance study of precursor diffusion during molecular layer deposition using cyclic azasilane, maleic anhydride, and water. 2019 , 37, 030909		4
582	Luminescent sequence-dependent materials through a step by step assembly of RE1¶,4-benzendicarboxylate¶E2 (REx = Y3+, Eu3+ and Tb3+) architectures on a silica surface. 2019 , 7, 4415-4423		4
581	Chemical vapor deposition of monolayer-thin WS crystals from the WF and HS precursors at low deposition temperature. 2019 , 150, 104703		7
580	Quantitative Evaluation of Long-Range and Cooperative Ion Effect on Water in Polyamide Network. 2019 , 123, 2948-2955		4
579	Wettability of Fully Hydroxylated and Alkylated (001) EQuartz Surface in Carbon Dioxide Atmosphere. 2019 , 123, 9027-9040		41
578	Computational Modelling of Structure and Catalytic Properties of Silica-Supported Group VI Transition Metal Oxide Species. 2019 , 315-344		1
577	An experimental and modelling study of water vapour adsorption on SBA-15. 2019 , 282, 53-53		9
576	Superconducting Diamond on Silicon Nitride for Device Applications. 2019 , 9, 2911		15
575	Experimentation and modeling of surface chemistry of the silica-water interface for low salinity waterflooding at elevated temperatures. <i>Colloids and Surfaces A: Physicochemical and Engineering Aspects</i> , 2019 , 570, 233-243	5.1	5
574	. 2019 , 26, 284-291		8
573	A Critical Review of Solid Materials for Low-Temperature Thermochemical Storage of Solar Energy Based on Solid-Vapour Adsorption in View of Space Heating Uses. 2019 , 24,		24
572	Molecular mechanisms of mesoporous silica formation from colloid solution: Ripening-reactions arrest hollow network structures. 2019 , 14, e0212731		4
571	Atomistic Study of Dynamic Contact Angles in CO-Water-Silica System. 2019 , 35, 5324-5332		10
570	Sol-Gel Synthesis and Characterization of Hybrid Materials for Biomedical Applications. 2019 , 445-475		1
569	Catalytic materials based on silica and alumina: Structural features and generation of surface acidity. 2019 , 104, 215-249		39
568	Application of the CLAYFF and the DREIDING Force Fields for Modeling of Alkylated Quartz Surfaces. 2019 , 35, 5746-5752		8
567	Smart Mesoporous Silica Nanoparticles for Protein Delivery. 2019 , 9,		29

566	Cumulative directional calcium gluing between phosphate and silicate: A facile, robust and biocompatible strategy for siRNA delivery by amine-free non-positive vector. 2019 , 209, 126-137	10
565	Post-synthesis deposition of mesoporous niobic acid with improved thermal stability by kinetically controlled solgel overcoating. 2019 , 7, 23803-23811	3
564	Effect of Surface Silanol Groups on Friction and Wear between Amorphous Silica Surfaces. 2019 , 35, 5463-54	7012
563	Adsorption layer structure at soil mineral/biopolymer/supporting electrolyte interface T he impact on solid aggregation. 2019 , 284, 117-123	7
562	Constraining silicon isotope exchange kinetics and fractionation between aqueous and amorphous Si at room temperature. 2019 , 253, 267-289	8
561	Effect of different waste filler and silane coupling agent on the mechanical properties of powder-resin composite. 2019 , 224, 940-956	20
560	Biocompatibility of Amine-Functionalized Silica Nanoparticles: The Role of Surface Coverage. 2019 , 15, e1805400	24
559	Silica-supported orthophosphoric acid (OPA/SiO2): preparation, characterization, and evaluation as green reusable catalyst for pinacolic rearrangement. 2019 , 16, 1029-1040	1
558	Relation between working properties and structural properties from 27Al, 29Si and 31P NMR and XRD of acid-based geopolymers from 25 to 1000°C. 2019 , 228, 293-302	14
557	High-Magnification SEM Micrograph of Siloxanes. 2019,	
556	Selective Elimination of Bitter Peptides by Adsorption to Heat-treated Porous Silica Gel. 2019 , 25, 179-186	3
555	Niobium pentoxide nanomaterials with distorted structures as efficient acid catalysts. 2019 , 2,	30
554	Preparation and antibacterial behaviour of nanostructured Ag@SiO2Benicillin with silver	_
	nanoplates. 2019 , 43, 16612-16620	5
553		7
553 552	nanoplates. 2019 , 43, 16612-16620	
	nanoplates. 2019 , 43, 16612-16620 Microporosity Quantification via NMR Relaxometry. 2019 , 123, 30486-30491 Dielectric and Electrostatic Properties of the Silica Nanoparticle Water Interface by EPR of	7
552	nanoplates. 2019, 43, 16612-16620 Microporosity Quantification via NMR Relaxometry. 2019, 123, 30486-30491 Dielectric and Electrostatic Properties of the Silica Nanoparticle Water Interface by EPR of pH-Sensitive Spin Probes. 2019, 123, 29972-29985 Influence of the Interactions at the Graphene-Substrate Boundary on Graphene Sensitivity to UV	3

548	Current trends, challenges, and perspectives of anti-fogging technology: Surface and material design, fabrication strategies, and beyond. 2019 , 99, 106-186	83
547	Calcium Ion Bridging of Aqueous Carboxylates onto Silica: Implications for Low-Salinity Waterflooding. 2019 , 33, 127-134	8
546	Importance of the Order of Addition of the Alumina Precursor and its Type Into Al-SBA-15 Mesoporous Materials for Use as Water Adsorbents. 2019 , 22,	4
545	Characterization of Multimodal Silicas Using TG/DTG/DTA, Q-TG, and DSC Methods. 2019 , 3, 6	8
544	Investigation of citric acid-assisted sol-gel synthesis coupled to the self-propagating combustion method for preparing bioactive glass with high structural homogeneity. 2019 , 97, 669-678	13
543	Bi-functionalization of glass surfaces with poly-l-lysine conjugated silica particles and polyethylene glycol for selective cellular attachment and proliferation. 2019 , 54, 2501-2513	1
542	Characterization of magnesium silicate hydrate (M-S-H). 2019 , 116, 309-330	53
541	Impact of MoS layer transfer on electrostatics of MoS/SiO interface. 2019 , 30, 055702	10
540	Adsorption and Photocatalytic Decomposition of Gaseous 2-Propanol Using TiO2-Coated Porous Glass Fiber Cloth. 2019 , 9, 82	4
539	Polymorphic foam clay for inhibiting the spontaneous combustion of coal. 2019 , 122, 263-270	20
538	Characterization and implication of phytolith-associated potassium in rice straw and paddy soils. 2019 , 65, 1354-1369	4
537	Dynamic adsorptiondesorption of methyl ethyl ketone on MCM-41 and SBA-15 decorated with thermally activated polymers. 2019 , 71, 465-480	14
536	Methyltrichlorosilane modified hydrophobic silica aerogels and their kinetic and thermodynamic behaviors. 2019 , 89, 448-457	12
535	Nanoscale Imaging and Stabilization of Silica Nanospheres in Liquid Phase Transmission Electron Microscopy. 2019 , 36, 1800374	7
534	Nanosilica decorated multiwalled carbon nanotubes (CS hybrids) in natural rubber latex. 2019 , 161, 170-180	15
533	A comparative study on mesocellular foam silica with different template removal methods and their effects on enzyme immobilization. 2019 , 26, 1059-1068	6
532	A new method to prepare mesoporous silica from coal gasification fine slag and its application in methylene blue adsorption. 2019 , 212, 1062-1071	87
531	Non-firing ceramics: Activation of silica powder surface by a planetary ball milling. 2019 , 30, 461-465	7

530	Heterogenization of a cyclocarbonation catalyst: Optimization and kinetic study. 2019 , 334, 140-155	7
529	Nanostructured silica used in super-insulation materials (SIM), hygrothermal ageing followed by sorption characterizations. 2019 , 183, 626-638	11
528	Modified coal fly ash waste as an efficient heterogeneous catalyst for dehydration of xylose to furfural in biphasic medium. 2019 , 239, 726-736	21
527	Time-of-day-dependent behavior of surficial lunar hydroxyl/water: Observations and modeling. 2019 , 321, 486-507	14
526	Preparation of pervious concrete with 3-thiocyanatopropyltriethoxysilane modified fly ash and its use in Cd[(II)]sequestration. 2019 , 212, 1-7	22
525	Detailed investigation of the surface mechanisms and their interplay with transport phenomena in alumina atomic layer deposition from TMA and water. 2019 , 195, 399-412	19
524	Removal of Congo red by thermally and chemically modified halloysite: equilibrium, FTIR spectroscopy, and mechanism studies. 2019 , 16, 4253-4260	7
523	One Step up the Ladder of Prebiotic Complexity: Formation of Nonrandom Linear Polypeptides from Binary Systems of Amino Acids on Silica. 2019 , 25, 1275-1285	10
522	Synthesis of Mesoporous Silicon with Uniform Pore Size Using the Ashes of Husks from Panicum Miliare Millet: A Novel Recyclable Bio-waste. 2019 , 11, 2345-2351	1
521	Adhesion force behaviors between two silica surfaces with varied water thin film due to substrate temperature studied by AFM. 2020 , 96, 855-872	6
520	Progress in the Design of Cooperative Heterogeneous Catalytic Materials for CIL Bond Formation. 2020 , 30, 1901385	7
519	Characterization of amorphous silica based catalysts using DFT computational methods. 2020 , 354, 3-18	35
518	Preparation, stabilization and characterization of 3-(methacryloyloxy) propyl trimethoxy silane modified colloidal nanosilica particles. <i>Colloids and Surfaces A: Physicochemical and Engineering Aspects</i> , 2020 , 585, 124066	6
517	Instability of geophysical flows at arbitrary latitude. 2020 , 191, 831-842	
516	Cationic starch as the effective flocculant of silica in the presence of different surfactants. 2020 , 234, 116132	8
515	Efficient degradation of methylene blue by Co(II) complexes constrained to the hall of mesoporous silica decorated by Pt nanoparticles. 2020 , 259, 126776	3
514	Adsorption isotherm and kinetic modeling of a novel procedure for physical modification of silica gel using aqueous solutions of 4,4?-(1,2-ethanediyldinitrilo)bis-(2-pentanone) for preconcentration of Ni(II) ion. 2020 , 55, 2919-2932	4
513	Reducing the thermal hazard of hydrophobic silica aerogels by using dimethyldichlorosilane as modifier. 2020 , 93, 111-122	5

(2020-2020)

512	Understanding the Synthesis of Supported Vanadium Oxide Catalysts Using Chemical Grafting. 2020 , 26, 1052-1063	6
511	Surface area of ferrihydrite consistently related to primary surface charge, ion pair formation, and specific ion adsorption. 2020 , 532, 119304	13
510	Minocycline Reduces Chemoradiation-Related Symptom Burden in Patients with Non-Small Cell Lung Cancer: A Phase 2 Randomized Trial. 2020 , 106, 100-107	7
509	Adsorption of Methyl Chloride on Molecular Sieves, Silica Gels, and Activated Carbon. 2020 , 43, 436-446	6
508	Interfacial reactions of Cu(II) adsorption and hydrolysis driven by nano-scale confinement. 2020 , 7, 68-80	13
507	Covalently attachment of aliphatic linear non-branched alcohols to silicon oxide and glass substrates in liquid paraffin solvent. 2020 , 509, 145102	1
506	The PAlxFe2-xO3 nanomagnets as MRI contrast agents: Factors influencing transverse relaxivity. Colloids and Surfaces A: Physicochemical and Engineering Aspects, 2020, 589, 124423	2
505	Integrating Reactors and Catalysts through Three-Dimensional Printing: Efficiency and Reusability of an Impregnated Palladium on Silica Monolith in Sonogashira and Suzuki Reactions. 2020 , 12, 1762-1771	11
504	Structure and sum-frequency generation spectra of water on uncharged Q silica surfaces: a molecular dynamics study. 2020 , 22, 2033-2045	7
503	Grafting metal complexes onto amorphous supports: from elementary steps to catalyst site populations via kernel regression. 2020 , 5, 66-76	11
502	Imbibition and dewetting of silica colloidal crystals: An NMR relaxometry study. 2020, 561, 741-748	8
501	Formation mechanisms of chitosan-silica hybrid materials and its performance as solid support for KR-12 peptide adsorption: Impact on KR-12 antimicrobial activity and proteolytic stability. 2020 , 9, 890-901	16
500	Mass transport in a partially filled horizontal drum: Modelling and experiments. 2020, 214, 115448	3
499	Thermally-Induced morphological evolution of spherical silica nanoparticles using in-operando X-ray scattering measurements. <i>Colloids and Surfaces A: Physicochemical and Engineering Aspects</i> , 5.1 2020 , 586, 124260	5
498	Ionic Diffusion, Nanoparticle Formation and Trapping Within Sol-Gel Made Pillared Planar Nanochannels in a Simple Microfluidic Device. 2020 , 6, 392-403	
497	Phase of iron oxide out of thermally treated magnetite nanoparticles. 2020, 497, 165999	3
496	Biomedical application of mesoporous silica nanoparticles as delivery systems: a biological safety perspective. 2020 , 8, 9863-9876	13
495	Improving	7

494	Polymerization Kinetics of Cyanate Ester Confined to Hydrophilic Nanopores of Silica Colloidal Crystals with Different Surface-Grafted Groups. 2020 , 12,	9
493	Charge Transport in 2D MoS2, WS2, and MoS2WS2 Heterojunction-Based Field-Effect Transistors: Role of Ambipolarity. 2020 , 124, 23368-23379	7
492	A Framework for Pore-Scale Simulation of Effective Electrical Conductivity and Permittivity of Porous Media in the Frequency Range From 1[mHz to 1[GHz. 2020 , 125, e2020JB020515	2
491	Adsorption of Iron(III) Ions on Porous Glass with Different Pore Space Structures. 2020 , 46, 242-248	2
490	CO2 capture and conversion by an organosilane-modified cementitious material. 2020 , 253, 119198	O
489	Influence of salt concentration on the formation of Pickering emulsions. 2020 , 16, 7342-7349	4
488	Surface Reactivity and Dissolution Properties of Alumina-Silica Glasses and Fibers. 2020 , 12, 36740-36754	10
487	ArgonWater DBD pretreatment and vapor-phase silanization of silica: Comparison with wet-chemical processes. 2020 , 17, 1900265	O
486	Taming the thermodiffusion of alkali halide solutions in silica nanopores. 2020 , 12, 23626-23635	4
485	Two-Dimensional Layers of Colloidal CdTe Quantum Dots: Assembly, Optical Properties, and Vibroelectronic Coupling. 2020 , 124, 25873-25883	5
484	Hydrophobic Modification on the Surface of SiO Nanoparticle: Wettability Control. 2020 , 36, 14924-14932	5
483	Surface Properties and Porosity of Silica Particles Studied by Wide-Angle Soft X-ray Scattering. 2020 , 124, 16663-16674	2
482	The correlation of tear deviation and resistance with the bound rubber content in rubber-silica composites. 2020 , 90, 106762	1
481	Evidence for low-energy ions influencing plasma-assisted atomic layer deposition of SiO2: Impact on the growth per cycle and wet etch rate. 2020 , 117, 031602	7
480	Nonporous Inorganic Nanoparticle-Based Humidity Sensor: Evaluation of Humidity Hysteresis and Response Time. 2020 , 20,	6
479	Multi-analytical characterisation of wheat biominerals: impact of methods of extraction on the mineralogy and chemistry of phytoliths. 2020 , 12, 1	1
478	Use of the Indirect Photoluminescence Peak as an Optical Probe of Interface Defectivity in MoS2. 2020 , 7, 2000413	4
477	A comprehensive study on the gelation process of silica gels from sodium silicate. 2020 , 9, 10157-10165	6

(2020-2020)

476	Surface modification of SiO2 nanoparticles with PDMAEMA brushes and Ag nanoparticles as antifungal coatings using electron beam assisted synthesis. 2020 , 253, 123438	12
475	Influence of Drug-Silica Electrostatic Interactions on Drug Release from Mesoporous Silica-Based Oral Delivery Systems. 2020 , 17, 3435-3446	5
474	Thermal stability and pyrolysis characteristics of MTMS aerogels prepared in pure water. 2020, 22, 1	10
473	Surface structure of linear nanopores in amorphous silica: Comparison of properties for different pore generation algorithms. 2020 , 153, 124708	3
472	Effect of Particle Specific Surface Area on the Rheology of Non-Brownian Silica Suspensions. 2020 , 13,	2
471	A Simple Low-Temperature Glass Bonding Process with Surface Activation by Oxygen Plasma for Micro/Nanofluidic Devices. 2020 , 11,	5
470	Preparation of mesoporous silica thin films at low temperature: a comparison of mild structure consolidation and template extraction procedures. 2020 , 96, 287-296	3
469	Abrasion Indicators for Smart Surfaces Based on a Luminescence Turn-On Effect in Supraparticles. 2020 , 1, 2000023	10
468	Synthetic amorphous silica nanoparticles: toxicity, biomedical and environmental implications. 2020 , 5, 886-909	69
467	Efficient Cu catalyst for 5-hydroxymethylfurfural hydrogenolysis by forming CuDBi bonds. 2020 , 10, 7323-7330	6
466	Nontraditional Catalyst Supports in Surface Organometallic Chemistry. 2020 , 10, 11822-11840	40
465	Effect of Poly(vinyl butyral) Comonomer Sequence on Adhesion to Amorphous Silica: A Coarse-Grained Molecular Dynamics Study. 2020 , 12, 47879-47890	5
464	Thermal deactivation kinetics and thermodynamics of a silica gel using surface area data. 2020 , 146, 1505	2
463	Injection and Retention Characterization of Trapped Charges in Electret Films by Electrostatic Force Microscopy and Kelvin Probe Force Microscopy. 2020 , 217, 2000190	3
462	Reversible Formation of Silanol Groups in Two-Dimensional Siliceous Nanomaterials under Mild Hydrothermal Conditions. 2020 , 124, 18045-18053	3
461	Intrinsic water layering next to soft, solid, hydrophobic, and hydrophilic substrates. 2020 , 153, 224702	1
460	Hydroxyl Groups Induce Bioactivity in Silica/Chitosan Aerogels Designed for Bone Tissue Engineering. In Vitro Model for the Assessment of Osteoblasts Behavior. 2020 , 12,	6
459	Relative humidity is not a direct factor to influence adhesion force between two silica surfaces. 2020 , 1-16	3

458	Structuring Edible Oils With Fumed Silica Particles. 2020 , 4,	4
457	Molecular Dynamics Simulations of Mineral Surface Wettability by Water Versus CO2: Thin Films, Contact Angles, and Capillary Pressure in a Silica Nanopore. 2020 , 124, 25382-25395	13
456	Band alignment at interfaces of two-dimensional materials: internal photoemission analysis. 2020 , 32, 413002	4
455	Atmospheric Water Harvesting: A Review of Material and Structural Designs. 2020 , 2, 671-684	102
454	Recent Developments in Thermally Insulating Materials Based on Geopolymers Review Article. 2020 , 37, 995-1014	4
453	Unraveling Particle Size and Roughness Effects on the Interfacial Catalytic Properties of Pickering Emulsions. <i>Colloids and Surfaces A: Physicochemical and Engineering Aspects</i> , 2020 , 599, 124800	7
452	Surface Preparation as a Step in the Fabrication of Biosensors Based on Silicon Nanowire Field-Effect Transistors: Review. 2020 , 14, 337-346	O
451	Catalytic Mechanisms of Zirconium-Containing Active Sites over the SBA-15 Zeolite Framework for Xylose Conversion to Methyl Lactate. 2020 , 124, 13102-13112	2
450	Deactivation Mechanism of Cu/SiO2 Catalysts in the Synthesis of Ethylene Glycol via Methyl Glycolate Hydrogenation. 2020 , 59, 12381-12388	9
449	The tensile strength of dust aggregates consisting of small elastic grains: constraints on the size of condensates in protoplanetary discs. 2020 , 496, 1667-1682	13
448	Rapid post-mortem oxygen isotope exchange in biogenic silica. 2020 , 284, 61-74	0
447	Toward Long-Lasting Low-Haze Antifog Coatings through the Deposition of Zeolites. 2020 , 59, 13042-13050	O
446	Oxidative destruction of phenol on Fe/SiO catalysts. 2020 , 81, 2189-2201	O
445	Silica surface states and their wetting characteristics. 2020 , 8, 145-157	7
444	From Femtosecond to Nanosecond Laser Microstructuring of Conical Aluminum Surfaces by Reactive Gas Assisted Laser Ablation. 2020 , 21, 1644-1652	5
443	Hansen solubility parameters obtained via molecular dynamics simulations as a route to predict siloxane surfactant adsorption. 2020 , 575, 326-336	7
442	Fluorocarbon versus hydrocarbon organosilicon surfactants for wettability alteration: A molecular dynamics approach. 2020 , 88, 224-232	6
441	Production of silica gel from waste metal silica residue. 2020 , 275, 128125	2

440	Grafting of iron on amorphous silica surfaces from ab initio calculations. 2020 , 152, 214706	10
439	Intrinsic Chemical Reactivity of Silicon Electrode Materials: Gas Evolution. 2020 , 32, 3199-3210	10
438	Gas dehydration using the ionic liquid [EMIM][MeSO3] supported on silica gel [Structural and water vapor sorption properties. 2020 , 398, 124689	10
437	TPD characterization of Al-OD-Si sites at the interface of bilayer Al0.42Si0.58O2/Ru(0001) thin-films 2020 , 696, 121595	
436	Area-selective chemical vapor deposition of cobalt from dicobalt octacarbonyl: Enhancement of dielectric-dielectric selectivity by adding a coflow of NH3. 2020 , 38, 033401	7
435	Polymer-coated cationic silica nanoparticles for slow-release Pickering emulsions. 2020 , 298, 559-568	2
434	Grafting Silicone at Room Temperature-a Transparent, Scratch-resistant Nonstick Molecular Coating. 2020 , 36, 4416-4431	32
433	On the Role of Silica Carrier Curvature for the Unloading of Small Drug Molecules: A Molecular Dynamics Simulation Study. 2020 , 109, 2018-2023	2
432	Quantum Chemical Analysis of the Processes of Synthesis of Vanadium Oxide Structures on the Silica Surface. 2020 , 90, 880-888	1
431	A PTFE helical capillary microreactor for the high throughput synthesis of monodisperse silica particles. 2020 , 401, 126063	8
430	Experimental study of substrate roughness on the local glass transition of polystyrene. 2020 , 152, 244901	10
429	Efficient Catalysis of Phosphate Ester Hydrolysis by Bare Silica. 2020 , 124, 17111-17120	0
428	Isomerization of Dinene oxide to campholenic aldehyde in the presence of Al-SiO2 and magnetic Al-SiO2/Fe3O4 catalysts. 2020 , 130, 919-934	
427	Water Uptake by Silica Nanopores: Impacts of Surface Hydrophilicity and Pore Size. 2020 , 124, 15188-15194	10
426	Correlation of Dielectric Breakdown and Nanoscale Adhesion in Silicon Dioxide Thin Films. 2020,	1
425	Effect of microstructural damage on the mechanical properties of silica nanoparticle-reinforced silicone rubber composites. 2020 , 235, 107195	13
424	Development of mesoporous materials from biomass ash with future applications as adsorbent materials. 2020 , 299, 110085	7
423	Unveiling the origin of the anti-fogging performance of plasma-coated glass: Role of the structure and the chemistry of siloxane precursors. 2020 , 141, 105401	6

422	Tuning the highly dispersed metallic Cu species via manipulating Brāsted acid sites of mesoporous aluminosilicate support for CO2 hydrogenation reactions. 2020 , 269, 118804	13
421	The importance of residual water for the reactivity of MPTMS with silica on the example of SBA-15. 2020 , 513, 145802	4
420	Surface modification of feldspar porcelain by corona discharge and its effect on bonding to resin cement with silane coupling agent. 2020 , 105, 103708	5
419	Insight into Kinetics and Mechanisms of AOT Vesicle Adsorption on Silica in Unfavorable Conditions. 2020 , 36, 1937-1949	6
418	Activation of Low-Valent, Multiply MM Bonded Group VI Dimers toward Catalytic Olefin Metathesis via Surface Organometallic Chemistry. 2020 , 39, 1035-1045	7
417	Aldol condensation of acetic acid and formaldehyde to acrylic acid over a hydrothermally treated silica gel-supported B-P-V-W oxide. 2020 , 594, 117472	8
416	Extraction of nano-porous silica from hydrosodalite produced via modification of low-grade kaolin for removal of methylene blue from wastewater. 2020 , 95, 1989-2000	6
415	Enhanced Menshutkin S2 Reactivity in Mesoporous Silica: The Influence of Surface Catalysis and Confinement. 2020 , 142, 5636-5648	15
414	L-Lysine-modified FeO nanoparticles for magnetic cell labeling. 2020 , 190, 110879	14
413	Effect of PDDA surfactant on the microstructure and properties of electrodeposited SiO2/Ni nanocomposites. 2020 , 163, 110229	3
412	Salt-Responsive Zwitterionic Polymer Brush Based on Modified Silica Nanoparticles as a Fluid-Loss Additive in Water-Based Drilling Fluids. 2020 , 34, 1669-1679	22
411	Temporally Anticorrelated Subdiffusion in Water Nanofilms on Silica Suggests Near-Surface Viscoelasticity. 2020 , 14, 3041-3047	7
410	Degradation kinetics of isoproturon and its subsequent products in contact with TiO2 functionalized silica nanofibers. 2020 , 387, 124143	9
409	Isolated Molybdenum(VI) and Tungsten(VI) Oxide Species on Partly Dehydroxylated Silica: A Computational Perspective. 2020 , 124, 3002-3013	8
408	MoSDeF, a Python Framework Enabling Large-Scale Computational Screening of Soft Matter: Application to Chemistry-Property Relationships in Lubricating Monolayer Films. 2020 , 16, 1779-1793	12
407	Nanostructure evolution of silica aerogels under rapid heating from 600IIC to 1300IIC via in-situ TEM observation. 2020 , 46, 12489-12498	15
406	Evaluation of surface energetics of zirconium-containing mesoporous silica using novel universal isotherm model. 2020 , 26, 607-618	2
405	Enhanced Selectivity and Stability of Cu/SiO2 Catalysts for Dimethyl Oxalate Hydrogenation to Ethylene Glycol by Using Silane Coupling Agents for Surface Modification. 2020 , 59, 9414-9422	13

404	Specificity and affinity of multivalent ions adsorption to kaolinite surface. 2020 , 190, 105557		17
403	Solar photocatalytic degradation of organic pollutants in textile industry wastewater by ZnO/pumice composite photocatalyst. 2020 , 8, 103907		17
402	Colloidal stability and dynamic adsorption behavior of nanofluids containing alkyl-modified silica nanoparticles and anionic surfactant. 2020 , 308, 113079		16
401	Hydrothermal SiO Nanopowders: Obtaining Them and Their Characteristics. 2020 , 10,		6
400	Development of an Adsorbing System Made of DMS-1 Mesh Modified by Amino Groups to Remove Pb(II) Ions from Water. 2020 , 13,		
399	Area Occupied by a Water Molecule Adsorbed on Silica at 298 K: Zeta Adsorption Isotherm Approach. 2020 , 124, 9269-9280		5
398	Tuning molecular adsorption in SBA-15-type periodic mesoporous organosilicas by systematic variation of their surface polarity. 2020 , 11, 3702-3712		4
397	Nanosized copper(ii) oxide/silica for catalytic generation of nitric oxide from S-nitrosothiols. 2020 , 8, 4267-4277		7
396	Macroporous geopolymers designed for facile polymers post-infusion. 2020 , 110, 103591		8
395	Influences of heating rate on the nano-porous structure of silica aerogel. 2021 , 39, 123-130		1
394	Desiccated Microclimates for Heritage Metals: Creation and Management. 2021 , 66, 127-153		1
393	Capillary contact angle for the quartz-distilled water-normal decane interface at temperatures up to 200 LC. Colloids and Surfaces A: Physicochemical and Engineering Aspects, 2021 , 609, 125608	5.1	4
392	Mesoporous magnesium carbonate for use in powder cosmetics. 2021 , 43, 57-67		1
391	Accessibility and strength of H-acceptor hydroxyls of ordered mesoporous silicas probed by pyridine donor. 2021 , 28, 323-335		2
390	How to design nanoporous silica nanoparticles in regulating drug delivery: Surface modification and porous control. 2021 , 263, 114835		11
389	Addition of modified hollow mesoporous organosilica in anhydrous SPEEK/IL composite membrane enhances its proton conductivity. 2021 , 620, 118897		4
388	Effect of thermal treatment on the surface/interfacial behaviour of Au@SiO2 nanoparticles in the presence of CTAB surfactant molecules. 2021 , 381, 503-508		6
387	Creating Brfisted acidity at the SiO2-Nb2O5 interface. 2021 , 394, 387-396		3

386	CO2 solubility in brine in silica nanopores in relation to geological CO2 sequestration in tight formations: Effect of salinity and pH. 2021 , 411, 127626	8
385	100th Anniversary of Macromolecular Science Viewpoint: Polymeric Materials by Liquid-Phase Transmission Electron Microscopy 2021 , 10, 14-38	13
384	Perspectives on additives for polymers. Part 2. Aspects of photostabilization and role of fillers and pigments. 2021 , 27, 211-239	7
383	Structure and thermoelectric properties of higher manganese silicides synthesized by pack cementation. 2021 , 47, 243-251	5
382	Development of Ni/ZnO desulfurization adsorbent with high stability: Formation of Zn2SiO4 and the impact from substrate. 2021 , 409, 127374	2
381	Abnormally large and small adhesion forces between plasma-treated silicon surfaces studied on AFM. 2021 , 97, 305-327	1
380	Structure Characterizations and Molecular Dynamics Simulations of Melt, Glass, and Glass Fibers. 2021 , 89-216	
379	Bulk supercooled water adsorbed films on silica surfaces: specific heat by Monte Carlo simulation. 2021 , 23, 2275-2285	
378	Structural Model for the Estimation of the Equivalent Permittivity of Nanodielectrics Based on Polyethylene and Epoxy Resins. 2021 , 9, 123927-123938	
377	Mixed gel electrolytes: Synthesis, characterization, and gas release on PbSb electrode. 2021 , 10, 325-335	
376	Competitive adsorption of phenol and toluene onto silica-supported transition metal clusters for biofuel purification.	3
375	Glass surface as strong base, 'green' heterogeneous catalyst and degradation reagent. 2021 , 12, 9816-9822	5
374	Risks and Limitations Associated with XLPE Nanocomposites and Blends. 2021 , 411-456	
373	Surface organometallic and coordination chemistry approach to formation of single site heterogeneous catalysts. 2021 ,	
372	Natural rubber and epoxidized natural rubber in combination with silica fillers for low rolling resistance tires. 2021 , 247-316	0
371	Biologically active composite based on fumed silica and Anoectochilus formosanus Hayata extract. 2021 , 75, 2575-2583	2
370	Modeling the solid/liquid interfacial properties of methylimidazole confined in hydrophobic silica nanopores. 2021 , 231, 116333	
369	Physicochemical and electrochemical characterization of Nafion-type membranes with embedded silica nanoparticles: Effect of functionalization. 2021 , 370, 137689	2

368	Carrier and dilution effects of CO on thoron emissions from a zeolitized tuff exposed to subvolcanic temperatures. 2021 , 8, 201539	
367	Cr[CH(SiMe3)2]3/SiO2 catalysts for ethene polymerization: The correlation at a molecular level between the chromium loading and the microstructure of the produced polymer. 2021 , 394, 131-141	2
366	Microwave heating and synthesis method influence in SiO2@rO2 mixed oxides preparation and its use as heterogeneous catalyst for biodiesel obtainment. 2021 , 132, 921-934	
365	Atomic-Level Material Removal Mechanisms of Si(110) Chemical Mechanical Polishing: Insights from ReaxFF Reactive Molecular Dynamics Simulations. 2021 , 37, 2161-2169	1
364	Electronic charge transfer during metal/SiO2 contact: Insight from density functional theory. 2021 , 129, 065304	5
363	Physical Origin of the Mechanochemical Coupling at Interfaces. 2021 , 126, 076001	2
362	PoreMS: a software tool for generating silica pore models with user-defined surface functionalisation and pore dimensions. 1-11	6
361	Simulations of the IR and Raman spectra of water confined in amorphous silica slit pores. 2021 , 154, 104503	2
360	Covalent Hybrid Elastomers Based on Anisotropic Magnetic Nanoparticles and Elastic Polymers. 2021 , 3, 1324-1337	4
359	Approaches Toward In Situ Reinforcement of Organic Rubbers: Strategy and Recent Progress. 1-32	1
358	Adsorption of constitutional isomers of cyclic monoterpenes on hydroxylated silica surfaces. 2021 , 154, 124703	О
357	Understanding the Confinement Effects and Dynamics of Methylimidazole in Nanoscale Silica Pores. 2021 , 125, 7421-7430	O
356	Ultrasmooth cobalt films on SiO2 by chemical vapor deposition using a nucleation promoter and a growth inhibitor. 2021 , 39, 023414	2
355	Density Functional Theory Study on the Morphology Evolution of Hydroxylated Cristobalite Silica and Desilication in the Presence of Methanol. 2021 , 125, 7868-7879	Ο
354	Unravelling the Role of Al-alkyl Cocatalyst for the VOx/SiO2 Ethylene Polymerization Catalyst: Diethylaluminum Chloride Vs. Triethylaluminum. 2021 , 13, 2278-2292	3
353	Selective chemical vapor deposition of HfB2 on Al2O3 over SiO2 and the acceleration of nucleation on SiO2 by pretreatment with Hf[N(CH3)2]4. 2021 , 39, 023415	2
352	Effects of alumina airborne-particle abrasion on the surface properties of CAD/CAM composites and bond strength to resin cement. 2021 , 40, 431-438	2
351	Characterization of H4SiW12O40 supported on mesoporous silica (SBA-15), non-structured amorphous silica and 🗟 lumina. 2021 , 395, 387-398	1

350	Hydroxylation methods for mesoporous silica and their impact on surface functionalisation. 2021 , 317, 110989	5
349	Impact of molecular layer on emergent photovoltaic response in silicon unraveled by photoelectron spectroscopy. 2021 , 544, 148807	2
348	Alkoxylation Reaction of Alcohol on Silica Surfaces Studied by Sum Frequency Vibrational Spectroscopy. 2021 , 125, 8638-8646	5
347	Complex Formation and Dissociation Dynamics on Amorphous Silica Surfaces. 2021 , 125, 4566-4581	3
346	A comparative study of different techniques for quantum dot nano-particles immobilization on glass surface for fabrication of solid phase fluorescence opto-sensors. 2021 , 23, 100907	2
345	A molecular model for obsidian hydration dating. 2021 , 36, 102824	
344	Activation of Peroxymonosulfate by Chrysotile to Degrade Dyes in Water: Performance Enhancement and Activation Mechanism. 2021 , 11, 400	1
343	Tailoring Interfacial Properties in PolymerBilica Nanocomposites via Surface Modification: An Atomistic Simulation Study. 2021 , 3, 2576-2587	4
342	Characterization of Hybrid Materials Prepared by Sol-Gel Method for Biomedical Implementations. A Critical Review. 2021 , 14,	10
341	A Review of Engineering Dielectric Properties of Nanocomposites through Effectively Removed Interfacial Water. 2021 , 28, 448-459	
340	The effect of short silica fibers (0.3 Th 3.2 Th) on macrophages. 2021 , 769, 144575	O
339	Individual Contributions of Adsorbed and Free Chains to Microscopic Dynamics of Unentangled poly(ethylene Glycol)/Silica Nanocomposite Melts and the Important Role of End Groups: Theory and Simulation. 2021 , 54, 4470-4487	5
338	XANES reflects coordination change and underlying surface disorder of zinc adsorbed to silica. 2021 , 28, 1119-1126	0
337	Hydroxylation of Apollo 17 Soil Sample 78421 by Solar Wind Protons. 2021 , 126, e2021JE006845	3
336	Effect of surfactant concentration on the formation of Fe2O3@SiO2 NIR-reflective red pigments. 2021 , 47, 13147-13155	9
335	Influence of seawater on alkali-activated slag concrete. 2021 , 54, 1	4
334	Heterogeneous Interactions of Prevalent Indoor Oxygenated Organic Compounds on Hydroxylated SiO Surfaces. 2021 , 55, 6623-6630	2
333	First-principles study of the surface of silica and sodium silicate glasses. 2021 , 103,	2

332	Wafer-Scale Growth of a MoS2 Monolayer via One Cycle of Atomic Layer Deposition: An Adsorbate Control Method. 2021 , 33, 4099-4105	4
331	Room temperature and ambient pressure deposition of Cu-BTC MOF on SBA-15 functionalized silica supports by simple spray layer-by-layer method. 2021 , 27, 102388	1
330	Mechanisms of shale water wettability alteration with chemical groups after CO2 injection: Implication for shale gas recovery and CO2 geo-storage. 2021 , 90, 103922	5
329	Binding of CO and O on Low-Symmetry Pt Clusters Supported on Amorphous Silica. 2021 , 125, 13780-13787	1
328	Improving the flame retardance of hydrophobic silica aerogels through a facile post-doping of magnesium hydroxide. 2021 , 32, 1891-1901	3
327	Surface charge density measurement of a single protein molecule with a controlled orientation by AFM. 2021 , 120, 2490-2497	3
326	The effect of nanosilica sizes in the presence of nonionic TX100 surfactant on CO2 foam flooding. 2021 ,	Ο
325	Electrical properties of CaWO4BiO2 composites. 2021 , 364, 115626	О
324	Modeling Contact Angle vs. Temperature for the Quartz-Water-Decane System. 2021 , 1-13	
323	Preparation and hydrophobicity modification of poly(vinylidene fluoride-co-hexafluoropropylene) membranes for pervaporation separation of volatile organic compound from water. 2021 , 42, 4684-4697	2
322	Anticorrosive Enamels: Evaluation of Nanocomposite Additives on Enamel Efficiency on Cold Rolled Steel. 2021 , 30, 4103-4116	
321	Nano surface modification of poly(ethylene terephthalate) fabrics for enhanced comfort properties for activewear. 2021 , 98, 217-230	2
320	Elucidating the Role of Water-Related Traps in the Operation of Polymer Field-Effect Transistors. 2021 , 7, 2100393	2
319	Effects of CO and temperature on phytolith dissolution. 2021 , 772, 145469	7
318	Controlled Grafting Synthesis of Silica-Supported Boron for Oxidative Dehydrogenation Catalysis. 2021 , 125, 12636-12649	6
317	Effect of copper dispersion on SBA-15 and SBA-16 affinity towards carbon dioxidell approach through thermal programmed desorption. 2021 , 23, 1	1
316	Effect of Surface Silanol Density on the Proton Conductivity of Polymer-Surface-Functionalized Silica Nanoparticles. 2021 , 9, 10093-10099	2
315	Atmospheric Pressure Dielectric Barrier Discharge Plasma-Enhanced Optical Contact Bonding of Coated Glass Surfaces. 2021 , 11, 6755	

314	Oil Displacement Efficiency of a Silica/HPAM Nanohybrid. 2021, 35, 13077-13085	1
313	Labeling and Probing the Silica Surface Using Mechanochemistry and O NMR Spectroscopy*. 2021 , 27, 12574-12588	4
312	Ultrafast Dynamics and Liquid Structure in Mesoporous Silica: Propagation of Surface Effects in a Polar Aprotic Solvent. 2021 , 125, 10018-10034	2
311	High-temperature oxidation resistance and thermal stability of higher manganese silicide powder synthesized by pack cementation. 2021 , 873, 159842	3
310	Synthesis of MgCl2/vermiculite and its water vapor adsorption-desorption performance.	3
309	Structure of the Water Molecule Layer between Ice and Amorphous/Crystalline Surfaces Based on Molecular Dynamics Simulations. 2021 , 125, 9601-9609	O
308	Permittivity Characterization of Dielectric Surfaces Using Nanofabricated In-Plane Capacitors. 2021 , 68, 4033-4038	1
307	Design of Silica Nanoparticles-Supported Metal Catalyst by Wet Impregnation with Catalytic Performance for Tuning Carbon Nanotubes Growth. 2021 , 11, 986	2
306	Sustainable Thermochemical Extraction of Amorphous Silica from Biowaste. 1	O
305	Silica coating of Fe3O4 magnetic nanoparticles with PMIDA assistance to increase the surface area and enhance peptide immobilization efficiency. 2021 , 47, 23078-23087	2
304	Effects of material texture and packing density on the interfacial polarization of granular soils. 1-58	1
303	Dynamical evolution and thermal history of asteroids (3200) Phaethon and (155140) 2005 UD. 2021 , 366, 114535	8
302	Effects of the acidity and shape selectivity of dealuminated zeolite beta on butene transformations. 2021 , 300, 120694	2
301	The pH dependence of the isotopic composition of boron adsorbed on amorphous silica. 2021 , 308, 1-20	O
300	Compressibility, stiffness and electrical resistivity characteristics of sanddiatom mixtures. 1-14	1
299	Investigating the Mineralogical and Chemical Effects of CO2 Injection on Shale Wettability at Different Reservoir Temperatures and Pressures. 2021 , 35, 14838-14851	2
298	Alteration of potash-lime silicate glass in atmospheric medium: study of mechanisms and kinetics using 18O and D isotopes. 2021 , 570, 121020	1
297	Effects of rice-straw derived phytoliths on the surface charge properties of paddy soils. 2021 , 400, 115234	1

296	Some critical observations about the degradation of glass: The formation of lamellae explained. 2021 , 569, 120984	2
295	Preparation of fractal-like silica particles based on StBer method by using tetrabutylammonium hydroxide as co-catalyst. <i>Colloids and Surfaces A: Physicochemical and Engineering Aspects</i> , 2021 , 5.1 626, 127091	О
294	Vapor-phase grafting of a model aminosilane compound to Al2O3, ZnO, and TiO2 surfaces prepared by atomic layer deposition. 2021 , 562, 149996	3
293	Size-dependent dissociation of surface hydroxyl groups of silica in aqueous solution. <i>Colloids and Surfaces A: Physicochemical and Engineering Aspects</i> , 2021 , 629, 127446	О
292	Recovery and characterization of useful benzene derivatives from spent engine oil through solvent extraction. 2021 , 175, 51-60	7
291	Understanding geopolymer binder-aggregate interfacial characteristics at molecular level. 2021 , 149, 106582	5
290	Functionalization of biosourced silica and surface reactions with mercury in aqueous solutions. 2021 , 423, 129745	2
289	Molecular investigation on the desorption process of alkane contaminant from fused silica surface in nonionic surfactant solution. 2021 , 565, 150516	O
288	On nanocomposite fabrication: using rheology to characterize filler/polymer interactions in epoxy-based nanocomposites. 2021 , 22, 100559	0
287	Oxo/imido heterometathesis: From molecular stoichiometric studies to well-defined heterogeneous catalysts. 2021 , 448, 214112	О
286	Preparation of MS/MIL-101(Cr) composite material and its properties of atmospheric water collection. 2021 , 304, 122572	1
285	Aqueous solutions of AOT as a dispersion medium for stabilization of SiO2 nanoparticles. 2021 , 343, 117591	1
284	Crystal face dependent wettability of Equartz: Elucidation by time-of-flight secondary ion mass spectrometry techniques combined with molecular dynamics. 2022 , 607, 1699-1708	О
283	Preparation and application of porous materials from coal gasification slag for wastewater treatment: A review. 2022 , 287, 132227	14
282	Effect of deposition temperature and surface reactions in atomic layer deposition of silicon oxide using Bis(diethylamino)silane and ozone. 2022 , 571, 151231	2
281	Lithium Adsorption Mechanism for Li2TiO3. 2021 , 19-27	
280	Effects of nanoconfinement and surface charge on iron adsorption on mesoporous silica. 2021 , 8, 1992-2005	3
279	A novel hemocompatible core@shell nanosystem for selective targeting and apoptosis induction in cancer cells. 2021 , 8, 2697-2712	3

278	CO Oxidation Efficiency and Hysteresis Behavior over Mesoporous Pd/SiO2 Catalyst. 2021, 11, 131	5
277	Thin-film Engineering by Atomic-layer Deposition for Ultra-scaled and Novel Devices. 2005 , 31-38	1
276	Acceleration of cement hydration from supplementary cementitious materials: Performance comparison between silica fume and hydrophobic silica. 2020 , 112, 103688	20
275	Effect of cleaning methods on the dissolution of diatom frustules. 2020 , 224, 103826	5
274	Impact of Adsorbed Water on the Interaction of Limonene with Hydroxylated SiO: Implications of EHydrogen Bonding for Surfaces in Humid Environments. 2020 , 124, 10592-10599	5
273	Modeling Enantiomeric Separations as an Interfacial Process Using Amylose Tris(3,5-dimethylphenyl carbamate) (ADMPC) Polymers Coated on Amorphous Silica. 2020 , 36, 1113-1124	12
272	On the Structure and Lithium Adsorption Mechanism of Layered HTiO. 2021 , 13, 8361-8369	8
271	Amine-Functionalized Nanoporous Silica Monoliths for Heterogeneous Catalysis of the Knoevenagel Condensation in Flow. 2021 , 6, 425-437	4
270	In situ TEM observation of liquid-state Sn nanoparticles vanishing in a SiO2 structure: a potential synthetic tool for controllable morphology evolution from corelhell to yolklhell and hollow structures. 2020 , 2, 1456-1464	1
269	Microconical surface structuring of aluminium tubes by femtosecond laser processing. 2020 , 4, 111001	2
268	Multiphysics model of chemical aging in frictional contacts. 2018, 2,	8
267	In situ x-ray studies of the incipient ZnO atomic layer deposition on In0.53Ga0.47As. 2020 , 4,	3
266	Effect of Silicon, Vanadium, and Tungsten Oxide Additives on the Electrical Properties of Composites Based on CaWO4. 2020 , 94, 2482-2487	2
265	Facile fabrication of mesostructured natural rubber/silica nanocomposites with enhanced thermal stability and hydrophobicity. 2019 , 14, 382	4
264	Bouncing of Hydroxylated Silica Nanoparticles: an Atomistic Study Based on REAX Potentials. 2020 , 15, 67	7
263	THE EFFECT OF SIO2 NANOPARTICLES ON PERFORMANCE OF CEMENT-BASED MATERIALS. 2018 , 3, 6-16	1
262	DEHYDRATION AND REHYDRATION OF AN ION-LEACHABLE GLASS USED IN GLASS-IONOMER CEMENTS. 2017 , 106-109	2
261	Evaluation of Interaction between Metal Ions and Nonionic Surfactants Containing Polyoxyethylene Chain by Measurement of Streaming Potential. 2018 , 67, 453-459	1

260	Forced Electrocodeposition of Silica Particles into Nickel Matrix by Horizontal Impinging Jet Cell. 2017 , 05, 51-63	1
259	Functionalization of Silica Surface with UV-Active Molecules by Multivalent Organosilicon Spacer. 2016 , 06, 163-174	4
258	Multinuclear Solid-state NMR Investigation of Nanoporous Silica Prepared by Sol-gel Polymerization Using Sodium Silicate. 2011 , 32, 3644-3649	13
257	Thermal Modulation of Photoluminescence from Single-Layer MoS2. 2014 , 35, 3077-3080	9
256	The role of contact angle and pore width on pore condensation and freezing. 2020, 20, 9419-9440	11
255	Silica particles with fluorescein-labelled cores for evaluating accessibility through fluorescence quenching by copper 2021 , 3, 6459-6467	1
254	Light Transmission and Surface Topography of KU-1 Optical Quartz After Sputtering and Cleaning from Al Films in RF Discharge of H2(D2)Ne Mixtures. 2021 , 15, 1029-1038	
253	Key factor analysis of nano silica on the dispersion in underfill. 2021,	
252	Naked eye detection of cyanide ion in water: highly selective azo-azomethine chromogenic receptor immobilized onto solid scaffolds. 1	1
251	Composite Films of HDPE with SiO and ZrO Nanoparticles: The Structure and Interfacial Effects. 2021 , 11,	Ο
250	Roles of paper composition and humidity on the adhesion between paper sheet and glass: a molecular dynamics study. 1	Ο
249	Supported MoOx and WOx Solid Acids for Biomass Valorization: Interplay of Coordination Chemistry, Acidity, and Catalysis. 13603-13648	2
248	Dehydration of Fructose to 5-Hydroxymethylfurfural: Effects of Acidity and Porosity of Different Catalysts in the Conversion, Selectivity, and Yield. 2021 , 3, 1189-1202	1
247	Surface Chemistry of Nanohybrids with Fumed Silica Functionalized by Polydimethylsiloxane/Dimethyl Carbonate Studied Using H, C, and Si Solid-State NMR Spectroscopy. 2021 , 26,	0
246	Study of the stability of CsI and iodine oxides (IOx) aerosols and trapping efficiency of small aerosols on sand bed and metallic filters under irradiation. 2021 , 142, 104013	Ο
245	Effective reduction of biofilm through photothermal therapy by gold core@shell based mesoporous silica nanoparticles. 2021 , 328, 111489	4
244	Evaluation and Interpretation of the Experimental Data. 2008 , 119-190	
243	Solid Additives. 2009, 723-755	1

242	Water Associated with Bio-Objects: Cells and Tissues. 2013 , 806-905	
241	An Ellipsometric Model for Establishing Thickness of Thin Water Nanolayers on the Silicon Wafers. 2015 , 139-145	
240	Quantitative Analysis of Grafted Methacrylate Groups by Michael Addition Reaction between Primary and Secondary Amino Groups on the Silica Nanoparticle Surface with 3-(Acryloyloxy)-2-Hydroxypropyl Methacrylate. 2015 , 39, 300-310	
239	Corrosion resistance of nanosilicasilicate conversion coatings on aluminum prepared by the dip immersion method. 2015 , 57, 402-408	1
238	Organic Modification of Hydroxylated Nanoparticles: Silica, Sepiolite, and Polysaccharides. 2016 , 1061-1100	
237	THE HYDRATION OF AN ION-LEACHABLE GLASS USED IN GLASS-IONOMER CEMENTS. 2016 , 243-247	2
236	Identification of Heterogeneous Surface Properties via Fluorescent Probes. 2016, 353-370	
235	Chapter 2 Preparation of Nanoparticles. 2016 , 9-40	
234	Chapter 10 Suppression of Surface Erosion by Surface-Treated Fillers. 2016 , 281-318	
233	Thermal Effect of Er3+Ions Embedded in Smart Nano-Composite Oxide Material Prepared by Sol-Gel Technique. 2017 , 132, 1277-1283	2
232	Amine-Functionalized Mesoporous Silica Nanoparticles: A New Nanoantibiotic for Bone Infection Treatment. 2017 , 3,	1
231	Chapter 14 Whispering Gallery Mode Resonators as Opto-Mechanical Probes to Nanoparticle-Microcavity Interaction and Charge. 2018 , 267-276	
230	Low temperature bonding of heterogeneous materials using Al2O3 as an intermediate layer. 2018,	О
229	Microstructural origin of compressive in situ stresses in electron-gun-evaporated silica thin films. 2019 , 3,	1
228	Longitudinal position dependence of the second-harmonic generation of optically trapped silica microspheres. 2020 , 45, 3196-3199	
227	Hydrophilic direct bonding and debonding of ultrathin glass substrates for high-temperature devices. 2020 , 59, 070901	
226	Synthesis of Surface-Porous Sorbents Based on Silicon Dioxide and Studying Their Adsorption Properties. 2020 , 93, 1211-1220	1
225	Silica-Supported Sulfuric Acid as Doping Agent in Synthesis of a New Composite of Poly(o-methoxyaniline) Under Solid-State Condition. 17, 115-126	

224	Thermal decomposition of volcanic glass (rhyolite): Kinetic deconvolution of dehydration and dehydroxylation process. 2021 , 179082	2
223	Unified Description of the Specific Heat of Ionic Bulk Materials Containing Nanoparticles. 2021, 15, 563-574	2
222	Food grade silica nanoparticles cause non-competitive type inhibition of human salivary \(\hat{\text{\text{m}}}\)mylase because of surface interaction. 2021 , 2, 632-641	1
221	Thin Oxide Films as Model Systems for Heterogeneous Catalysts. 2020 , 267-328	Ο
220	Direct-Bandgap Bilayer WSe /Microsphere Monolithic Cavity for Low-Threshold Lasing. 2021 , e2106502	1
219	Nanopore networks in colloidal silica assemblies characterized by XCT for confined fluid flow modeling. 2021 , 208, 109780	
218	Atmospheric-Pressure Plasma-Enhanced Spatial ALD of SiO Studied by Gas-Phase Infrared and Optical Emission Spectroscopy. 2021 , 125, 24945-24957	2
217	Effects of Water on the Dielectric Response of Calcined Silica-based Polyethylene Nanocomposites. 2020 ,	
216	Precipitated Silica and Non-Black Fillers. 2020 , 451-532	
215	Capillary-condensed water in nonporous nanoparticle films evaluated by impedance analysis for nanoparticle devices. 2020 , 31, 455701	1
214	A DFT study of the aldol condensation reaction in the processing of ethanol to 1,3-butadiene on a MgO/SiO2 surface.	O
213	Organometallic Chemistry on Oxide Surfaces. 2021 ,	
212	Synthesis of silica nanoparticles for biological applications. 2022 , 377-412	О
211	Self-Assembly of Au-FeO Hybrid Nanoparticles Using a Sol-Gel Pechini Method. 2021 , 26,	1
210	Role of Mesoporous Silica Nanoparticles as Drug Carriers: Evaluation of Diverse Mesoporous Material Nanoparticles as Potential Host for Various Applications. 2022 , 205-234	O
209	Influence of ionic strength and surfactant concentration on the alkane contaminant desorption in solution: A molecular dynamics simulation. 2021 , 118154	1
208	Organosilica Nanoparticles with Ordered Trimodal Porosity and Selectively Functionalized Mesopores .	
207	Nanoantibiotics Based in Mesoporous Silica Nanoparticles: New Formulations for Bacterial Infection Treatment 2021 , 13,	3

206	Cluster Model Simulations of Metal-Doped Amorphous Silicates for Heterogeneous Catalysis.	2
205	日本日本日本日本日本日本日本日本日本日本日本日本日本日本日本日本日本日本日本	
204	A simple liquid state H NMR measurement to directly determine the surface hydroxyl density of porous silica. 2021 , 57, 12804-12807	
203	CO2 capture and CO2/CH4 separation by silicas with controlled porosity and functionality. 2022 , 332, 111651	O
202	Revealing the dehydration/deuteration processes at the liquid-solid interface by nuclear magnetic resonance spectroscopy. <i>Colloids and Surfaces A: Physicochemical and Engineering Aspects</i> , 2022 , 5.1 637, 128260	1
201	Quantifying the effect of polynuclear hydroxocomplex adsorption on the charge reversals at solid surfaces. 2022 , 10, 107126	Ο
200	Assessment of nanoparticle immersion depth at liquid interfaces from chemically equivalent macroscopic surfaces 2021 , 611, 670-683	1
199	Chemical and Microstructural Properties of Designed Cohesive M-S-H Pastes 2022, 15,	O
198	Proton transport over nanoparticle surface in insulating nanoparticle film-based humidity sensor.	
197	Evidence for Entropically Controlled Interfacial Hydration in Mesoporous Organosilicas 2022,	Ο
196	Hydrometallurgical Leaching Behavior and Kinetic Modeling of Blast Furnace Slag in Hydrochloric Acid. 2022 , 8, 170	0
195	Contact angle hysteresis. 2022 , 101574	5
194	Surface Protolysis and Its Kinetics Impact the Electrical Double Layer 2022 , 128, 056001	2
193	Effects of pH and vanadium concentration during the impregnation of Na-SiO2 supported catalysts for the oxidation of propane. 2022 , 520, 112158	O
192	Mechanism and Free-Energy Landscape of Peptide Bond Formation at the SilicalWater Interface. 2821-2830	1
191	Density functional theory study on the selective capping of cobalt on copper interconnect. 2022 , 585, 152750	Ο
190	Surface Organometallic Chemistry and Catalysis. 2022 ,	
189	Microstructure and Segmental Dynamics of Industrially Relevant Polymer Nanocomposites. 2022 , 251-290	

188	Core vs. surface labelling of mesoporous silica nanoparticles: advancing the understanding of nanoparticle fate and design of labelling strategies.	1
187	Internal Gas Composition and Pressure in As-drawn Hollow Core Optical Fibers. 2022, 1-1	O
186	In situ plasma cleaning of large-aperture optical components in ICF.	3
185	Improvement of the Thermal Insulation Performance of Silica Aerogel by Proper Heat Treatment: Microporous Structures Changes and Pyrolysis Mechanism 2022 , 8,	2
184	Wettability of Shale/Oil/Brine Systems: A New Physicochemical and Imaging Approach. 2022,	O
183	Soft-Hard Segment Combined Carbonized Polymer Dots for Flexible Optical Film with Superhigh Surface Hardness 2022 ,	2
182	Relation between Reactive Surface Sites and Precursor Choice for Area-Selective Atomic Layer Deposition Using Small Molecule Inhibitors 2022 , 126, 4845-4853	5
181	Heterogeneous Interactions between Carvone and Hydroxylated SiO2.	2
180	Study on the Effect of Amorphous Silica from Waste Granite Powder on the Strength Development of Cement-Treated Clay for Soft Ground Improvement. 2022 , 14, 4073	
179	Computational Insights into the Multisite Nature of the Phillips CrOx/SiO2 Catalyst for Ethylene Polymerization: The Perspective of Chromasiloxane Ring Size and F Modification. 2022 , 12, 3589-3603	O
178	Enhanced morphology and hydrophilicity of PVDF flat membrane with modified CaCO3@SMA additive via thermally induced phase separation method. 2022 , 107, 444-455	2
177	Atom-by-Atom Synthesis of Multiatom-Supported Catalytic Clusters by Liquid-Phase Atomic Layer Deposition. 2022 , 10, 3455-3465	O
176	Influence of the Support on Propene Oxidation over Gold Catalysts. 2022, 12, 327	0
175	Relevance of Colloid Inherent Salt Estimated by Surface Complexation Modeling of Surface Charge Densities for Different Silica Colloids. 2022 , 6, 23	
174	Competitive Protein Adsorption on Charge Regulating Silica-Like Surfaces: The Role of Protonation Equilibrium 2022 ,	
173	Applicability of the linearized Poisson-Boltzmann theory to contact angle problems and application to the carbon dioxide-brine-solid systems 2022 , 12, 5710	1
172	Simulations of Glass Water Interactions. 2022 , 490-521	1
171	Effect of protein adsorption on the dissolution kinetics of silica nanoparticles 2022 , 214, 112466	1

170	Impact of initial states on the vapor hydration of iodine-bearing borosilicate glass. 2022 , 587, 121584	O
169	Silicon foliar spraying in the reproductive stage of cotton plays an equivalent role to boron in increasing yield, and combined boron-silicon application, without polymerization, increases fiber quality. 2022 , 182, 114888	O
168	Dependence of the Hydration of the Lunar Surface on the Concentrations of TiO2, Plagioclase, and Spinel. 2022 , 14, 47	
167	Hygrothermal aging effect on the properties of PMMA nanocomposites reinforced by ceramic nanoparticles. 2022 , 56, 727-741	1
166	Understanding the Olefin Polymerization Initiation Mechanism by Cr(III)/SiO2 Using the Activation Strain Model. 2022 , 126, 296-308	3
165	Silica-Mediated Monohydrolysis of Dicarboxylic Esters. 2021 , 2021, 6773-6776	O
164	Bisphenol A Adsorption on Silica Particles Modified with Beta-Cyclodextrins 2021 , 12,	O
163	The nature of column boundaries in micro-structured silicon oxide nanolayers. 2021 , 9, 121107	1
162	From inert silica carrier derivatives to a source of bioavailable silicium in the field of cosmetic, pharmaceutical, luxury, and food industries. 2022 , 525-544	
161	Nanosilica-mediated plant growth and environmental stress tolerance in plants: mechanisms of action. 2022 , 325-337	
160	A comparative study of the dissolution mechanisms of amorphous and crystalline feldspars at acidic pH conditions. 2022 , 6,	О
159	Surface Hydroxyl Dependent Adsorption of Ruthenium on SiO2 (001) - Understanding MetalBupport Interaction. 2022 , 153396	O
158	Does the Roll-off Angle Depend on Work of Adhesion?. 2022 ,	0
157	Data_Sheet_1.pdf. 2019 ,	
156	[Novel submicron nonporous silica material modification with high carbon content and its application in reversed-phase pressurized capillary electrochromatography] 2022 , 40, 88-99	
155	Comparison between the Optical Performance of Photonic Bandgap and Antiresonant Hollow Core Fibers after Long-Term Exposure to the Atmosphere. 2022 ,	
154	Electron-Stimulated Hydroxylation of Silica Bilayer Films Grown on Ru(0001): A Combined HREELS and EPR Study. 2022 , 126, 7956-7964	О
153	Water Harvesting from Air: Current Passive Approaches and Outlook. 2022 , 4, 1003-1024	7

152	Improving the physical and mechanical properties and alkali resistance of fireclay-based castables by modifying their structure with SiO2 sol. 2022 ,	O
151	Original Basic Activation for Enhancing Silica Particle Reactivity: Characterization by Liquid Phase Silanization and Silica-Rubber Nanocomposite Properties 2022 , 14,	O
150	High-performance MoS2/p+-Si heterojunction field-effect transistors by interface modulation.	O
149	Biocatalytic asymmetric synthesis of secondary allylic alcohols using Burkholderia cepacia lipase immobilized on multiwalled carbon nanotubes 2022 ,	
148	Tuning Molecular Inhibitors and Aluminum Precursors for the Area-Selective Atomic Layer Deposition of Al2O3.	1
147	A Chemical Nanoreactor Based on a Levitated Nanoparticle in Vacuum 2022,	2
146	Size effect and mucus role on the intestinal toxicity of the E551 food additive and engineered silica nanoparticles 2022 , 1-18	1
145	The coordination chemistry of oxide and nanocarbon materials 2022,	2
144	Auto-Fluorescence in Phytoliths Mechanistic Understanding Derived From Microscopic and Spectroscopic Analyses. 2022 , 10,	O
143	Removal of Pb2+, Cr3+ and Hg2+ ions from aqueous solutions using SiO2 and amino-functionalized SiO2 particles.	
142	Engineering mesoporous silica nanoparticles for drug delivery: where are we after two decades?.	19
141	Influence of Electron beam radiation on the properties of Surface-Modified Titania-Filled gel polymer electrolytes using vinyltriethoxysilane (VTES) for lithium battery application. 2022 , 4, 100383	
140	Molecular Dynamics Simulations of Reverse Osmosis in Silica Nanopores. 2022 , 126, 9161-9172	1
139	Effect of Chemical and Thermal Treatment Priority on Physicochemical Properties and Removal of Crystal Violet Dye from Aqueous Solution. 2022 , 7,	O
138	Vibrational spectroscopic evaluation of hydrophilic or hydrophobic properties of oxide surfaces.	1
137	Thermal-mechanical-photo-activation effect on silica micro/nanofiber surfaces: origination, reparation and utilization.	
136	Bioinspired Mesoporous Silica for Cd(II) Removal from Aqueous Solutions.	O
135	Chemical Creep and Its Effect on Contact Aging. 1368-1373	

134 Modeling of linear nanopores in a-SiO2 tuning pore surface structure. **2022**, 112077

133	Two-Dimensional Ultrathin Silica Films.	1
132	The Nature of Interface Interactions Leading to High Ionic Conductivity in LiBH4/SiO2 Nanocomposites.	O
131	Effect of Inorganic Acid Concentration on Sandstone Surface Chemistry Examined via Nuclear Magnetic Resonance.	
130	Gas Adsorption and Diffusion Behaviors in Interfacial Systems Composed of a Polymer of Intrinsic Microporosity and Amorphous Silica: A Molecular Simulation Study. 2022 , 38, 7567-7579	
129	Adhesion and Cohesion of Silica Surfaces with Quartz Cement: A Molecular Simulations Study.	1
128	Intrinsic properties of multi-component glass surfaces exposed to aqueous hydrofluoric (HF) and/or hydrochloric (HCl) acid-based treatments. 2022 , 592, 121766	О
127	New insights into the interaction of triethylphosphine oxide with silica surface: exchange between different surface species. 2022 , 24, 16755-16761	
126	Effect of the Drying Procedure of Hydrophobic Hybrid Sonogels for Organic Solvent Remediation: Structure, Mechanical Properties and Absorption Performance.	
125	A General Route to Flame Aerosol Synthesis and in situ Functionalization of Mesoporous Silica.	
124	A General Route to Flame Aerosol Synthesis and in situ Functionalization of Mesoporous Silica.	
123	Two-Phase Conceptual Framework of Phosphatase Activity and Phosphorus Bioavailability. 13,	1
122	Photocatalytic activities of siliceous termite hill-based composites in the degradation of dye.	
121	Understanding the Role of Fe Doping in Tuning the Size and Dispersion of GaN Nanocrystallites for CO2-Assisted Oxidative Dehydrogenation of Propane. 2022 , 12, 8527-8543	2
120	Insight on the Dependence of the Drug Delivery Applications of Mesoporous Silica Nanoparticles on Their Physical Properties.	О
119	Addition of silicon to boron foliar spray in cotton plants modulates the antioxidative system attenuating boron deficiency and toxicity. 2022 , 22,	1
118	Experiment study on normalized compression behaviour of marine diatomaceous soil considering microstructure of biogenic silica. 2022 , 125, 103254	
117	Rice husk silica as a sustainable filler in the tire industry. 2022 , 15, 104086	1

116	Contact time dependence of adhesion force at silica/silica interface on AFM: Influence of relative humidity and contact history. 2022 , 600, 154175	1
115	Interactions and dynamics of cations and interlayer quest molecules in nontronite and nontroniteformamide intercalation. 2022 , 228, 106637	О
114	Materials and devices for atmospheric water harvesting. 2022 , 3, 100976	1
113	Metabolically Doping of 3D Diatomaceous Biosilica with Titanium. 2022 , 15, 5210	
112	Preparation and characterization of mesoporous amorphous nano-silica and nano-cristobalite for value enhancement of low-cost Egyptian waste materials. 2022 ,	О
111	PREPARATION OF SILVER DOPED RICE HUSK SILICA COMPOSITES USING SOL GEL METHOD. 2022 , 365-373	
110	Amorphous silica dissolution kinetics in freshwater environments: Effects of Fe2+ and other solution compositional controls. 2022 , 158239	О
109	Sorbents for Atmospheric Water Harvesting: from Design Principles to Applications.	1
108	Sorbents for Atmospheric Water Harvesting: from Design Principles to Applications.	2
107	A Tag-and-Count Approach for Quantifying Surface Silanol Densities on Fused Silica Based on Atomic Layer Deposition and High-Sensitivity Low-Energy Ion Scattering. 2022 , 154551	O
106	Silica as a Model Ice-Nucleating Particle to Study the Effects of Crystallinity, Porosity, and Low-Density Surface Functional Groups on Immersion Freezing.	1
105	The influence of sediment diagenesis and aluminium on oxygen isotope exchange of diatom frustules. 2022 , 333, 362-372	
104	A clean dispersant for nano-silica to enhance the performance of cement mortars. 2022, 371, 133647	O
103	Interfacial engineering of epoxy/silica nanocomposites by amino-rich polyethyleneimine towards simultaneously enhanced rheological and thermal-mechanical performance for electronic packaging application. 2022 , 245, 110214	O
102	SO2 sensing mechanism of nanostructured SiC-SiOxC core shell: An operando DRIFT investigation. 2022 , 371, 132497	
101	Improving the colloidal stability of PEGylated BaTiO3hanoparticles with surfactants. 2022, 111701	1
100	Effect of geometric modification of fumed nanoscale silica for medical applications on adsorption of human serum albumin: Physicochemical and surface properties. 2022 , 220, 1294-1308	О
99	Effect of counter-surface chemical activity on mechanochemical removal of GaAs surface. 2022 , 176, 107928	О

98	Light-responsive Pickering emulsions based on azobenzene-modified particles. 2022 , 18, 5770-5781	1
97	A molecular dynamics study of nonlinear spectra and structure of charged (101) quartz/water interface.	О
96	A wear-resistant silicon nano-spherical AFM probe for robust nanotribological studies. 2022 , 24, 23849-23857	0
95	Surface activities of silica powders produced by milling. 2022,	О
94	Self-assembled monolayers for silicon passivated contacts. 2022 ,	О
93	Substrate stiffness reduces particle uptake by epithelial cells and macrophages in a size-dependent manner through mechanoregulation.	O
92	Recent advances in the applications of mesoporous silica in heterogeneous catalysis. 2022 , 12, 5765-5794	1
91	Comparative characteristics of the structure and physicochemical properties of silica synthesized by pyrogenic and fluoride methods.	О
90	Tailoring the Hydroxyl Density of Glass Surface for Anionic Ring-Opening Polymerization of Polyamide 6 to Manufacture Thermoplastic Composites. 2022 , 14, 3663	0
89	Well-structured 3D channels within GO-based membranes enable ultrafast wastewater treatment.	О
88	Influence of 虧i 3 N 4 whiskers on sintering and crystallization of fused silica ceramics.	0
87	A comprehensive review of anionic azoldyes adsorption on surface-functionalised silicas.	О
86	Passivation of Mid-Gap Electronic States at Calcium Aluminosilicate Glass Surfaces upon Water Exposure: An Ab Initio Study. 2022 , 126, 7709-7719	О
85	Comparative Characteristics of the Structure and Physicochemical Properties of Silica Synthesized by Pyrogenic and Fluoride Methods.	О
84	The Modulation of Electrokinetic Streaming Potentials of Silicon-Based Surfaces through Plasma-Based Surface Processing. 2022 , 38, 11837-11844	0
83	Interactions during the Adsorption of Heterocycles on Zeolites, Silica Gels, and Activated Carbons.	О
82	Siliceous termite hill supported ZnO-TiO2 as a solar light responsive photocatalyst: Synthesis, characterization and performance in degradation of methylene blue dye. 2022 , 34, 102360	О
81	Atomic Layer Deposition of Silicon Oxide Films Using Bis(dimethylaminomethylsilyl)trimethylsilylamine and Ozone: First-principle and Experimental Study.	O

80	The Effects of Humidity on Dielectric Permittivity of Surface Modified TiO2 and MgO Based Polypropylene Nanocomposites. 2022 , 1-1	0
79	Effect of Superhydrophobic Coating and Nanofiller Loading on Facial Elastomer Physical Properties. 2022 , 15, 7343	Ο
78	Advanced Dye Sorbents from Combined Stereolithography 3D Printing and Alkali Activation of Pharmaceutical Glass Waste. 2022 , 15, 6823	1
77	Bioactive nanoglasses and xerogels (SiO2faO and SiO2faOP2O5) as promising candidates for biomedical applications. 2022 ,	1
76	Functional rubber composites based on silica-silane reinforcement for green tire application: the state of the art. 2022 , 3,	1
75	Mesoporous Spherical Silica Filler Prepared from Coal Gasification Fine Slag for Styrene Butadiene Rubber Reinforcement and Promoting Vulcanization. 2022 , 14, 4427	O
74	Immobilization of Metronidazole on Mesoporous Silica Materials. 2022 , 14, 2332	O
73	Structural and acidity analysis of heteropolyacids supported on faujasite zeolite and its effect in the esterification of oleic acid and n-butanol. 2022 , 532, 112737	Ο
72	A perfect pair: Niobium- and gallium-doped ceramic biomaterial enabled by coupled synthesis method with potential application for bone regeneration and cancer-targeted therapy. 2023 , 599, 121962	0
71	Effect of the indoor humidity control characteristics for amine grafted functionalized mesoporous silica nanomaterials. 1-10	O
70	Theoretical modelling of electrostatic interactions in pH-dependent drug loading and releasing by functionalized mesoporous silica nanoparticles.	О
69	Using low-field NMR relaxation to optimise particulate dispersions. 2022, 118065	О
68	n-Pentanol lubrication of silica layers passivated with hydroxyl groups under constant shear stress and load, and isothermal conditions.	О
67	Adhesion, friction and tribochemical reactions at the diamondBilica interface. 2023, 203, 601-610	Ο
66	Synthesis and characterization of KF/waste glass catalyst for use in the transesterification process under pressurized conditions. 2023 , 203, 56-67	О
65	Role of particle size on the cohesive strength of non-sintered (green) ceramics. 2023, 658, 130653	Ο
64	Hydroxylation structure of quartz surface and its molecular hydrophobicity. 2023, 612, 155884	O
63	Regulating the states of Ni species by controlling the silanols of MCM-41 support to promote the hydrogenation of maleic anhydride. 2023 , 335, 127030	О

62	Comparative study of interzeolite transformed metallosilicates for the chemisorption of benzene, toluene, and xylenes. 2023 , 612, 155851	О
61	Arc Formation on Solar Array Surfaces Under Energetic Electron Irradiation and Vacuum Exposure. 2022 , 1-8	O
60	Phase and Structural Thermal Evolution of BiBiD Catalysts Obtained via Laser Ablation. 2022, 12, 4101	1
59	Contact Electrification of Biological and Bio-Inspired Adhesive Materials on SiO2 Surfaces: Perspectives from DFT Calculations. 2022 , 7, 216	O
58	Low-temperature Cu/Zn/SBA-16 integrating carbon membrane reactor for hydrogen production and high CO conversion through water-gas shift reaction. 2022 ,	О
57	Adsorption of a water-soluble molecular rotor fluorescent probe on hydrophobic surfaces. 2022 , 12,	O
56	Transition Metal Dichalcogenide TiS2 Prepared by Hybrid Atomic Layer Deposition/Molecular Layer Deposition: Atomic-Level Insights with In Situ Synchrotron X-ray Studies and Molecular Surface Chemistry. 2022 , 34, 10885-10901	О
55	Significantly Enhancing CO2 Adsorption on Amine-Grafted SBA-15 by Boron Doping and Acid Treatment for Direct Air Capture. 2022 , 123030	O
54	Potentials of Cellulose and Silica-based Materials for Enzyme Immobilization.	0
53	A Form of Non-Volatile Solid-like Hexadecane Found in Micron-Scale Silica Microtubule. 2023 , 16, 9	O
52	Controlled Growth of Platinum Nanoparticles on Amorphous Silica from Grafted Pt D isilicate Complexes. 2022 , 7, 47120-47128	О
51	Adsorption of 6-MHO on two indoor relevant surface materials: SiO2 and TiO2.	O
50	Thermo-sensitive hydrogels for forward osmosis with NIR light-induced freshwater recovery.	О
49	Fundamentals of antifogging strategies, coating techniques and properties of Inorganic materials; a comprehensive review. 2023 ,	O
48	Illustrating new understanding of adsorbed water on silica for inducing tetrahedral cobalt(II) for propane dehydrogenation. 2023 , 14,	1
47	Layer-by-Layer siRNA Particle Assemblies for Localized Delivery of siRNA to Epithelial Cells through Surface-Mediated Particle Uptake. 2023 , 6, 83-92	O
46	Composition Effect on Interfacial Reactions of Sodium Aluminosilicate Glasses in Aqueous Solution. 2023 , 127, 269-284	0
45	Review: 3-Aminopropyltriethoxysilane (APTES) Deposition Methods on Oxide Surfaces in Solution and Vapor Phases for Biosensing Applications. 2023 , 13, 36	O

44	Mechanistic Study on Molecular Layer Deposition of Titanicone from TiCl4 and Ethylene Glycol. 2023 , 127, 2258-2265	O
43	Magnetoresponsive fluorescent coreBhell nanoclusters for biomedical applications.	O
42	Adsorption of CO32/IHCO3Ibn the Quartz Surface: Cluster Formation, pH effects, and Mechanistic Aspects.	0
41	Surface Hydroxyl-Determined Migration and Anchoring of Silver on Alumina in Oxidative Redispersion. 2277-2285	1
40	The role of carbon dioxide and water in the degradation of zeolite 4A, zeolite 13X and silica gels. 2023 , 47, 5249-5261	0
39	Stimuli-Responsive Silica Silanol Conjugates: Strategic Nanoarchitectonics in Targeted Drug Delivery.	O
38	Influence of Henna Extracts on Static and Dynamic Adsorption of Sodium Dodecyl Sulfate and Residual Oil Recovery from Quartz Sand. 2023 , 8, 13118-13130	O
37	Preparation of SiO2 coated carbon fibers and its interfacial properties with cement paste matrix.	O
36	Effect of Hydrophobic Moieties on the Assembly of Silica Particles into Colloidal Crystals.	O
35	Experimental investigation of hydrophobic and hydrophilic silica nanoparticles on extended surfactant properties: Micro-emulsion, viscosity, and adsorption behaviors. 2023 , 223, 211582	O
34	Hydrothermal rehydroxylation of SBA-15 material: Effect of initial silanol concentration and pore size on the textural properties. 2023 , 28, 101725	0
33	Reinforcement mechanism of silica surface hydroxyl: The opposite effect. 2023 , 623, 157000	O
32	Impact of silica nanoparticles architectures on the photosensitization of O2 by immobilized Rose Bengal. 2023 , 440, 114648	0
31	Functionalized silica nanoparticles within a multicomponent oil emulsion by molecular dynamic study. 2023 , 732, 122283	O
30	Co-deposition characteristics of hydrates and sands in gas-salty water-sands flow system. 2023 , 346, 128276	0
29	Utilization of palm oil as an alternative processing oil in carbon black-filled natural rubber compounds. 2023 , 194, 116270	O
28	Nanoscale insights into the interfacial characteristics between calcium silicate hydrate and silica. 2023 , 616, 156478	0
27	Atomistic investigation on interfacial properties of glass surfaces modeling plasma modification and the influence of wettability conditions on adhesion. 2023 , 122, 103330	O

26 Effects of Interfacial Hydroxylation Microstructure on Quartz Flotation by Sodium Oleate. **2023**, 39, 2182-21910

25	Computational investigation of ⊞iO2 surfaces as a support for Pd. 2023 , 25, 6121-6130	O
24	Aminosilane-Modified Ordered Hierarchical Nanostructured Silica for Highly-Selective Carbon Dioxide Capture at Low Pressure. 2023 , 1, 720-733	0
23	Fluorination of TiN, TiO2, and SiO2 Surfaces by HF toward Selective Atomic Layer Etching (ALE). 2023 , 13, 387	O
22	Prediction of glassy silica etching with hydrogen fluoride gas by kinetic Monte Carlo simulations. 2023 , 158, 094709	0
21	Investigation on morphology and chemistry of the Beilby layer on polished fused silica. 2023 , 49, 17116-17122	О
20	Removal of Methylene Blue from Aqueous Solution by Mixture of Reused Silica Gel Desiccant and Natural Sand or Eggshell Waste. 2023 , 16, 1618	0
19	Dissolution control and stability improvement of silica nanoparticles in aqueous media. 2023, 25,	O
18	Wet Milling of Alginate Alco- and Hydrogel Composites: A Facile Top-Down Approach for Continuous Production of Aerogel Microparticles. 2200674	O
17	Insights into the Coating Integrity and its Effect on the Electrochemical Performance of CoreBhell Structure SiO x @C Composite Anodes. 2201623	O
16	Synthesis and Characterization of Solfiel-Derived SiO 2 fao Particles: Size Impact on Glass (Bio)Properties. 2200184	0
15	Single-Collision Statistics Reveal a Global Mechanism Driven by Sample History for Contact Electrification in Granular Media. 2023 , 130,	O
14	Surface modification of TiO2 nanoparticles with organic molecules and their biological applications. 2023 , 11, 2334-2366	0
13	The role of silanol groups on the reaction of SiO 2 and anhydrous hydrogen fluoride gas.	Ο
12	Improving the sustainability of greenItyre tread compound by using recovered silica filler. 2023 , 26, 37-46	0
11	Synthesis of Organoalkoxysilanes: Versatile OrganicIhorganic Building Blocks. 2023 , 3, 280-297	O
10	High mobility of asteroid particles revealed by measured cohesive force of meteorite fragments. 2023 , 9,	0
9	Biomimetic Hygroscopic Fibrous Membrane with Hierarchically Porous Structure for Rapid Atmospheric Water Harvesting. 2214813	Ο

CITATION REPORT

8	Effect of the drying procedure on hybrid sono-aereogels for organic solvent remediation. 2023,	О
7	Sour Gas Adsorption on Silica Gels. 2023 , 8, 12592-12602	O
6	Localised strain and doping of 2D materials.	О
5	Sustainable charged composites with amphiphobic surfaces for harsh environment E olerant non-contact mode triboelectric nanogenerators. 2023 , 112, 108428	O
4	Structural and Surface Changes of SiO2 Flint Aggregates under Thermal Treatment for Potential Valorization. 2023 , 13, 647	0
3	A Review of Mineral and Rock Wettability Changes Induced by Reaction: Implications for CO2 Storage in Saline Reservoirs. 2023 , 16, 3484	O
2	n-Pentanol Lubrication of Silica Layers Passivated with Hydroxyl Groups Under Constant Shear Stress and Load and Isothermal Conditions. 2023 , 71,	0
1	Binding and Orientation of Carbamate Pesticides on Silica Surfaces.	O